RSC Advances

REVIEW

View Article Online
View Journal | View Issue

Cite this: *RSC Adv.*, 2022, **12**, 19764

Inhibitory potential of nitrogen, oxygen and sulfur containing heterocyclic scaffolds against acetylcholinesterase and butyrylcholinesterase

Rami J. Obaid,[a] Nafeesa Naeem,[b] Ehsan Ullah Mughal,[*b] Munirah M. Al-Rooqi,[a] Amina Sadiq,[c] Rabab S. Jassas,[d] Ziad Moussa[e] and Saleh A. Ahmed[*af]

Heterocycles are the key structures in organic chemistry owing to their immense applications in the biological, chemical, and pharmaceutical fields. Heterocyclic compounds perform various noteworthy functions in nature, medication, innovation *etc.* Most frequently, pure nitrogen heterocycles or various positional combinations of nitrogen, oxygen, and sulfur atoms in five or six-membered rings can be found. Inhibition of acetylcholinesterase (AChE) and butyrylcholinesterase (BChE) enzymes is a popular strategy for the management of numerous mental diseases. In this context, cholinesterase inhibitors are utilized to relieve the symptoms of neurological illnesses like dementia and Alzheimer's disease (AD). The present review focuses on various heterocyclic scaffolds and their role in designing and developing new potential AChE and BChE inhibitors to treat AD. Moreover, a detailed structure–activity relationship (SAR) has been established for the future discovery of novel drugs for the treatment of AD. Most of the heterocyclic motifs have been used in the design of new potent cholinesterase inhibitors. In this regard, this review is an endeavor to summarize the biological and chemical studies over the past decade (2010–2022) describing the pursuit of new N, O and S containing heterocycles which can offer a rich supply of promising AChE and BChE inhibitory activities.

Received 16th May 2022
Accepted 27th June 2022

DOI: 10.1039/d2ra03081k

rsc.li/rsc-advances

[a]*Department of Chemistry, Faculty of Applied Sciences, Umm Al-Qura University, Makkah 21955, Saudi Arabia. E-mail: saahmed@uqu.edu.sa; saleh_63@hotmail.com*

[b]*Department of Chemistry, University of Gujrat, Gujrat-50700, Pakistan. E-mail: ehsan.ullah@uog.edu.pk*

[c]*Department of Chemistry, Govt. College Women University, Sialkot-51300, Pakistan*

[d]*Department of Chemistry, Jamoum University College, Umm Al-Qura University, 21955 Makkah, Saudi Arabia*

[e]*Department of Chemistry, College of Science, United Arab Emirates University, P.O. Box 15551, Al Ain, Abu Dhabi, United Arab Emirates*

[f]*Department of Chemistry, Faculty of Science, Assiut University, 71516 Assiut, Egypt*

Ehsan Ullah Mughal is a Tenured Associate Professor of Organic Chemistry at the Department of Chemistry in University of Gujrat, Gujrat, Pakistan. He obtained his PhD from Bielefeld University, Germany in 2013 under the supervision of Prof. Dr Dietmar Kuck. For postdoctoral studies, he joined the group of Prof. Dr Xinliang Feng, Max-Planck-Institute for Polymer Research, Mainz, Germany. His current research interests include the design and synthesis of bioactive heterocycles, synthetic flavonoids, transition metals-based terpyridine complexes and their uses in the fabrication of DSSCs and as efficient photo-catalysts, and organic functional materials for the applications in organic electronics.

Saleh A. Ahmed received his PhD in photochemistry (photochromism) under the supervision of Prof. Heinz Dürr in Saarland University, Saarbrücken, Germany. He has more than 20 years of experience as post-doctoral fellow, senior researcher and visiting professor in France, Japan, Germany, Italy and USA. Since 2010 he is a senior professor of organic chemistry (photochemistry) at Assiut University, Egypt. He had successfully published more than 200 publications. His current research interests include synthesis and photophysical properties of novel organic compounds, developments of synthetic methodologies for the synthesis of novel organic compounds with unique theoretical and biological applications.

1 Introduction

Heterocyclic chemistry constitutes one of the most significant subclasses of organic chemistry. Heterocycles are cyclic organic compounds that contain at least one hetero-atom such as nitrogen, oxygen, sulfur *etc.*[1,2] Among the heterocyclic compounds, five or six-membered heterocycles with one, or two, or three hetero atoms in their nucleus have attained special interest owing to their stability and ubiquitous occurrence in natural as well as synthetic compounds.[3–5] Synthetic heterocyclic chemistry is used in a variety of domains including medicine, pharmacology, biocidal formulation, polymer science, electronics, agriculture, biology, optics, anticorrosive agents, agrochemicals, photo-stabilizers and material sciences.[6–8] In particular, they considered one of the significant classes of organic compounds, which are used in many biological fields on account of their multiple uses in treating various illnesses.[9,10] Many biological compounds, such as vitamins, hemoglobin, hormones, DNA, RNA, and others contain these heterocyclic rings as a key structural constituent. These structures can also be found in several FDA-approved medications that are used to treat a variety of disorders.[11] Furthermore, heterocyclic compounds have a wide range of biological applications as antifungal, anticonvulsant, antibacterial, antioxidant, antidiabetic, anti-inflammatory, enzyme inhibitors, herbicidal action, antiallergic, anticancer tumor, anti-HIV, and insecticidal agents.[12–22]

N-containing heterocycles are such organic compounds which contain one or more than one N-atom present in five- or six-membered ring systems (Fig. 1).[23,24] Likewise, the *O*-containing heterocycles are also important scaffolds in organic chemistry mainly because of their diverse biological functions. The various subclasses of *O*-containing heterocycles are chromones, coumarins, furan, oxazole, and benzofuran *etc.* A substantial number of *O*-containing heterocycles exhibit a broad range of pharmacological activities such as antimicrobial, anti-HIV, antimalaria, anticancer, anti-tubercular, and diabetic activities.[25–28] Moreover, *S*-containing heterocyclic compounds are often associated with foul odors but are widely used in various biological processes. Organosulfur compounds are fundamental entities in primary (cystine and methionine amino acids) and secondary metabolites (biotin and thiamine), and are also used in medicines, dyes, and agrochemicals *etc.*[29,30] Many *S*-containing bioactive molecules, such as glutathione, hydrogen sulfide, and taurine play a crucial role in maintaining cellular redox equilibrium in living organisms. Additionally, *S*-containing β-lactam ring system is present in commercially available antibiotics such as penicillin and cephalosporin.[31–35]

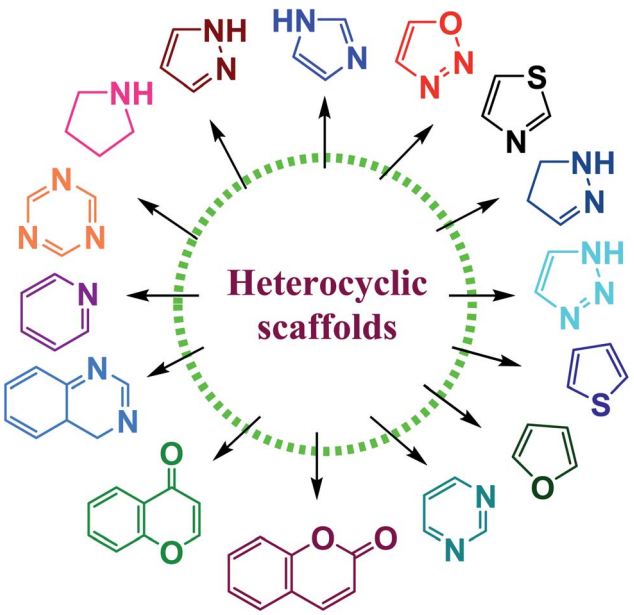

Fig. 1 Various heterocyclic scaffolds.

The applications of heterocyclic motifs in medicinal chemistry and chemical sciences are very vast as illustrated by the marketed medicines containing N, O, and S heteroatoms. The exceptional function of these heteroatoms in a variety of interactions with essential biological targets broadens the possibility of drug design and development. In this context, four cholinesterase (ChE) inhibitors (tacrine, donepezil, rivastigmine, and galantamine) have been approved as safe and non-toxic drugs for the symptomatic treatment of Alzheimer's disease (AD). Although, there are six types of these inhibitors which are commercially available in the market (Fig. 2).[36–42] However, the drugs based-on edrophonium and pyridostigmine structural motifs have been found to show toxicity. Due to their toxic nature, such inhibitors have been commercially banned now.

Since heterocyclic compounds occupy a crucial rank in organic chemistry[43,44] and comprise a significant share of the chemical and biological sciences, they are used as potent motifs for many bio-evaluations.[45–48] Such compounds play a vital role in the discovery of novel pharmacologically bioactive molecules.[49] Indeed, with respect to the pharmaceutical industry, heterocyclic nuclei are remarkably ubiquitous with over 60% of the top most selling pills having at least one heterocyclic scaffold as part of the whole structure of the molecule.[50] Furthermore, molecules containing heterocyclic scaffolds frequently demonstrate enhanced solubilities and can ease salt formation, both of which are recognized to be necessary for bioavailability and oral absorption.[51] In this regard, various heterocycles show evidence of various biological and pharmacological activities partly due to certain parallels with many natural and synthetic molecules with known bioactivity.[52]

Therefore, there has been continuous research related to synthesis of more potent and highly efficacious cholinesterase inhibitors by modifying the main template moieties of available inhibitors for AD management. The present review discusses a variety of most significant heterocyclic structures, containing N, O and S atoms, exhibiting high potential as cholinesterase inhibitors in a concise way. Structure–activity relationship has also been established. To the best of our knowledge, such structures have not been considered before against acetylcholinesterase and butyrylcholinesterase enzymes.

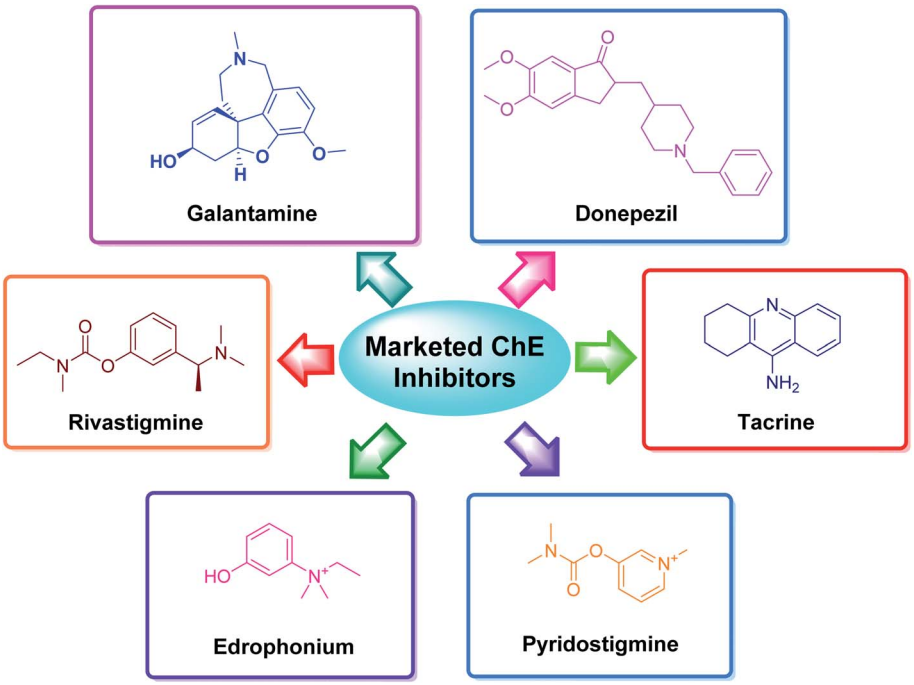

Fig. 2 Selected examples of commercially available cholinesterase inhibitors.

2 Cholinesterase enzymes

Cholinesterases are essential enzymes present in vertebrates and insects that hydrolyze the acetylcholine (ACh) in the central and peripheral nervous system.[53,54] In the body, ChE act as neurotransmitters responsible for the conduction of nerve impulses to the cholinergic synapses.

Acetylcholinesterase (AChE; EC 3.1.1.7) and butyrylcholinesterase (BChE); (EC 3.1.1.8) are two forms of cholinesterases. BChE is an enzyme closely related to AChE and serves as a cholinergic neurotransmission co-regulator that hydrolyzes ACh. During the progression of Alzheimer's disease, investigations have revealed an increase in BChE activity (40–90%) in the most affected parts of the brain, such as the temporal cortex and hippocampus. During the early phases of senile plaque development, enhanced BChE activity is also significant in Aβ-aggregation. As a result, inhibition of AChE and BChE has been identified as a significant target for the effective management of AD, as evidenced by a rise in ACh availability in brain areas and a decrease in Aβ deposition.[55] However, BChE is primarily found in peripheral tissues, including plasma, with only a trace amount present in the brain. Moreover, the possible benefit of selective inhibition of AChE over BChE may include a lower risk of peripheral cholinesterase enzyme inhibition and related side effects.[56]

Cholinergic theory states, Alzheimer's disease (AD) symptoms are largely produced by structural alterations in cholinergic synapses, the damage of subtypes of acetylcholine (ACh) receptors, the death of acetylcholine-generating neurons, and, as a result, cholinergic neurotransmission degradation. These problems cause AChE, an ACh-hydrolyzing enzyme to accumulate.[57] Apart from a small number of familial instances caused by genetic abnormalities, no viable therapy options exist for most patients, and the illness's primary causes remain unknown. The following are the main categories of pharmacotherapeutic tactics for the treatment of AD: (i) therapies that prevent the commencement of the disease by isolating the main progenitors; (ii) disease-modifying treatments that stop or reverse disease development; and (iii) symptomatic treatments that target the disease's cognitive signs and protect patients from further cognitive decline.[58,59] Because cholinergic neuron damage is prevalent in disease states, the present pharmacotherapeutic method founded on cholinesterase inhibitors offers a viable therapeutic aim for partial stabilization of cognitive function in AD patients. However, these compounds only have a short-term effect, usually 1–3 years, and they have no effect on disease progression.[60–62]

2.1 Alzheimer's disease and properties of various kinds of cholinesterase

Alzheimer's disease (AD) is a progressive chronic illness that causes gradual neurodegeneration. It was first characterized by Alois Alzheimer in 1907. Alzheimer's disease produces gradual cognitive dysfunction, including difficulty in making decisions, language problems, mood swings, learning, orientation, and other behavioral issues. Aging is the most important risk factor for Alzheimer's disease.[63,64] Physical activity, on the other hand, can help to lower dementia rates. The enzyme cholinesterase (ChE) is a promising therapeutic target for Alzheimer's disease (AD). The loss of neurotransmission and the deterioration of cholinergic neurons in the brain are the main causes of cognitive decline in Alzheimer's patients.[65,66]

According to the cholinergic hypothesis, the main cause of Alzheimer's disease is decline in acetylcholine synthesis. Brain atrophy is the most visible clinical feature in Alzheimer's disease as acetylcholine (ACh), a neurotransmitter involved in the transmission of electrical impulses from one nerve cell to another, is rapidly hydrolyzed by the acetylcholinesterase (AChE) enzyme.[67,68] According to the amyloid hypothesis, AChE has non-cholinergic effects such as promoting the formation of β-amyloid (Aβ), a proteolytic fragment produced from amyloid precursor protein (APP), and deposition in the brain of afflicted persons in the form of senile neurofibrillary tangles. The accumulation of Aβ is thought to have a key role in the onset and progression of Alzheimer's disease.[69–72]

Cholinesterase (ChE) is a choline-based esterase that hydrolyzes choline-based esters like acetylcholine (ACh), a neurotransmitter. The hydrolysis of cholinergic neurotransmitters is catalyzed by two enzymes known as AChE and BChE. AChE activity is prominent in the healthy brain, whereas BChE, which works as a coregulator of cholinergic neurotransmission, plays a supporting role.[73,74] AChE activity remains constant or decreases in individuals with AD, but BChE activity rises, resulting in an imbalance between BChE and AChE.[75] Consequently, both enzymes are involved in the control of ACh levels and act as a useful therapeutic target for treating cholinergic deficits[76] (Fig. 3). As a result, inhibiting both AChE and BChE at the same time may be beneficial in the latter phases of the illness.[77] Accordingly, AChE and BChE inhibitors have surfaced as effective symptomatic therapies for AD. So far, four acetylcholinesterase inhibitors (AChEIs) have been authorized for commercial use: galantamine, rivastigmine, tacrine, and donepezil. Nevertheless, tacrine was detached from clinical use due to unadorned adverse effects accompanying with hepatotoxicity.[78]

2.2 Properties of acetylcholinesterase

AChE is an esterase-like acetylcholine hydrolase enzyme (Fig. 4). Through cholinergic pathways, it plays an important role in brain function.

In 1991, the 3D structure of AChE was discovered in a Pacific electric ray (*Torpedo californica* (TcAChE)). The enzyme is mainly found in the central and peripheral nervous systems' synaptic gaps, and on red cell membranes.[79–81] ACh is a cholinergic system neurotransmitter that regulates a variety of processes, including cognition.[82] Botox, an exotoxin produced by the bacterium *Clostridium botulinum*, inhibits the discharge of ACh from cholinergic nerves blocking local neural conduction and muscle contraction. Botox is used in cosmetics to diminish facial creases, and for other therapeutic purposes.[83,84]

Inhibiting AChE by specific inhibitors is the therapeutic target to control *Myasthenia gravis*, glaucoma, Lewy body dementia, and AD.[85] Enzyme inhibitors are crucial in a variety of disease management situations.[86] AChE inhibitors are utilized in clinical practice to treat these problems, as they improve cholinergic function by increasing the amount of ACh in cholinergic synapses.[87] AChEIs were initially utilized in the treatment of myasthenia gravis, a neuromuscular condition that generates skeletal muscle weakening, in 1932. These inhibitors were first approved (1938) for the treatment of individuals with myasthenia gravis.[88] Antibodies targeting ACh receptors were developed later in 1960.[89,90] AChEIs have been utilized to protect retinal ganglion cells from ocular hypertension in glaucoma. The intraocular pressure was reduced, the

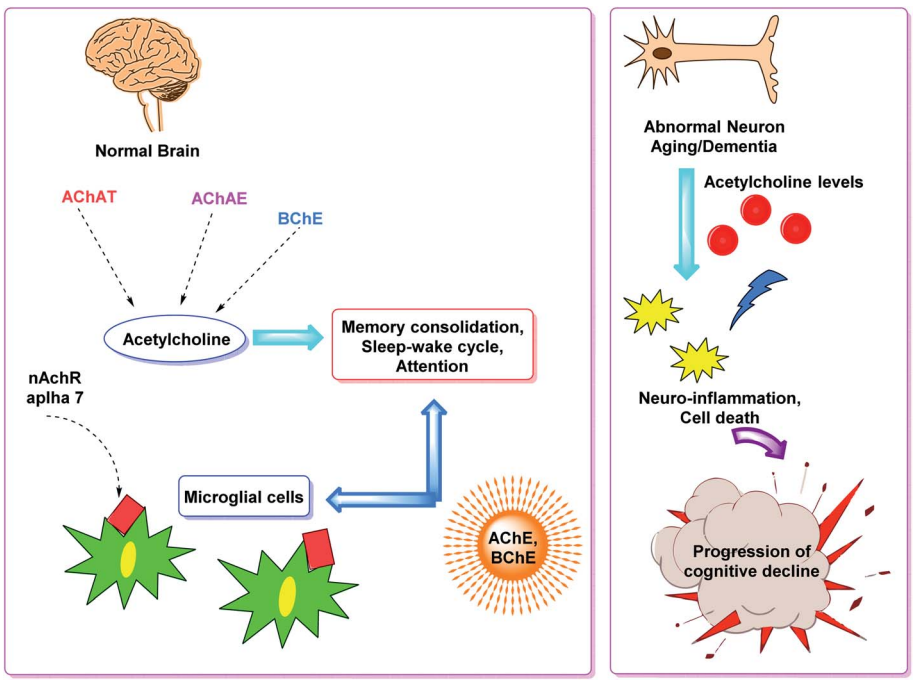

Fig. 3 Brain cholinergic signaling.

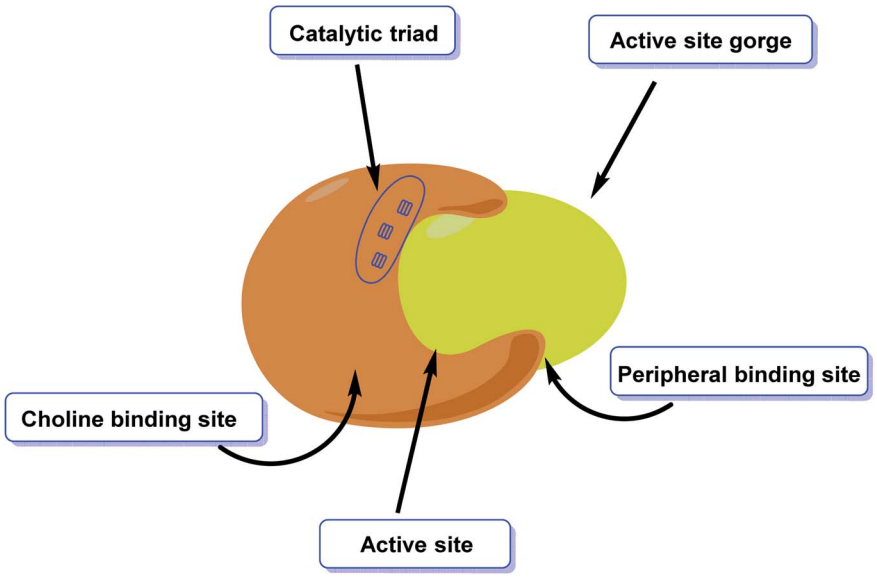

Fig. 4 Diagrammatic representation of the active site of acetylcholinesterase.

arteries were protected, and ocular blood flow was enhanced.[91,92] AChEIs can also treat the symptoms of AD, known as the most frequent kind of dementia defined by the accumulation of amyloid plaques,[93] which is triggered by the loss of ACh functions in the brain, which occurs most commonly in the elderly.[94] Many compounds have been approved to prevent AChE breakdown in the brain, which can boost ACh activity and lessen AD symptoms,[95] despite the fact that no treatments exist that to stop or reverse Alzheimer's progression (Fig. 5).

2.3 Properties of butyrylcholinesterase

BChE is found in a variety of organs, including the liver, where it is produced and released into the bloodstream.[96,97] BChE has a restricted neuronal distribution in the central nervous system as a pseudocholinesterase (CNS). In the human cerebral cortex, the number of BChE-rich neurons is around 2 orders of magnitude lower than the number of AChE-rich neurons. Glial origins are the most common.[98,99] Although the role of BChE in normal conditions is unknown, it has been linked to lipoprotein, drug, and detoxification metabolism.[100,101] It has a role in the breakdown of succinylcholine, an amyorelaxant used in surgical procedures. It also activates the antiasthmatic prodrug bambuterol and hydrolyzes medicines like heroin and physostigmine.[102] As a result, the level of BChE has been demonstrated to play an important role in diabetes, obesity, hepatic steatosis, and other diseases.[103] BChE knockout mice show no physiological abnormalities.[104] Similarly, BChE-deficient persons can live long and healthy lives.[105] BChE's compensating nature, on the other hand, is a prominent aspect. BChE compensates for the absence of AChE in the AChE-knockout mouse model, allowing normal cholinergic pathways to be maintained in AChE nullizygous animals.[106] Due to highly damaged cholinergic neurons, the amount of AChE reduces by 90% in advanced AD. Meanwhile, BChE levels and function rise to 105–165% of normal, making it the primary ACh metabolic enzyme.[107] Because of the critical role of BChE, ACh does not significantly increase in AChE knocked-out mice.[108,109] As a result, licensed selective AChE inhibitors such as galantamine and donepezil have a very limited effect on severe AD, which is linked to a significant drop in AChE levels in individuals with serious AD. In recent years, a growing number of researchers have focused their research efforts on the design of BChE inhibitors for the treatment of advanced AD.[110–112]

2.4 Mechanism of action of cholinesterase enzymes

As mentioned previously, there are two types of cholinesterase (ChE) enzymes: acetyl and butyrylcholinesterase (AChE and BChE). The ChE inhibitors are the most valuable agents for increasing ACh levels in neuronal cells by preventing the hydrolysis of ACh into choline and acetic acid. Clinical data suggest that BChE plays an significant role in the control of ACh and the maintenance of normal cholinergic activities, making it an additional intriguing target in the battle against AD.[113–115] As a result, addressing both ChEs (AChE and BChE) simultaneously might provide a remedial benefit in advanced and late-stage AD. Furthermore, both ChEs are known to play an important role in Aβ aggregation.[116] The Aβ is an insoluble protein fragment produced by beta secretase-1's catalytic proteolysis of amyloid precursor protein (BACE-1). The production of oligomers, fibrillary rods, or -sheets, which have been implicated in increasing neurotic damage and cognitive failure, is triggered by the buildup of Aβ aggregates.[117] Furthermore, the buildup of Aβ aggregates in mitochondria may result in the formation of free radicals, resulting in oxidative stress.[118] As a result, multitargeted therapeutics that inhibit ChEs (dual AChE and BChE), BACE-1, and Aβ aggregation while also having antioxidant potential could be useful in

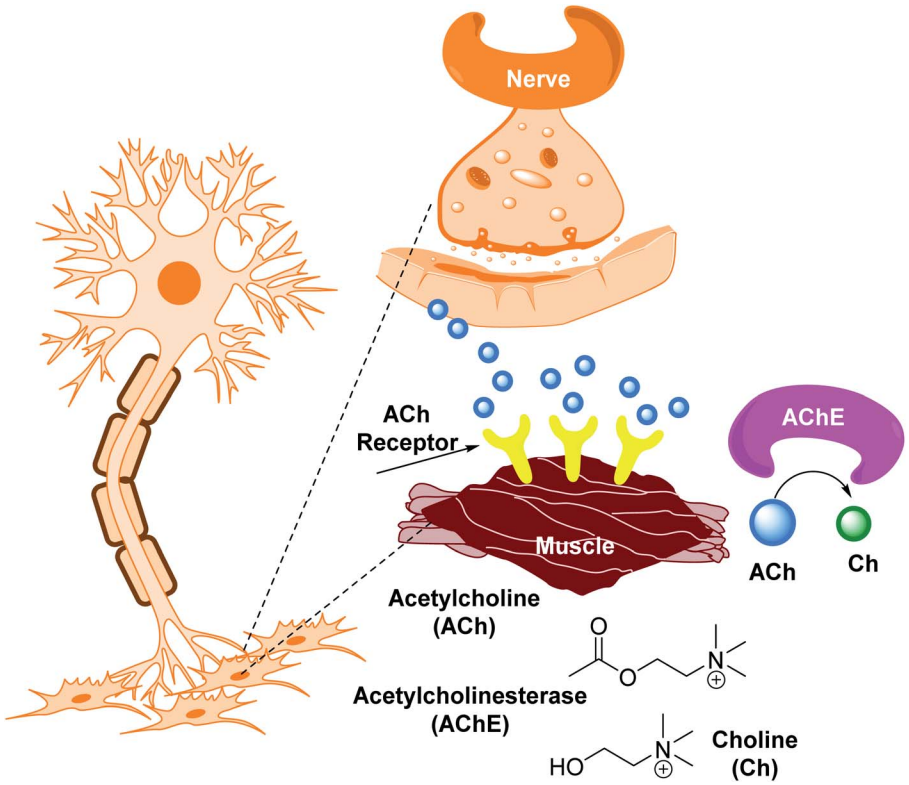

Fig. 5 Synthesis of acetylcholine.

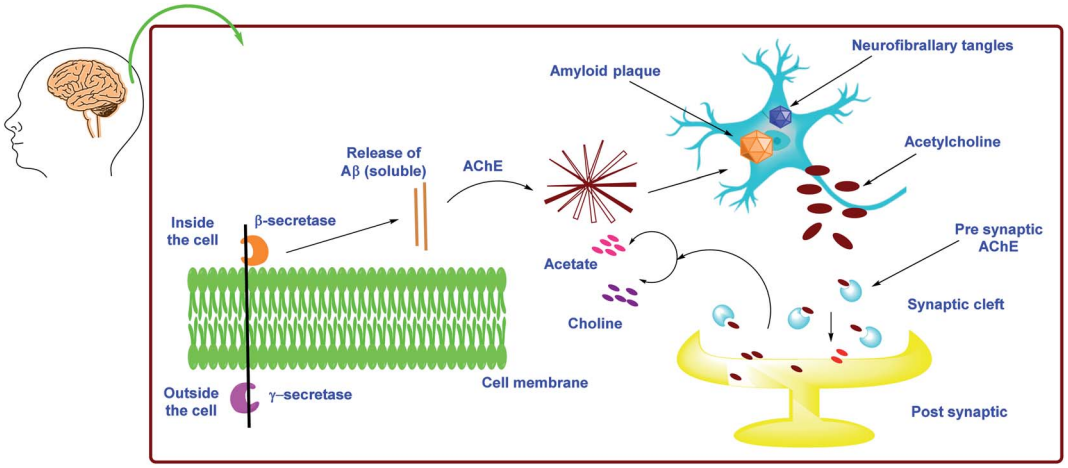

Fig. 6 Schematic representation of AD pathogenesis in light of the cholinergic and amyloid hypothesis.

slowing the progression of AD instead of just delivering symptomatic relief (Fig. 6).

3 Cholinesterase inhibition

Cognition is a blend of memory, attention, acquaintance, perception, skills, decision making, reminiscence, planning and judgment.[119,120] The loss of memory coupled with cognitive impairment are noted in a variety of conditions such as aging, head injury and neurodegenerative disorders like depression, schizophrenia, AD and Parkinson's disease[121–123] (Fig. 7).

Acetylcholine, glutamate, serotonin, and dopamine are neurotransmitters that regulate cognitive functioning. ACh, is an essential neurotransmitter in the control of learning and memory processes.[124–127] Low acetylcholine concentrations in the cortex, hippocampus, and basal forebrain have been linked to cognitive impairment and short-term memory loss.[128] By forming AChE-A complexes, AChE also causes the aggregation and deposition of A fibrils, resulting in cognitive dysfunction.

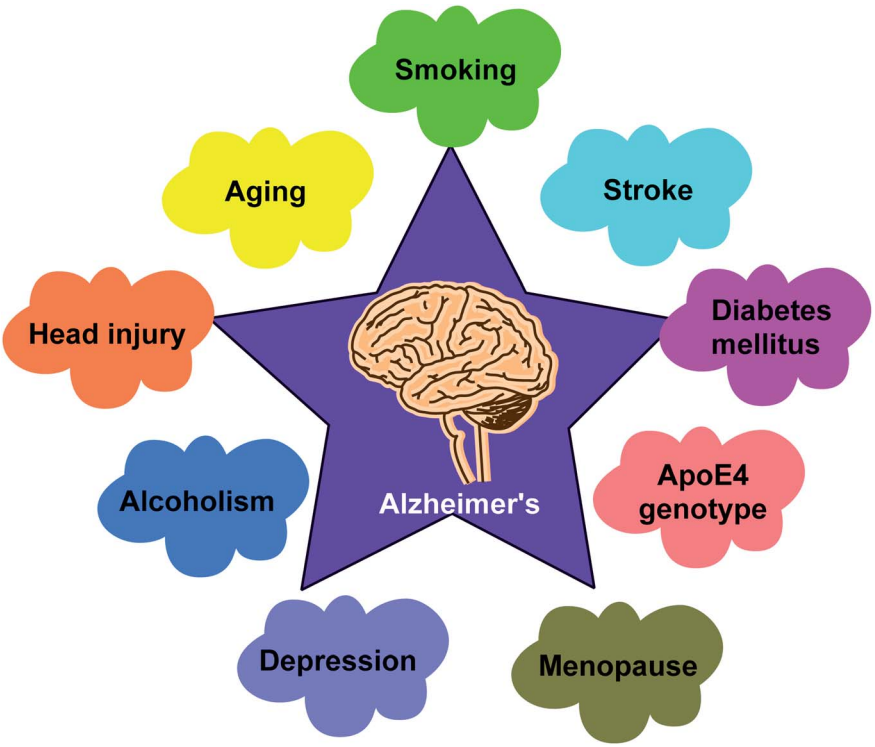

Fig. 7 Factors involved in AD progression.

As a result, increasing ACh by AChE inhibition and preventing Aβ aggregation are the best promising treatments to slowing dementia development.[129] Oxidative stress is another harmful component where excessive reactive oxygen species (ROS) production causes lipid peroxidation and protein oxidation, which causes oxidative damage and impairs cognitive function.[130–132]

The United States Food and Drug Administration (US FDA) has licensed three AChE inhibitors (rivastigmine, galantamine, and donepezil) to treat the symptoms of AD, however these drugs have no effect on disease progression.[133] These medications have several adverse effects, including urine incontinence and muscular cramping, which restricts their usage in the latter periods of the disorder.[134,135] As a result, it is critical to develop novel drugs that will obstruct ACh metabolism by blocking AChE and inhibiting Aβ aggregation and should demonstrate antioxidant activity to slow disease progression.[136,137]

3.1 Cholinesterase inhibition mechanism

Aggregation of β-amyloid proteins and decreased cholinergic neurotransmission, which degrade the structural proteins of neurons, are the two major targets of treatment methods for cognitive decline.[138] In the pathogenesis of cognitive decline, oxidative stress has also been implicated. ROS cause oxidative damage to the lipid and protein composition of neurons, resulting in changes in neuronal structure and function. The most severe and persistent biochemical alteration in cognitive impairment is cholinergic insufficiency (Fig. 8). Diminished levels of AChE, acetylcholine, and choline acetyltransferase have been reported in necropsy brain samples, indicating this. Choline esters are hydrolyzed by AChE, a hydrolase[139] exhibiting high catalytic activity where each molecule is capable of degrading around 25 000 acetylcholine (ACh) molecules/second, reaching the substrate's diffusion limit. The anionic and esteratic subsites of AChE's active site are separated by a membrane. The crystal structure of AChE has revealed the shape and mechanism of action of the enzyme.[140–150]

AChE is one of the most important enzymes in the serine hydrolase family, as it is engaged in the cleavage of ACh, exhausting ACh levels linked to memory and learning.[151] As a result, the cholinergic hypothesis for cognition problems implies that degeneration in ACh-containing neurons play a significant role in the cognitive decline linked to old age. Multiple cognition enhancers have been developed throughout the years, but the discovery and development of several possible AChE inhibitors has cleared the path for a more effective therapy and treatment methodology to cognitive decline.[152] As a result, cholinesterase inhibitors (ChEIs) are employed to treat cholinergic insufficiency. AChEIs have been designed using a variety of pharmacophoric scaffolds. The FDA has already authorized AChE inhibitors including physostigmine, rivastigmine, tacrine, and donepezil for the treatment of neurodegenerative illnesses like AD.[153,154]

4 Synthetic sources of ChE inhibitors

Donepezil and galantamine are agents that inhibit AChE function in a reversible and selective manner.[155] Rivastigmine, on the other hand, connects covalently to the receptors' active site

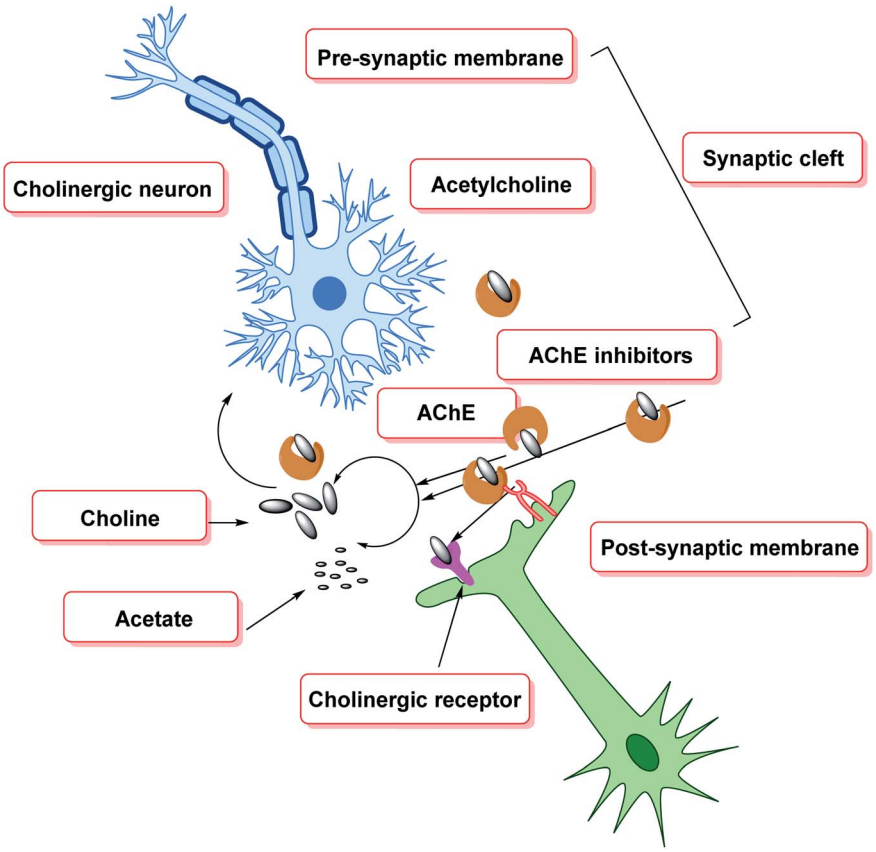

Fig. 8 Therapeutic strategies towards cognitive decline.

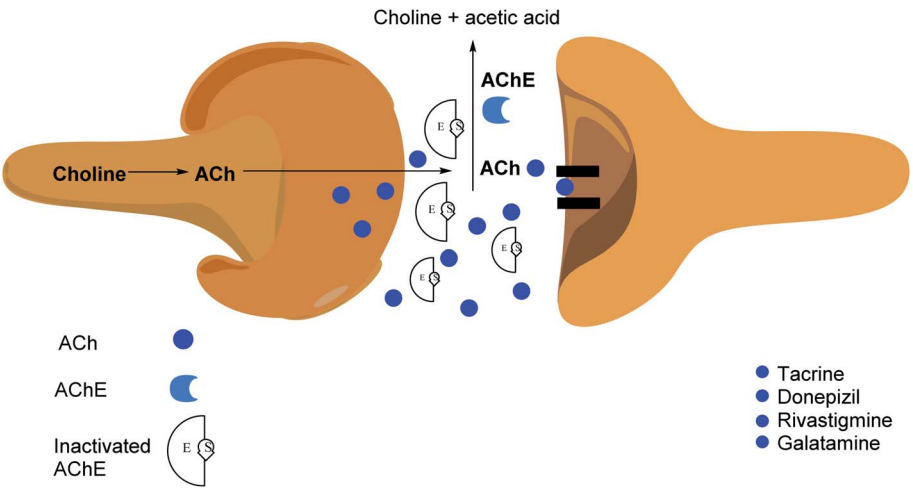

Fig. 9 Synthesis, storage, discharge and termination of acetylcholine's action.

and is thus referred to as a pseudo-irreversible drug due to the sluggish release of the substrates. Rivastigmine is additionally a dual inhibitor of AChE and BChE.[156,157] Rivastigmine is the only carbamate medicine that is prescribed to cure the symptoms of AD in patients. Other important functions of the carbamate group in pharmaceuticals include chemical stability, the ability to enhance permeability across cellular membranes, and participation in serine hydrolase inhibitors to cure asthma and pesticides for pest control.[158] The amino acid sequences of human AChE and BChE are about 89% similar.[159]

Surface specificity and gorge sensitivity, as well as the volume of the gorge exposed to entrance inhibitors, are the main differences between AChE and BChE. The entrance of the BChE gorge is noticeably broader than AChE, and the amino

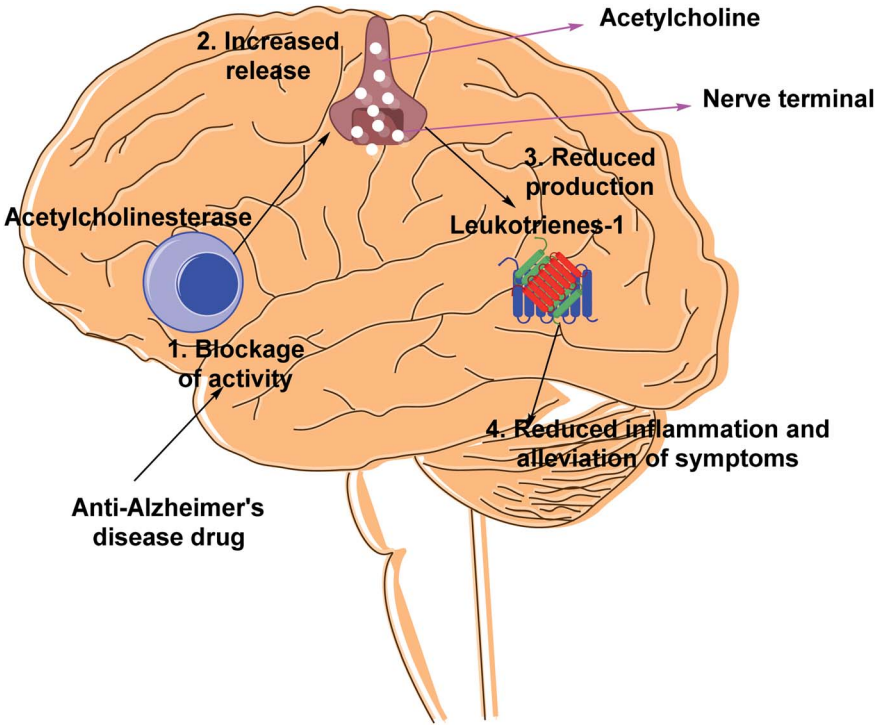

Fig. 10 Mechanism of action of anti-AD drug.

acid residues at the peripheral site of AChE and BChE are partly different, according to X-ray spectroscopic study (Fig. 9). Three aromatic amino acids are missing from the peripheral site of BChE, resulting in altered interactions between ligand and substrate.[160,161] The role of BChE in normal conditions of healthy brain activity is overlooked, even though BChE level rises in tandem with AD progression in the latter phases of the illness. Remarkably, the level of AChE begins to decrease in these situations[162–164] (Fig. 10).

5 Synthetic cholinesterase inhibitors

5.1 Nitrogen-, oxygen- and sulfur-based heterocycles

Taslimi *et al.* (2018) reported a series of substituted pyrazol-4-yl-diazene derivatives **1** and their *in vitro* cholinesterase (ChE) studies and suggested that all the analogs were potent AChE (K_i = 44.66–78.34 nM) and BChE (K_i = 50.36–88.36 nM) inhibitors even better than tacrine (standard) for the treatment of AD (Table 1). Later, inhibition of such metabolic enzymes has emerged as a promising factor for pharmacologic intervention in a range of disorders like epilepsy, obesity, and neurodegenerative diseases.[165]

Qin *et al.* (2019) prepared a series of δ-sulfonolactone-fused pyrazole motif using sulfur(VI) fluoride exchange chemistry employing pyrazolones and aryl sulfonyl fluorides. The *in vitro* enzyme screening demonstrated their ChE inhibitory action. Among the synthesized compounds, compounds **2**, **3**, and **4** were recognized as selective BChE inhibitors with IC_{50} = 0.20, 0.46 and 0.42 μM, respectively. Kinetic studies showed that BChE inhibition of compounds **3** and **4** were reversible, mixed, and non-competitive (K_i = 145 nM and 60 nM respectively). This type of inhibition exhibited remarkable neuroprotective activity and developed as promising therapeutics for AD treatment[166] (Table 1).

Şen *et al.* (2019) prepared a series of substituted pyrazole-based pyridazine derivatives and checked their inhibitory abilities against AChE inhibitors. These pharmacophores have gained special attention in many different synthetic drug designs due to their various bioactivities and the scaffolds of various bioactive natural compounds. All the synthesized analogs **5** and **6a–f** exhibited excellent AChE inhibition (**1–9** = 506 to 1022 nM). The discovery of novel inhibitors of AChE, one of the ChE enzymes, is particularly important for AD[167] (Table 1).

Singh *et al.* (2019) prepared several 3,5-diaryl-1*H*-pyrazole derivatives and evaluated them for their potencies against AChE and BChE inhibitors. All analogs demonstrated mild to good activity compared to the reference standard donepezil. Compound **7** (*p*-Cl) was found to be potent inhibitor of AChE and BChE with 2-folds increase in IC_{50} (IC_{50} = 1.937 μM for AChE; 1.166 μM for BChE). These results represent a valuable milestone for the design of new agents against AD[168] (Table 1).

Shaikh *et al.* (2020) reported novel scaffolds of N-substituted pyrazole derived α-amino phosphonates and evaluated their anti-ChE activity, where two of these analogs **8** (IC_{50} = 0.055 μM for AChE) and **9** (IC_{50} = 0.017 μM for AChE) showed strong efficacy against AChE. The remaining compounds possessed moderate to good BChE inhibition and performed better than the commercially available drugs galantamine and rivastigmine. This research produced promising lead compounds for further development as anti-Alzheimer agents[169] (Table 1).

Table 1 Chemical structures of pyrazole derivatives **1–9** and their IC_{50} values against cholinesterase enzymes

Compound no.	Chemical structure	IC_{50} values (μM) AChE	IC_{50} values (μM) BChE	References
1	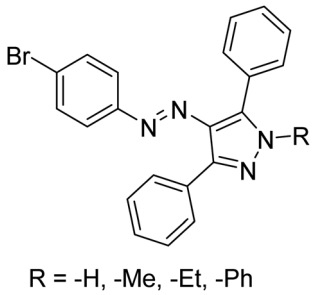 R = -H, -Me, -Et, -Ph	44.66–78.34 nM	50.36–88.36 nM	165
2	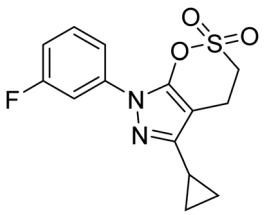	—	0.20	166
3	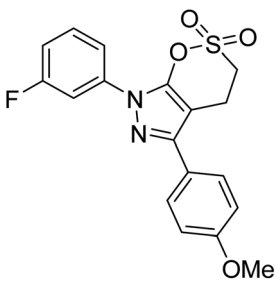	—	0.46	166
4	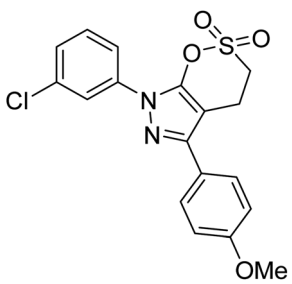	—	0.42	166
5	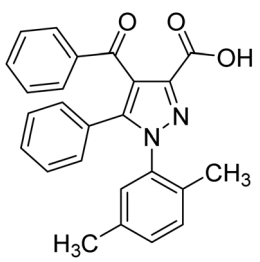	506–1022 nM	—	167

Table 1 (*Contd.*)

Compound no.	Chemical structure	IC_{50} values (μM) AChE	BChE	References
6	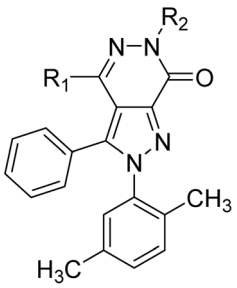 R_1 = -Ph (a-f) R_2 = -Ph (a), -H(b), -Ph$(CH_3)_2$ (c), -PH(NO_2) (d), -Ph$(Cl)_3$ (e), -PH(CF_3) (f)	506–1022 nM	—	167
7	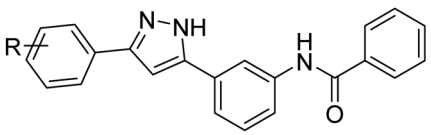 R = -H, -Cl, -Br, -F, -OCH_3, -CF_3, -CN, -CH_3	1.937	1.166	168
8	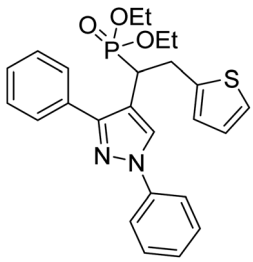	0.055	—	169
9	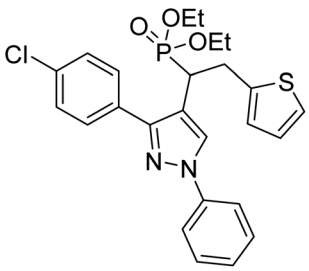	0.017	—	169

Limited SAR studies were conducted based on the central core and substitution pattern on the pyrazole scaffold (Fig. 11). Accordingly, it may be deduced that the variations observed in cholinesterase activity of the above-mentioned analogs is a consequence of variations in substitution pattern present on the main structural motif of the molecule. All these structural features are performing a considerable role in the inhibitory activity, though, observed variation in the activity of these analogs, which may be substantial in some cases, is ascribed to variability in the nature and positions of substituents on aryl rings. The smaller groups attached to the pyrazole ring promote higher AChE and BChE inhibitory abilities compared to bulky ones. Electron withdrawing atoms or groups (–F, –Cl, –Br, *etc.*) increase the activity whereas electron-donating groups (EDG) (–CH_3, –OCH_3 *etc.*) decrease the activity. Thus, ChE activity seems to be impacted by electronic and steric factors inherent to the inhibitor molecule.

In all the figures (Fig. 11 to 25) given below, the red arrow indicates the decrease in activity and green arrow indicates an increase in activity.

Ghalib *et al.* (2012) synthesized two indenoimidazoles by reacting ninhydrin with diphenylthiourea and diphenylurea for the treatment of AD. *In vitro* assays demonstrated that most of the compounds successfully inhibited ChEs in the μM range.

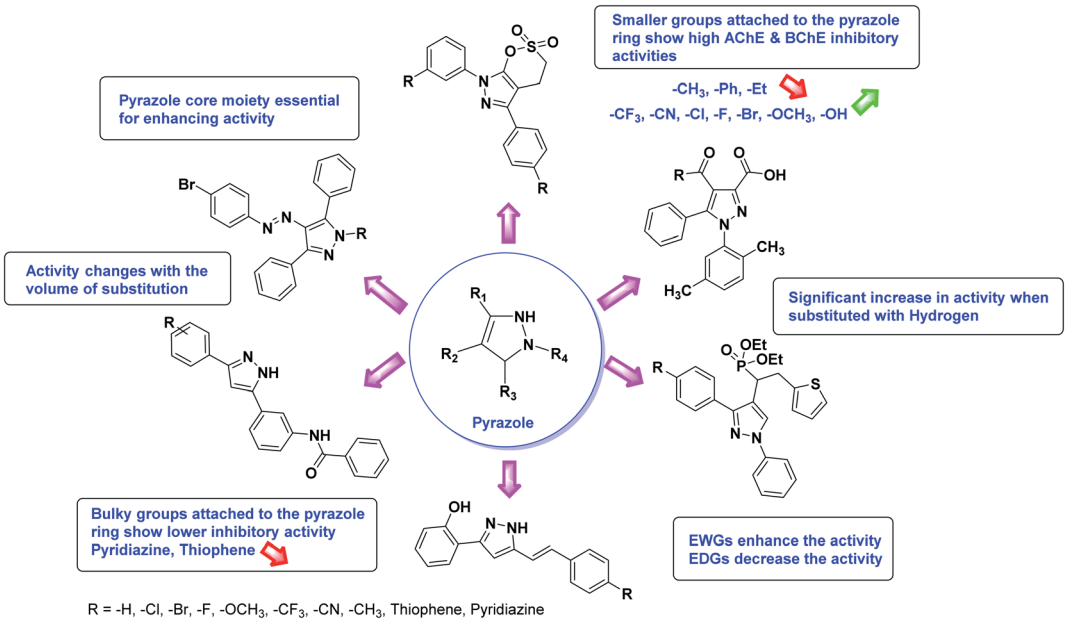

Fig. 11 SAR analysis of different pyrazole derivatives as AChE and BChE inhibitors.

Analogs **10** (IC_{50} = 177.69 μM for AChE and 90.20 μM for BChE) and **11** (IC_{50} = 274.69 μM for AChE and 101.20 μM for BChE) demonstrated good ChE enzyme. Moreover, **11** was found to be 3 times more selective BChE inhibitor, highlighting its potential for possible use in preventing further neurodegeneration as well for symptomatic treatment of Alzheimer patients. The AChE inhibitors are the mainstay drugs for the management of AD[170] (Table 2).

Yoon *et al.* (2013) synthesized a novel series of compounds containing benzimidazole core structure and evaluated their inhibitory potential against AChE and BChE inhibitors. Among the synthesized analogs, four benzimidazoles exhibited excellent AChE inhibition with IC_{50} < 10 μM. Compound **12** showed the highest inhibitory activity (–NO_2, IC_{50} = 5.12 μM for AChE and 8.63 μM for BChE). This work demonstrated that manipulating substituents on the 2nd position on the benzimidazole core as well as the 4th position on the aryl ring moiety could potentially result in novel analogs with potent ChE inhibition activity. The compounds containing EWGs at the 4th position in the phenyl ring are important for better activities as shown by **13** (–CF_3; IC_{50} = 9.74 μM for AChE and 6.59 μM for BChE), **14** (–COOH; IC_{50} = 16.38 μM for AChE and 11.44 μM for BChE) and **15** (–COOH; IC_{50} = 19.57 μM for AChE and 18.08 μM for BChE) compared to donepezil and rivastigmine. Compound **12–15** gave AChE inhibition activity with IC_{50} value <20 μM. The best inhibitor was **12** with IC_{50} of 8.63 μM (ref. 171) (Table 2).

Alam *et al.* (2018) described the preparation and AChE inhibition of imidazole iminium chloride derivatives. Among these, compound **16** was the best inhibitor of AChE with an IC_{50} value of 0.33 μM compared to the standard drug tacrine (IC_{50} = 0.20 μM)[172] (Table 2).

Inspired by multi-target-directed ligands (MTDLs), Xu *et al.* (2018) described the preparation of a new series of propargylamine-modified imidazole substituted pyrimidinyl thiourea derivatives. All compounds successfully inhibited AChE but displayed poor inhibitory activity toward BChE. Compound **17** was the best and most selective inhibitor having an IC_{50} = 0.324 μM. SAR studies demonstrated that the size of the propargylamine N-substituent strongly influenced the inhibitory profile. Moreover, the outcomes revealed that analog **17** may represent a multifunctional agent for the therapy of AD[173] (Table 2).

Menges *et al.* (2019) synthesized a series of mono and di-substituted imidazole derivatives and evaluated them *in vitro* for AChE and BChE inhibitory abilities. The synthesized derivatives exhibited excellent inhibition of AChE (IC_{50} = 17.3–120.9 nM) as well as BChE (IC_{50} = 27.02–151.2 nM) which was nearly equal to donepezil and 20–40 folds higher than the standard drug tacrine. Among them, compound **19** (substituted with α-naphthyl groups) displayed the most potent inhibition of both the esterases with IC_{50} values of 17.3 and 27.02 nM, respectively. The dimethoxy substituted imidazole derivative **18** and pyrene-substituted derivative **20** also displayed potent AChE and BChE inhibitory abilities with IC_{50} values of 17.3 and 17.32 nM (for AChE) and 41.67 and 64.28 nM (for BChE), respectively. SAR studies revealed that the nature of the substitution and their relative positions on the aromatic ring has a significant effect on the biological activity profile[174] (Table 2).

Arumugam *et al.* (2020) synthesized a small library of spiropyrrolidine tethered imidazole heterocyclic hybrids. These were evaluated for their *in vitro* ChEs inhibitory abilities, where analogs possessing *p*-CH_3 **21** and *p*-OCH_3 **22** substituents displayed potent activities with IC_{50} values of 2.02 and 2.05 μM against AChE and 12.40 and 11.45 μM against BChE enzyme, respectively, compared to galantamine (IC_{50} = 2.09 μM for AChE and 19.34 μM for BChE). Therefore, novel heterocycles

Table 2 Chemical structures of imidazole derivatives **10–24** and their IC_{50} values against cholinesterase enzymes

Compound no.	Chemical structure	IC_{50} values (μM) AChE	BChE	References
10	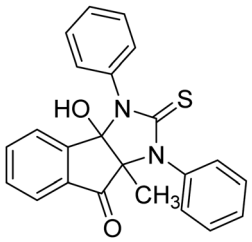	177.69	90.20	170
11	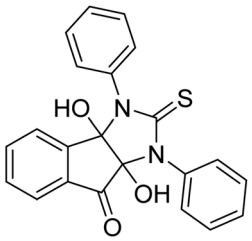	274.69	101.20	170
12	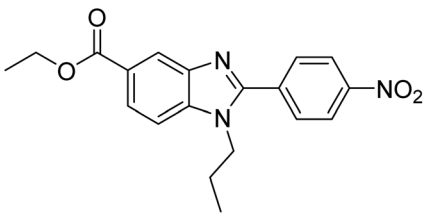	5.12	8.63	171
13	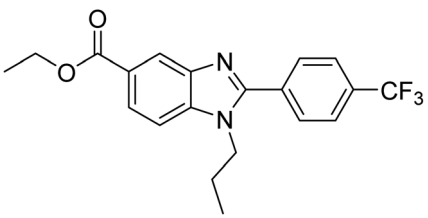	9.74	6.59	171
14	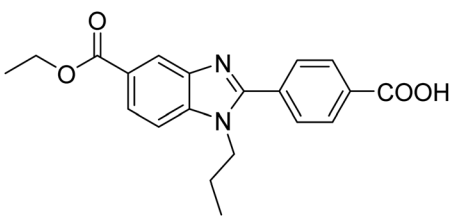	16.38	11.44	171
15	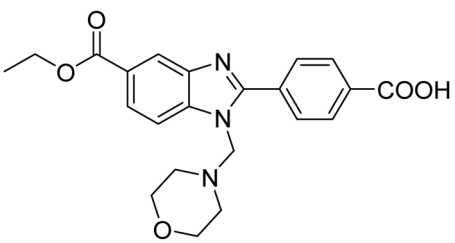	19.57	18.08	171
16	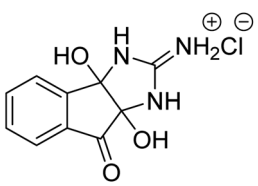	0.33	—	172

Table 2 (*Contd.*)

Compound no.	Chemical structure	IC_{50} values (μM) AChE	BChE	References
17	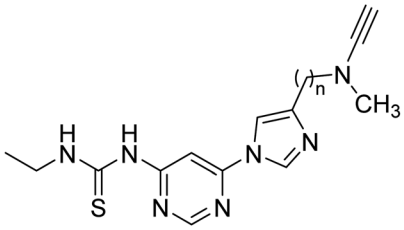	0.324	—	173
18	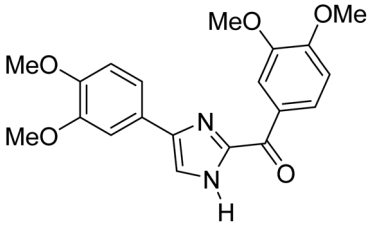	17.3 nM	41.67 nM	174
19	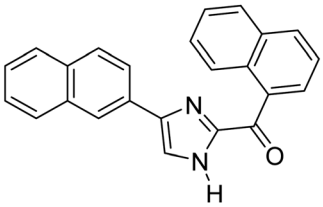	17.3 nM	27.02 nM	174
20	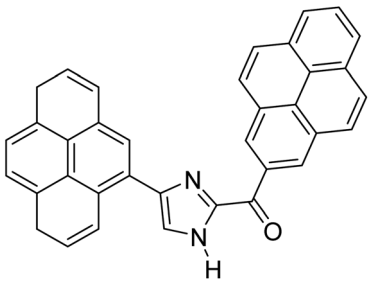	17.32 nM	64.28 nM	174
21	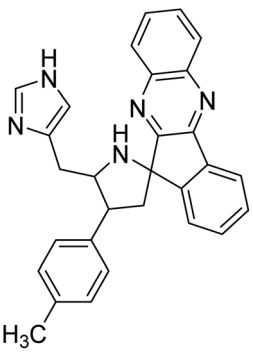	2.02	12.40	175

Table 2 (*Contd.*)

Compound no.	Chemical structure	IC_{50} values (μM) AChE	BChE	References
22	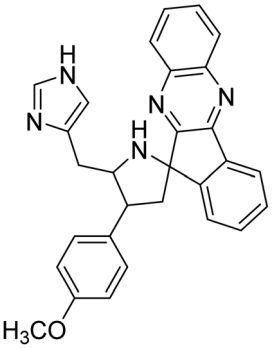	2.05	11.45	175
23	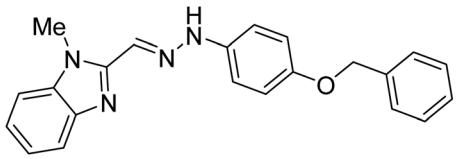	11.8	—	176
24	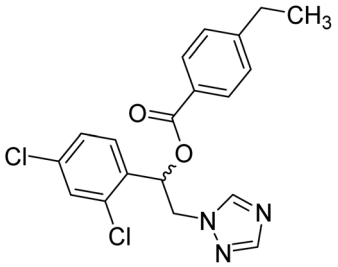	8.77	—	177

capable of suppressing the ChEs enzyme activity can compete with current ChEIs for promising AD treatments[175] (Table 2).

Boulebd *et al.* (2020) synthesized 10 hydrazones bearing a benzimidazole nucleus and assessed them for their anti-ChE activities. Among them, compound **27** (IC_{50} = 11.8 μM) was the best AChE inhibitor with an IC_{50} value comparable to that of the standard galantamine (IC_{50} = 8.9 μM). Furthermore, docking studies results revealed that these analogs inhibited the AChE enzyme mainly through H-bonds, π–π stacking, and hydrophobic interaction. These researchers succeeded in incorporating these two independently biologically active moieties (imidazole and hydrazone) into one molecule to generate compounds with new and/or enhanced biological activities[176] (Table 2).

Sari *et al.* (2021) reported a variety of azole antifungals like miconazole to possess ChE inhibitory effects. In this study, they have tested a set of azole antifungal analogs selected through virtual screening of an in-house library for their AChE and BChE inhibitory effects. Compound **24** showed potent and selective AChE inhibition, 70 times more potent (IC_{50} = 8.77 μM) than the standard. The study also yielded dual AChE/BChE inhibitors in addition to several potent AChE inhibitors. All the active compounds were imidazole derivatives and the modeling study showed that imidazole in the protonated state contributed greatly to the binding interactions with some key residues of AChE and BChE active site[177] (Table 2).

According to SAR studies, as represented in Fig. 12, the imidazole core moiety is essential for cholinesterase activity. Imidazole-based cholinesterase inhibitors proved excellent drugs against neurological diseases *i.e.*, Alzheimer's and Parkinson's disease. All the imidazole structural features perform a considerable role in the inhibitory activity, though, a slight variation in the activity of the reported analogs is attributed to variability in the nature and positions of substituents on aromatic rings. Smaller groups attached to the imidazole ring foster higher AChE and BChE inhibitory abilities compared to bulky ones. The AChE and BChE activities change with the volume of substitution. Electron withdrawing groups (–CF_3, –Cl, –NO_2, –COOH *etc.*) enhance the activity and electron-donating groups (–CH_3, –OCH_3 *etc.*) exhibit inhibitory effect. Thus, new imidazole derivatives are a gateway to many novel and cheap anticholinesterase drugs.

Abbasi *et al.* (2013) synthesized *S*-substituted analogs of 5-(2-nitrostyryl)-1,3,4-oxadiazole-2-thiol **25–30** and evaluated their ChE inhibitory activity. The analysis demonstrated that the synthesized analogs exhibit moderate to good activity against

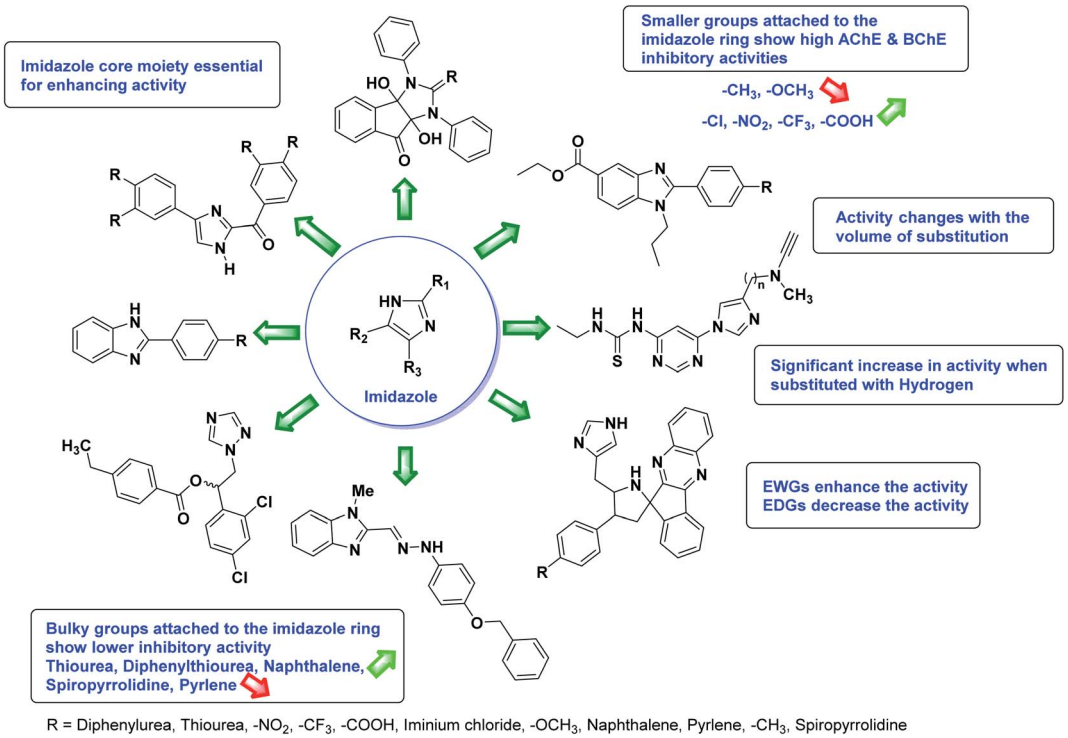

Fig. 12 SAR analysis of different imidazole derivatives as AChE and BChE inhibitors.

BChE and excellent inhibitory potential against AChE as evident from the IC_{50} values obtained for **25–30** (IC_{50} = 135, 254, 301, 289, >400, 101 μM for AChE and 132, 138, 74, 114, 80, 152 μM for BChE), respectively, relative to the reference standard eserine (IC_{50} = 0.04 mM for AChE and 0.85 mM for BChE). Hence, based on the outcome of this work, it was that halogenated analogs of 1,3,4-oxadiazoles **29** and **30** appear as good drug contenders for the treatment of AD.178 (Table 3).

Kamal *et al.* (2014) prepared a library of 2,5-disubstituted 1,3,4-oxadiazole analogs and evaluated their AChE inhibitory activity *in vitro*. All compounds showed good to moderate inhibitory activity toward the AChE enzyme. Amongst the surveyed oxadiazole analogs, compounds **31**, **32**, **33** and **34** (IC_{50} = 24.89, 13.72, 37.65, and 19.63 μM, respectively) stood out as the most promising inhibitors of AChE. Based on molecular modeling results, it was observed that the compounds **31–34** bind to the AChE enzyme in a similar fashion to donepezil. This investigation provided an insight for the future direction in the development of conjugates as potential AChE inhibitors[179] (Table 3).

Acridone-1,2,4-oxadiazole-1,2,3-triazole hybrids were prepared and assessed by Akbarzadeh *et al.* (2015) for their AChE and BChE inhibitory potential. Among the series, compound **35** was the most potent AChE activity (IC_{50} = 11.55 μM), being as potent as rivastigmine. Among all newly synthesized acridone-1,2,4-oxadiazole-1,2,3-triazoles, compounds **36** and **37** (IC_{50} = 11.55–77.79 μM) showed anti-AChE activity and **35** (IC_{50} = 11.55 μM) was found as potent as rivastigmine (IC_{50} = 11.07 μM). According to their findings, compound **35** possessing substitution-free acridone and 4-methoxyphenyl-1,2,4-oxadiazole groups displayed the best activity (IC_{50} = 11.55 μM)[180] (Table 3).

Siddiqui *et al.* (2017) described the preparation of 5-benzyl-1,3,4-oxadiazole-2-thiol derivatives and screened all the synthesized analogs against AChE and BChE. Among these, **38–42** demonstrated moderate to good anti-ChE activity (IC_{50} = 74.7, 129.6, 107.9, 70.84, 17.50 μM for AChE; **41**; 82.2, **42**; 72.7 μM for BChE, respectively) compared to eserine (IC_{50} = 0.04 μM for AChE, 0.85 μM for BChE) and was credited to the presence of the 3,4-dimethoxyphenylacetamide moiety[181] (Table 3).

Al-Harrasi *et al.* (2018) synthesized novel coumarin-oxadiazole hybrids and evaluated them against AChE and BChE in order to explore their potential for the prevention of AD. In the case of the coumarinyl oxadiazole series, **43** was lead candidate against AChE with an IC_{50} value of 6.07 μM, whereas compound **45** was found significantly active against BChE with an IC_{50} value of 0.15 μM. To realize the binding interaction of these compounds with AChE and BChE, molecular docking studies were performed. The docking studies of coumarinyl oxadiazole derivatives suggested that the compounds with high anti-BChE activity **43–45** provided MOE scores of −9.9, −7.4, and −8.2 kcal mol^{-1}, respectively, with the active site of BChE building π–π stacking with Trp82 and water bridged interaction. In the future, these compounds and their functionalized derivatives may be helpful in the development of potent drugs for AD[182] (Table 3).

Rehman *et al.* (2018) synthesized 5-substituted-1,3,4-oxadiazole-2yl-*N*-(2-methoxy-5-chlorophenyl)-2-sulfanyl acetamide derivatives and screened these derivatives against AChE and BChE. These findings revealed that the desired compounds

Table 3 Chemical structures of oxadiazole derivatives **25–84** and their IC_{50} values against cholinesterase enzymes

Compound no.	Chemical structure	IC_{50} values (μM) AChE	BChE	References
25	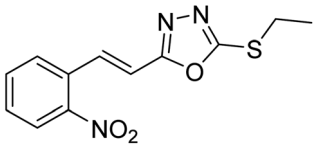	135	132	178
26	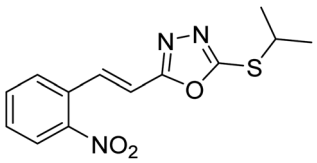	254	138	178
27	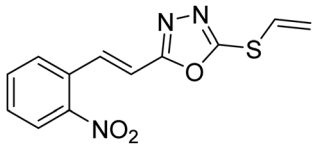	301	74	178
28	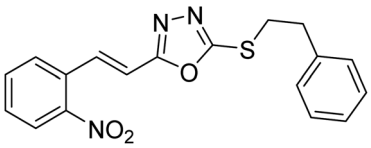	298	114	178
29	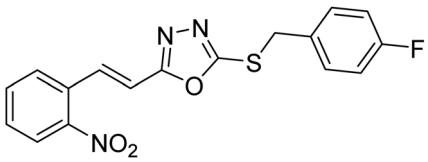	>400	80	178
30	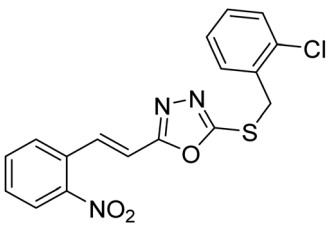	101	152	178
31	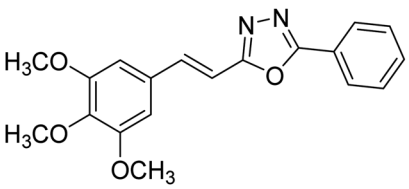	24.89	—	179
32	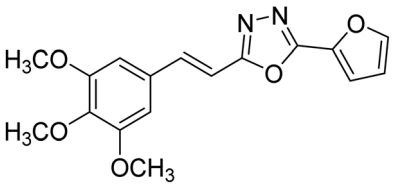	13.72	—	179
33	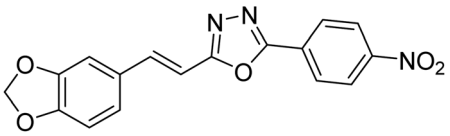	37.65	—	179

Table 3 (*Contd.*)

Compound no.	Chemical structure	IC_{50} values (μM) AChE	BChE	References
34	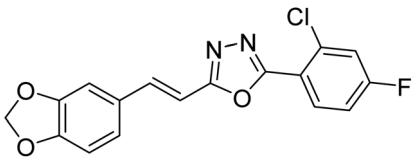	19.63	—	179
35	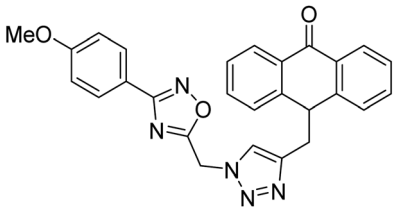	11.55	—	180
36	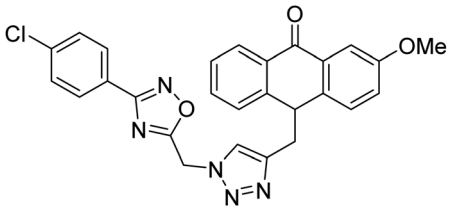	11.55–77.79	—	180
37	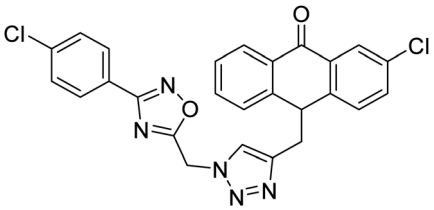	11.55–77.79	—	180
38	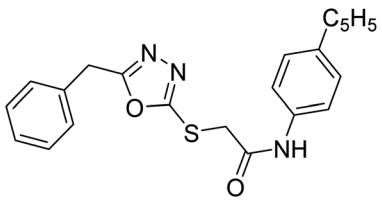	74.7	64.3	181
39	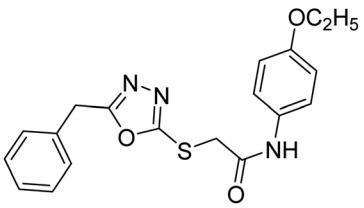	129.6	69.6	181
40	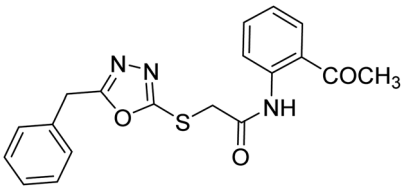	107.9	66.1	181

Table 3 (*Contd.*)

Compound no.	Chemical structure	IC_{50} values (μM) AChE	BChE	References
41	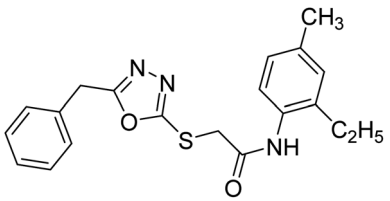	70.8	82.2	181
42	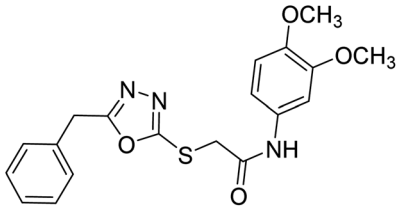	17.5	72.7	181
43	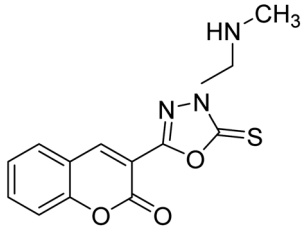	6.07	2.98	182
44	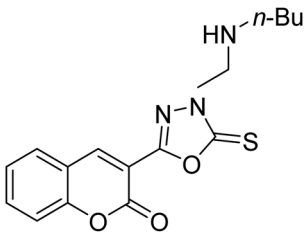	7.12	1.45	182
45	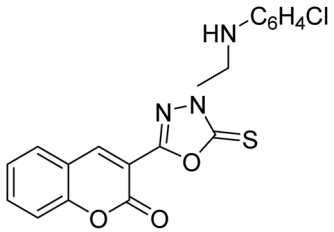	9.18	0.15	182
46	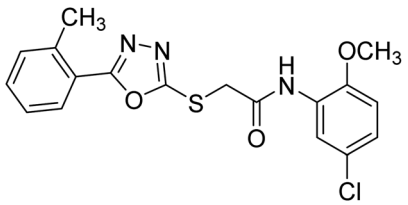	34.61	—	183
47	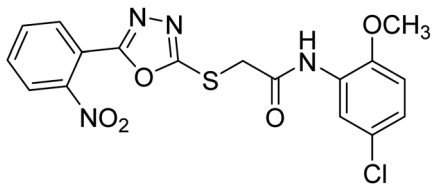	40.21	—	183

Table 3 (*Contd.*)

Compound no.	Chemical structure	IC_{50} values (μM) AChE	BChE	References
48	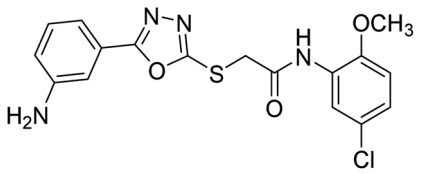	45.11	—	183
49	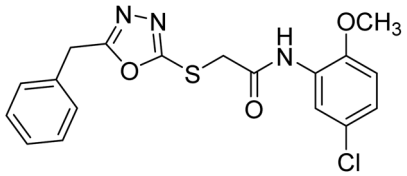	33.31	—	183
50	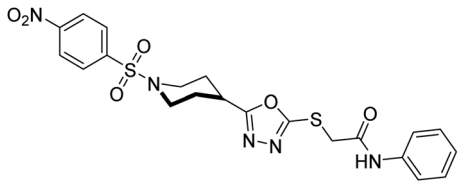	62.54	—	184
51	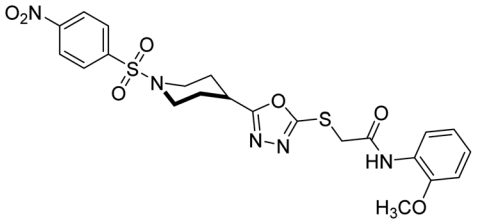	47.69	—	184
52	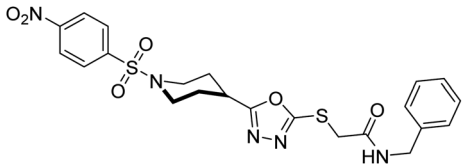	28.54	—	184
53	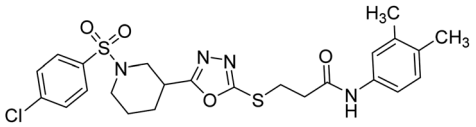	7.21	—	185
54	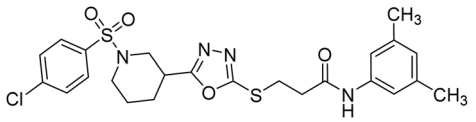	5.76	—	185
55	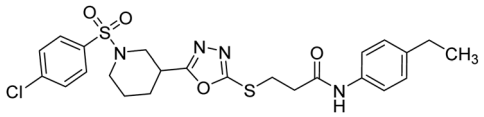	3.64	—	185
56	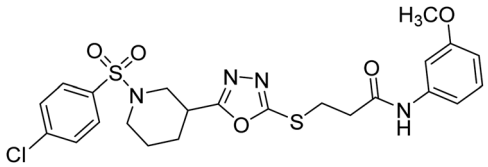	7.62	—	185

Table 3 (*Contd.*)

Compound no.	Chemical structure	IC_{50} values (μM) AChE	BChE	References
57	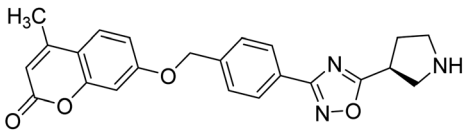	9.49	8.17	186
58	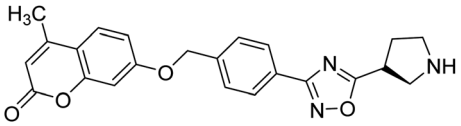	7.58	9.56	186
59	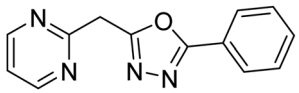	5.69	—	187
60	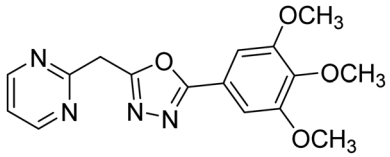	5.91	—	187
61	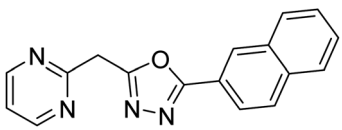	6.52	—	187
62	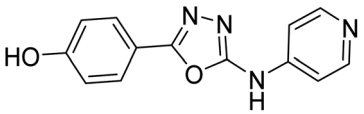	1.098	—	188
63	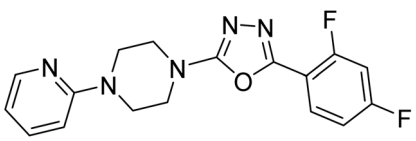	0.054	0.787	189
64	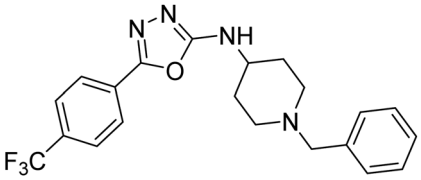	0.055	0.186	190
65	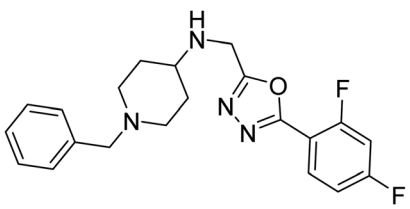	0.086	0.143	190
66	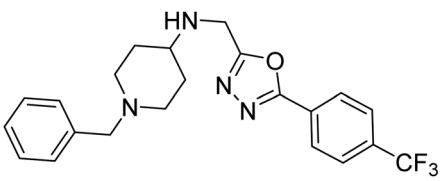	0.144	0.220	190

Table 3 (*Contd.*)

Compound no.	Chemical structure	IC_{50} values (μM) AChE	BChE	References
67	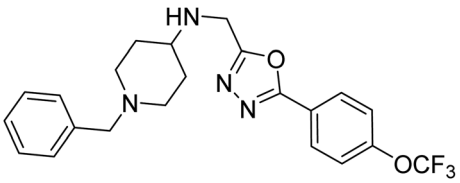	0.119	0.751	190
68	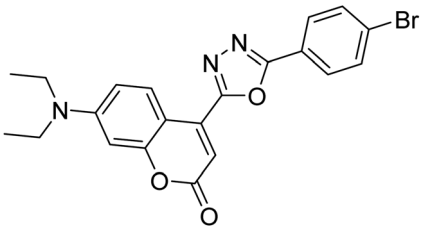	7.19	4.61	191
69	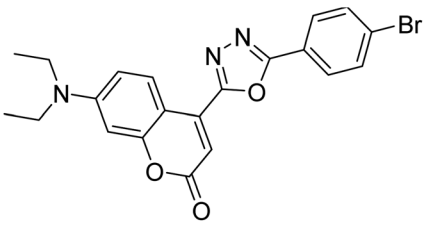	9.45	5.28	191
70	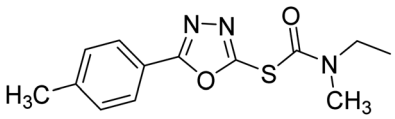	0.51–69.44	—	192
71	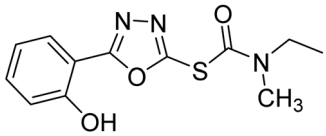	0.51–69.44	—	192
72	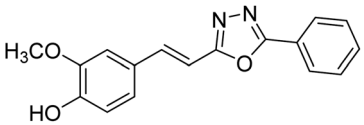	0.16	3.12	193
73	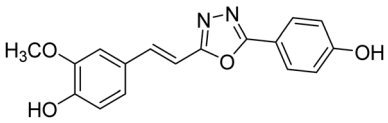	1.10	1.94	193
74	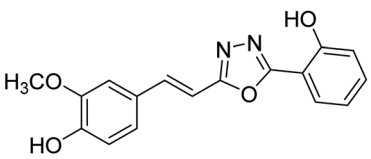	1.59	1.86	193
75	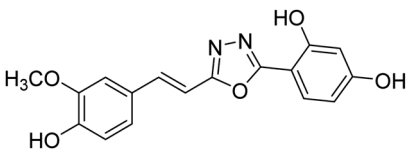	1.82	2.76	193

Table 3 (*Contd.*)

Compound no.	Chemical structure	IC_{50} values (μM) AChE	BChE	References
76	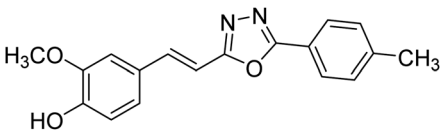	2.17	5.23	193
77	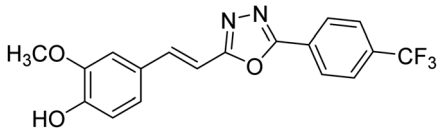	0.068	0.218	193
78	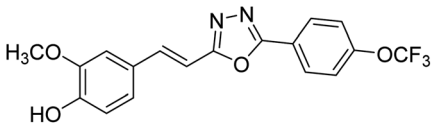	0.092	0.163	193
79	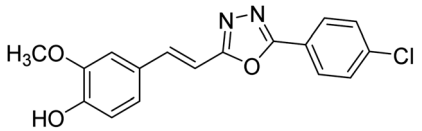	0.33	0.73	193
80	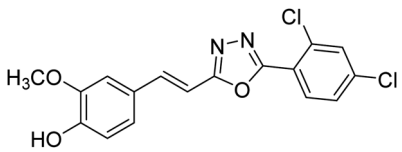	0.22	0.91	193
81	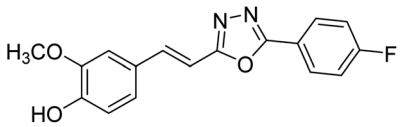	0.28	0.29	193
82	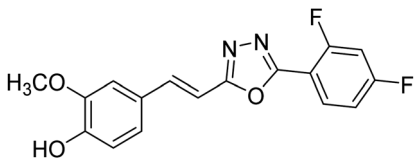	0.19	0.42	193
83	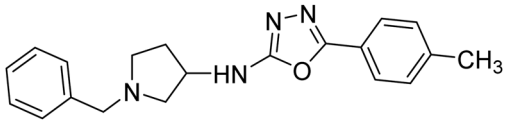	—	0.463	194
84	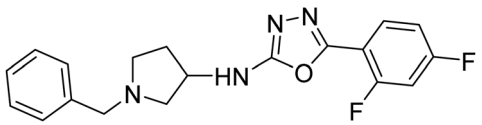	—	0.359	194

were potent AChE inhibitors relative to eserine (IC_{50} = 0.04 μM for AChE, 0.85 μM for BChE). Compounds **46**, **47** and **48** showed reasonably good inhibiting activity against AChE having an IC_{50} value of 34.61, 40.21 and 45.11 μM, respectively. Screening against the BChE enzyme showed that only one compound **49** exhibited excellent inhibitory potential having IC_{50} 33.31 μM. The current study emphasizes the research and development of new therapeutic approaches for AD[183] (Table 3).

Rehman *et al.* (2018) reported the green synthesis of *N*-(substituted)-2-(5-(1-(4-nitrophenylsulfonyl)piperidin-4-yl)-1,3,4-oxadiazol-2-ylthio) acetamide hybrids and their pharmacological applications to overcome enzymatic disorders. All the synthesized compounds were screened for AChE inhibition potential. Compounds **50**, **51**, and **52** were found to be very active AChE inhibitors having IC_{50} values 62.54, 47.69, and 28.54 and % inhibition values of 85.36, 88.72, and 89.75,

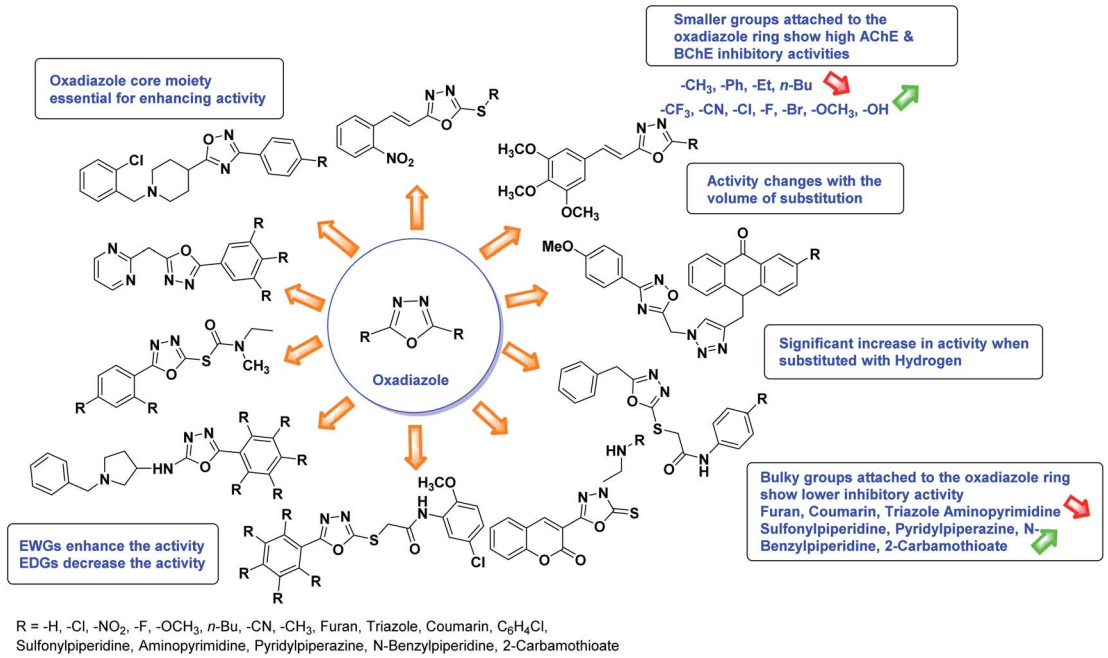

Fig. 13 SAR analysis of different oxadiazole derivatives as AChE and BChE inhibitors.

respectively. Eserine (IC_{50} = 0.04 μM) was the reference drug for AChE inhibition[184] (Table 3).

Rehman *et al.* (2018) synthesized N-substituted derivatives of 3-[(5-{1-[(4-chlorophenyl)sulfonyl]-3-piperidinyl}-1,3,4-oxadiazol-2-yl)sulfanyl]propenamide and assessed them as new drug contenders for AD. The synthesized products were tested for enzyme inhibition activity against the AChE enzyme. All the derivatives showed moderate to excellent inhibition activity against the ChE enzyme. Compounds bearing dimethyl phenyl groups, **53** and **54**, showed enhanced inhibitory ability against AChE with IC_{50} values of 7.21 μM and 5.76 μM, respectively, yet were less efficient than the reference drug eserine (IC_{50} value = 0.04 μM). The improved activity may be credited to the presence of 3,4-dimethyl phenyl and 3,5-dimethylphenyl groups due to the collective electron-donating positive inductive effect of two methyl groups. Compounds bearing mono-substituted phenyl groups like **55** and **56** exhibited excellent AChE inhibitory activity with IC_{50} values of 3.64 μM and 7.62 μM, respectively, compared to the reference drug[185] (Table 3).

Sun *et al.* (2018) synthesized a series of new chiral coumarin/1,2,4-oxadiazole hybrids and evaluated them for ChE inhibitory activity. Among them, enantiomers **57** and **58** showed potent BChE inhibitory activity with IC_{50} values of 8.17 and 9.56 μM, respectively, compared to tacrine (IC_{50} = 0.16 μM for AChE, 0.24 μM for BChE) and also exhibited good selectivity for BChE over AChE by 9.49- and 7.58-fold, respectively. In the current study, coumarin/1,2,4-oxadiazole hybrids **57** and **58** could be highlighted as a new chiral molecular template for developing multifunctional anti-AD drugs[186] (Table 3).

Shrivastava *et al.* (2019) synthesized new hybrids bearing a 2-aminopyrimidine (2-AP) moiety linked to substituted 1,3,4-oxadiazoles and evaluated them biologically. Among the synthesized derivatives, compound **59**, with a phenyl ring at the 5th position of the 1,3,4-oxadiazole core, exhibited considerable AChE inhibitory activity (IC_{50} = 5.69 μM). Compound **60**, bearing an EWG 3,4,5-trimethoxyphenyl group, showed significant AChE inhibitory potential (IC_{50} = 5.91 μM). Among all the evaluated derivatives, compound **61**, bearing a naphthyl ring, displayed the most significant AChE inhibitory activity (IC_{50} = 6.52 μM). The enhanced lipophilicity of compound **61** due to its naphthyl group may be the cause of its effective interactions with the active site residues of AChE. Thus, this study indicated that multitargeted *N*-(pyrimidin-2-yl)-1,3,4-oxadiazole derivatives are potential scaffolds for the treatment of dementia with compound **61** representing a promising lead for further research[187] (Table 3).

Shrivastava *et al.* (2019) synthesized novel hybrid bearing 4-aminopyridine tethered with substituted 1,3,4-oxadiazole nucleus and evaluated them for their potential AChE inhibitory property and antioxidant potential. Among all the compounds, **62** with 4-hydroxyl substituent promoted optimum AChE inhibition with the non-competitive type of enzyme inhibition (IC_{50} = 1.098 μM; K_i = 0.960 μM). These findings highlighted the potential of compound **62** as significant lead for the development of orally active therapeutics in the treatment of AD[188] (Table 3).

Shrivastava *et al.* (2019) designed and synthesized molecular hybrids of 2-pyridylpiperazine and 5-phenyl-1,3,4-oxadiazoles. Compound **63** comprising 2,4-difluoro substitution at the terminal phenyl ring emerged as the most promising AChE inhibitor lead (IC_{50} = 0.054 μM), BChE (IC_{50} = 0.787 μM). The enzyme kinetics study of **63** against AChE indicated a mixed type of inhibition (K_i = 0.030 μM). Compound **63** may be deemed as a notable lead with multifunctional actions against AD[189] (Table 3).

Shrivastava *et al.* (2019) synthesized multitargeted hybrids of substituted 5-phenyl-1,3,4-oxadiazoles and *N*-benzylpiperidine and assessed them against AD. The analyzed compounds showed moderate to excellent enzyme inhibition against hAChE and hBChE. Among them, **64** (IC_{50} = 0.055 μM for hAChE; 0.186 μM for hBChE), **65** (IC_{50} = 0.086 μM for hAChE; 0.143 μM for hBChE), **66** (IC_{50} = 0.144 μM for hAChE; 0.220 μM for hBChE) and **67** (IC_{50} = 0.119 μM for hAChE; 0.751 μM for hBChE) displayed balanced and noteworthy inhibition of hAChE and hBChE in nanomolar concentration range compared to donepezil (IC_{50} = 0.046 μM for hAChE; 1.94 μM for hBChE) and rivastigmine (IC_{50} = 2.58 μM for hAChE; 1.07 μM for hBChE). The results of *in vitro* assays corroborated their results, indicating that an increase in the chain length and suitable placement of the 1,3,4-oxadiazole between the *N*-benzylpiperidine core and terminal phenyl group would significantly improve the inhibitory potential against target enzymes. In conclusion, all these results emphasized **64** as a potential candidate for the treatment of AD[190] (Table 3).

Chen *et al.* (2020) synthesized 7-diethylaminocoumarin-based-1,3,4-oxadiazole analogs *via* I_2-induced oxidative cyclization. The *in vitro* outcome of these compound's activities inhibiting AChE showed that **68** and **69** had moderate inhibitory abilities with 69.19% and 65.06%, respectively. The preliminary SAR showed that the introduction of halogen atom on the *p*-position of the aryl ring of oxadiazole derivatives could lead to a promising AChE inhibitor. Molecular docking study suggested that **69** possessed an optimal docking pose with interactions inside AChE[191] (Table 3).

Safavi *et al.* (2020) synthesized a new series of 5-aryl-1,3,4-oxadiazole-2-carbamothioate compounds using structure-based drug discovery approaches. The potential of the synthesized compounds was evaluated against AChE and BChE to determine their IC_{50} values. The results of biological experiments demonstrated that most synthetic compounds exhibit moderate to excellent selective activity against BChE (0.51–69.44 μM). Docking studies showed the range of binding affinity for the best poses of individual conformers for any compound was between −7.81 **70** and −6.75 **71** kcal mol^{-1}. Recent essay data survey indicates that BChE plays a significant interest role in AD, especially at the advance stage of the disease, therefore these selective BChE inhibitors can be favorable drug candidates in the future[192] (Table 3).

Shrivastava *et al.* (2020) synthesized a series of molecular hybrids with ferulic acid and 1,3,4-oxadiazole framework for the treatment of AD and screened them for multifunctional inhibitory potential against AChE and BChE. Compound **77** was the most potent inhibitor of AChE (IC_{50} = 0.068 μM). It also showed equipotent inhibition of BChE with IC_{50} value of 0.218 μM. Compound **78** possessed the most significant inhibition of BChE with IC_{50} value 0.163 μM. Among all the tested compounds, analogs with 4-CF_3 and 4-OCF_3 substitution exhibited excellent AChE inhibitory profile **77**, IC_{50} = 0.068 μM; **78**, IC_{50} = 0.092 μM. Several findings suggested that inhibition of BChE is also a vital therapeutic strategy in the treatment of AD. The dual inhibition of AChE and BChE could be beneficial in halting the disease progression rather than providing symptomatic relief only. Therefore, the BChE inhibitory potential of all the target compounds was also evaluated. Several of the prepared compounds **72** (IC_{50} = 3.12 μM for BChE), **73** (IC_{50} = 1.94 μM for BChE), **74** (IC_{50} = 1.86 μM for BChE), **75** (IC_{50} = 2.76 μM for BChE) and **76** (IC_{50} = 5.23 μM for BChE) demonstrated micromolar inhibitory ability against BChE. The remaining compounds **79** (IC_{50} = 0.33 μM for AChE; 0.73 μM for BChE), **80** (IC_{50} = 0.22 μM for AChE; 0.91 μM for BChE), **81** (IC_{50} = 0.28 μM for AChE; 0.29 μM for BChE), and **82** (IC_{50} = 0.19 μM for AChE; 0.42 μM for BChE) prompted outstanding dual inhibitory ability against both cholinesterases compared to donepezil (IC_{50} = 0.046 μM for AChE; 1.94 μM for BChE) and rivastigmine (IC_{50} = 2.58 μM for AChE; 1.07 μM for BChE)[193] (Table 3).

Shrivastava *et al.* (2021) synthesized a hybrid of substituted 5-phenyl-1,3,4-oxadiazole and *N*-benzylpyrrolidine and the derivatives were at first screened for ChE inhibition ability. The results indicated that the highest BChE inhibition was attained with analogs (IC_{50}, **83:** 0.463 μM **84:** 0.359 μM) substituted by 4-CH_3, and 2,4-difluoro on the phenyl ring, respectively. Compound **84** also exhibited outstanding oral absorption attributes in a primary pharmacokinetic study[194] (Table 3).

SAR studies of different oxadiazoles demonstrate that various derivatives are active against AChE and BChE enzymes (Fig. 13). All the structural features contribute to the inhibitory activity in different capacities where any slight variation in the activity of these analogs is due to variability in the nature and positions of substituents on aryl rings. The smaller groups attached to the oxadiazole ring seem to promote higher AChE and BChE inhibitory abilities compared to bulky groups. The ChE activity changes with the size of substitution. Electron withdrawing groups (–F, –Cl, –Br, –CN, –OH, *etc.*) increase the activity and electron-donating groups (–CH_3, –OCH_3, Et, *n*-Bu *etc.*) decrease it. All the presented analogues so far have shown good to excellent ChE inhibitory abilities with a low risk of harmful side effects. Moreover, these species are economical and easy to synthesize in the laboratory, making them attractive for commercial development and marketing as drugs against cholinesterase.

Ucar *et al.* (2005) prepared some 1-*N*-substituted thiocarbamoyl-3-phenyl-5-thienyl-2 pyrazoline analogs and among the synthesized analogs, compound **85** selectively inhibited hAChE (IC_{50} = 0.09 μM) and is much more potent than rivastigmine (IC_{50} = 12.23 μM). Compound **85** carrying the *p*-OCH_3 group on the phenyl ring inhibited the hAChE non-competitively and reversibly. The obtained results suggested that ChE inhibitors have promising features in the therapy of AD's[195] (Table 4).

Jayaprakash *et al.* (2010) synthesized some 3,5-diaryl-2-pyrazoline-1-carbothioamides and assessed their AChE inhibitory profile. Compound **86** showed outstanding AChE inhibitory activity (IC_{50} = 19.45 μM) and **87** displayed better BChE inhibitory ability (IC_{50} = 6.31 μM).

All analogs tested were potent inhibitors of ChE[196] (Table 4).

Altintop *et al.* (2013) synthesized new pyrazoline derivatives and each analog was evaluated for its ability to inhibit AChE and BChE using a modification of Ellman's spectrophotometric

Table 4 Chemical structures of pyrazoline derivatives **85–113** and their IC_{50} values against cholinesterase enzymes

Compound no.	Chemical structure	IC_{50} values (μM) AChE	BChE	References
85	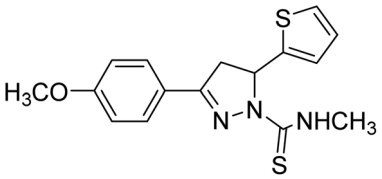	0.09	—	195
86	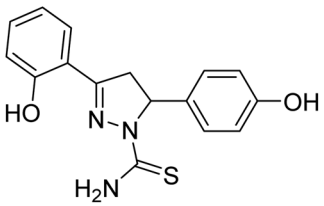	19.45	—	196
87	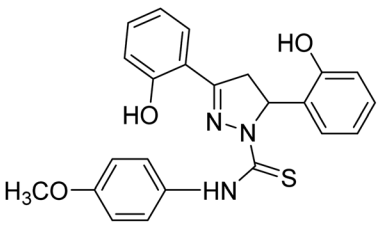	—	6.31	196
88	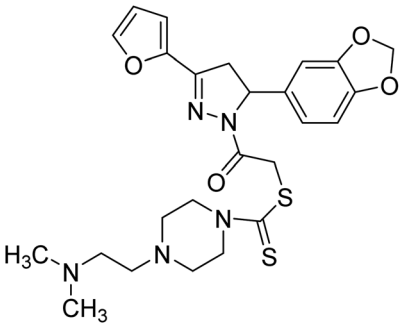	0.72 μg mL^{-1}	7.46 μg mL^{-1}	197
89	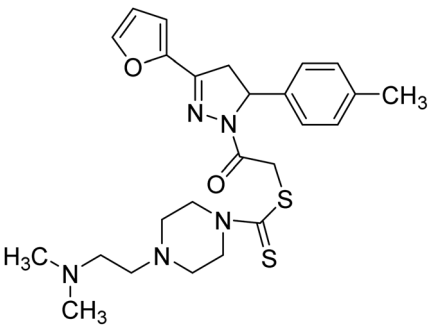	7.2 μg mL^{-1}	>80 μg mL^{-1}	197
90	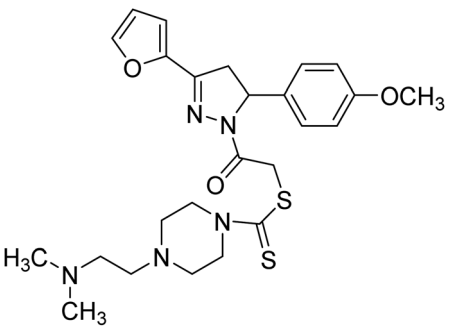	3.2 μg mL^{-1}	26.9 μg mL^{-1}	197

Table 4 (*Contd.*)

Compound no.	Chemical structure	IC_{50} values (μM) AChE	BChE	References
91	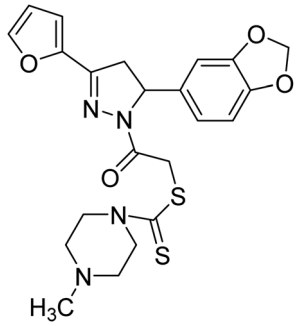	48 μg mL^{-1}	—	197
92	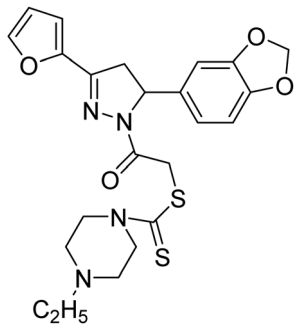	50.68 μg mL^{-1}	—	197
93	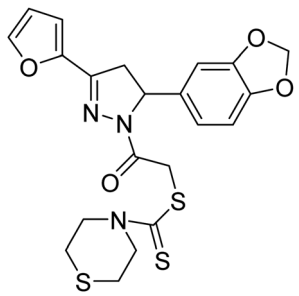	62 μg mL^{-1}	—	197
94	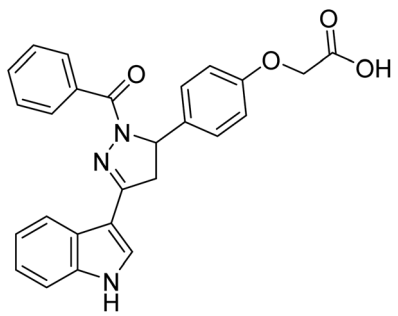	0.68	—	198
95	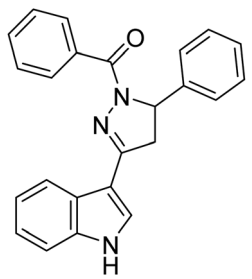	0.74	—	198

Table 4 (*Contd.*)

Compound no.	Chemical structure	IC_{50} values (μM) AChE	BChE	References
96	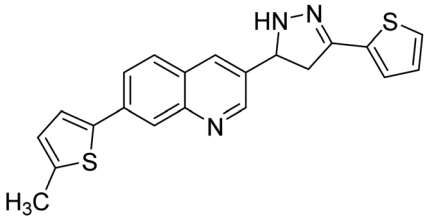	0.13	—	199
97	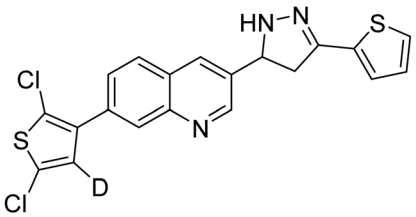	0.15	—	199
98	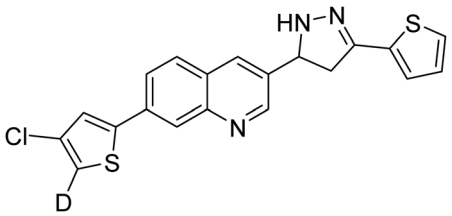	0.20	—	199
99	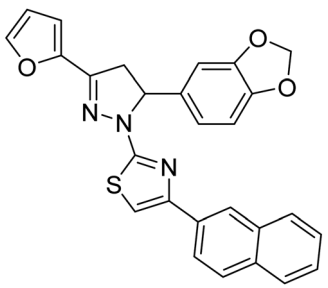	38.5	—	200
100	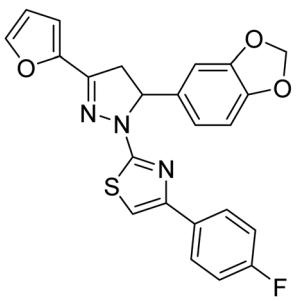	—	43.02	200
101	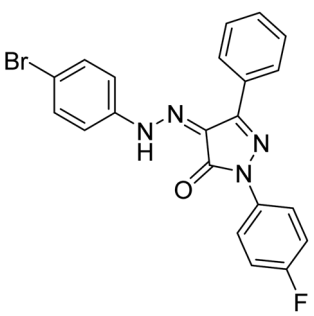	48.15	—	201

Table 4 (*Contd.*)

Compound no.	Chemical structure	IC_{50} values (μM) AChE	BChE	References
102	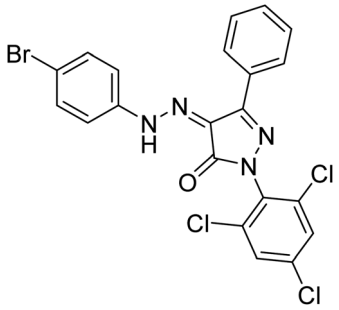	52.65	—	201
103	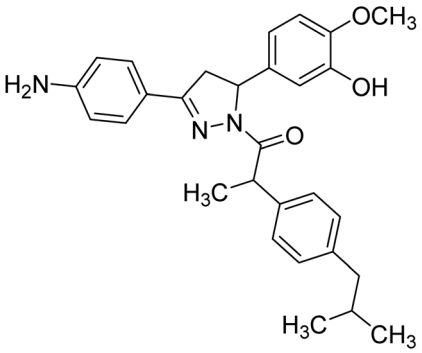	123 nM	—	202
104	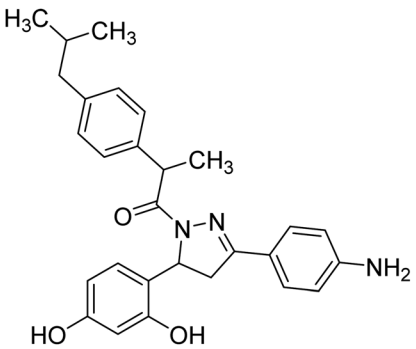	201 nM	—	202
105	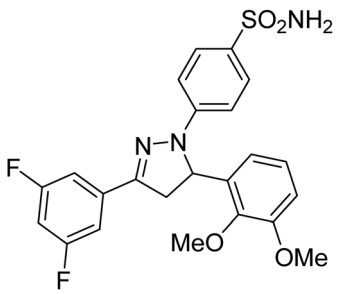	9.77 nM	—	203
106	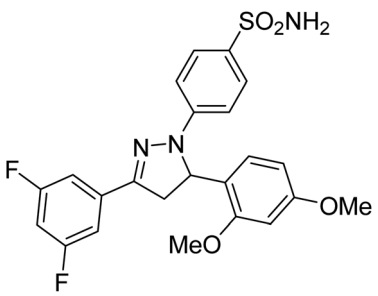	3.43 nM	—	203

Table 4 (*Contd.*)

Compound no.	Chemical structure	IC_{50} values (μM) AChE	BChE	References
107	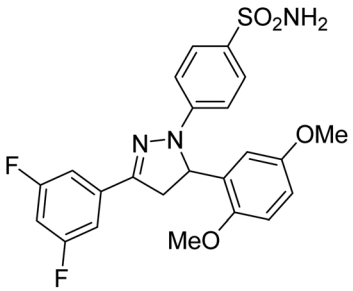	6.86 nM	—	203
108	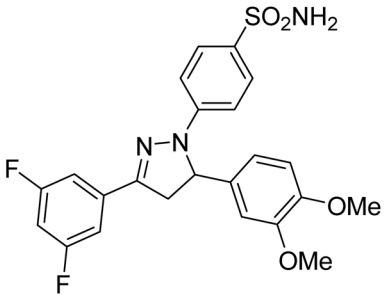	8.32 nM	—	203
109	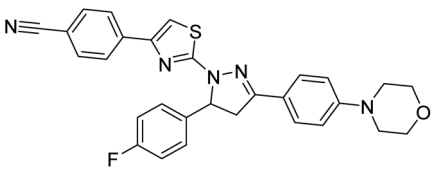	14.37 nM	—	204
110	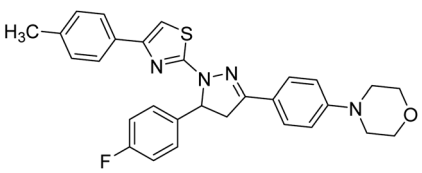	26.64 nM	—	204
111	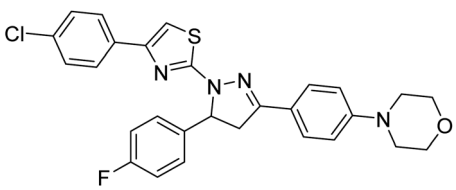	16.18 nM	—	204
112	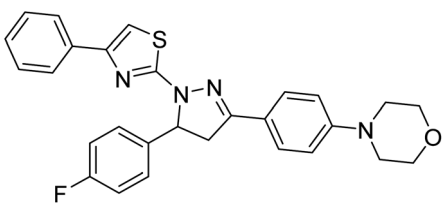	17.96 nM	—	204
113	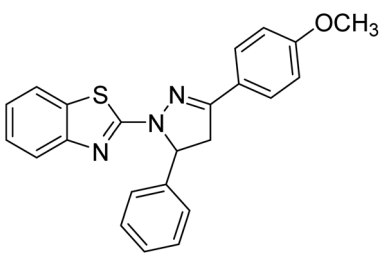	1.3	—	205

method. The most potent AChE inhibitor was found to be compound **88** followed by compounds **89** and **90**. Effective compounds against AChE are characterized by the presence of the 2-dimethylaminoethyl moiety, which resembles the trimethylammonium group and the ethylene bridge of acetylcholine. Among all compounds, compound **88** bearing 2-dimethylaminoethyl and 3,4-methylenedioxyphenyl moieties were also found to be highly effective inhibitor of BChE. Compound **88** can be regarded as the most promising anticholinesterase agent due to its inhibitory effect on AChE with an IC_{50} value of 0.72 μg mL^{-1} when compared with eserine (IC_{50} = 0.0013 μg mL^{-1}). Compounds **89** and **90** exhibited AChE inhibitory activity with IC_{50} values of 7.2 μg mL^{-1} and 2.32 μg mL^{-1}, respectively. Compounds **91**, **92** and **93** exhibited AChE inhibitory activity with IC_{50} values of 48, 50.68 and 62 μg mL^{-1}, respectively. Compound **88** also exhibited the highest inhibitory effect on BChE with an IC_{50} value of 7.46 μg mL^{-1} when compared with eserine (IC_{50} = 0.012 μg mL^{-1}). Compound **90** exhibited BChE inhibitory activity with an IC_{50} value of 26.93 μg mL^{-1}. Although compound **89** carries the 2-dimethylaminoethyl group, it was a weak inhibitor of BChE (IC_{50} > 80 μg mL^{-1})[197] (Table 4).

Chigurupati *et al.* (2016) synthesized novel indolopyrazoline derivatives and assessed them as prospective anti-Alzheimer compounds through AChE inhibition study (*in vitro*). Specifically, **94** shows AChE inhibition (IC_{50} = 0.68 μM), while **95** ranked second best compound with AChE inhibition (IC_{50} = 0.74 μM). This study described the first use of indolopyrazoline compounds as potential anti-Alzheimer drugs[198] (Table 4).

Iqbal *et al.* (2017) synthesized novel pyrazoline-based analogs and appraised their ChE inhibitory activity. Out of the synthesized compounds, compounds **96**, **97** and **98** were the best inhibitors against AChE with an IC_{50} of 0.13, 0.15 and 0.20 μM, respectively. Compound **96** exhibited 173-fold higher inhibitory ability compared to neostigmine (IC_{50} = 22.2 μM). All the 2-pyrazoline analogs showed comparatively less (<50%) inhibitory capacity against BChE[199] (Table 4).

Altintop *et al.* (2018) synthesized new thiazolyl-pyrazoline derivatives. The compounds were investigated for their inhibitory effects on AChE and BChE using a modification of Ellman's spectrophotometric method. As a part of this study, the compliance of the compounds to Lipinski's RO5 was evaluated. Naphthalene-substituted compound **99** was the most potent AChE inhibitor (IC_{50} = 38.5 μg mL^{-1}), whereas fluoro-substituted compound **100** was the most effective BChE inhibitor (IC_{50} = 43.02 μg mL^{-1}) in this series relative to the standard galantamine (IC_{50} = 97.17 μg mL^{-1} for AChE; 80.98 μg mL^{-1} for BChE)[200] (Table 4).

Turkan *et al.* (2019) synthesized novel pyrazoline analogs and assessed their AChE inhibitory activity. These pyrazoline analogs were efficient inhibitors of the AChE, with K_i values ranging between 48.2–84.1 μM for AChE. In this study, all the evaluated pyrazoline derivatives showed potent inhibition against the AChE enzyme, but compounds **101** and **102** showed outstanding inhibition profiles against AChE with K_i values of 48.15 and 52.65 μM, respectively. Tacrine molecule was employed as a control compound for AChE inhibition[201] (Table 4).

Mumtaz *et al.* (2019) synthesized a series of 1-(3-(4-aminophenyl)-5-phenyl-4,5-dihydro-1*H*-pyrazol-1-yl)-2-(4-isobutylphenyl)propan-1-one derivatives and evaluated their biological potential as potent ChE inhibitors. The top potent and most selective inhibitor for the AChE was analog **103** which had an inhibitory concentration of 123 nM. Compound **104** was discovered as a selective inhibitor of BChE with an IC_{50} value of 201 nM. The results showed that the attachment of different substituents at the *para*, *ortho*, and *meta* positions at the main moiety has a significant impact and contribution towards the inhibitory profile of ChE[202] (Table 4).

Gul *et al.* (2020) synthesized a novel series of 4-(3-(difluorophenyl)-5-(dimethoxyphenyl)-4,5-dihydropyrazol-1-yl) benzenesulfonamides since sulfonamide and pyrazoline pharmacophores have garnered attention in drug design due to their wide range of bioactivities including AChE, hCA-I and hCA-II inhibitory potencies. *In vitro* enzyme assays showed that the novel compounds had a significant inhibitory profile against hCA I, hCA II and AChE enzymes at the nanomolar levels. When AChE inhibitory activity of the 3,5-difluorophenyl derivatives as assessed, IC_{50} values were calculated in the range of 8.66–15.07 nM. Compounds **105–108** having IC_{50} values 9.77, 3.43, 6.86 and 8.32 nM, respectively can be considered as promising AChE inhibitors for the development of novel bioactive molecules[203] (Table 4).

Sever *et al.* (2020) prepared thiazolyl-pyrazolines analogs and evaluated their AChE inhibitory potential. *In vitro* studies demonstrated that all the compounds notably inhibited AChE even more than the reference drug tacrine. Compound **109** (IC_{50} = 14.37 nM for AChE) with the cyanophenyl substitution inhibited AChE with the lowest K_i value, whereas compound **110** (IC_{50} = 26.64 nM for AChE) with methyl substitution was determined as the most selective hCA I inhibitor. Compound **111** (IC_{50} = 16.18 nM for AChE) with the chloro substitution exhibited the most potent and selective inhibition towards AChE. In such a manner, compound **112** (IC_{50} = 17.96 μM) without any substitution was found as the best and most selective AChE enzyme inhibitor in this series. All compounds in the series stand out as excellent multi-targeted inhibitors for further investigations in AD treatment[204] (Table 4).

Gül *et al.* (2020) assessed a novel series of pyrazoline compounds as potent AChE inhibitors. Compound **113** (IC_{50} = 1.3 μM; K_i = 0.13 μM) possessed the highest AChE inhibitory effect in the series, proving 2-fold more potent than the standard tacrine (IC_{50} = 0.84 μM; K_i = 0.26 μM)[205] (Table 4).

The SAR analysis of pyrazoline derivatives summarized Fig. 14 has indicated that various derivatives are active against cholinesterase enzymes. All the structural features perform critical function in the inhibition where fine tuning of the activity of these analogs is possible with varying the nature and positions of substituents on aryl rings. The smaller groups attached to the pyrazoline ring foster higher AChE and BChE inhibitory abilities compared to bulky ones. The ChE activity changes with the size of substitution suggesting that steric and electronic factors are important in fine tuning the structure. In this context, electron withdrawing groups (–F, –Cl, –Br, *etc.*) have been found to increase the activity and electron-donating

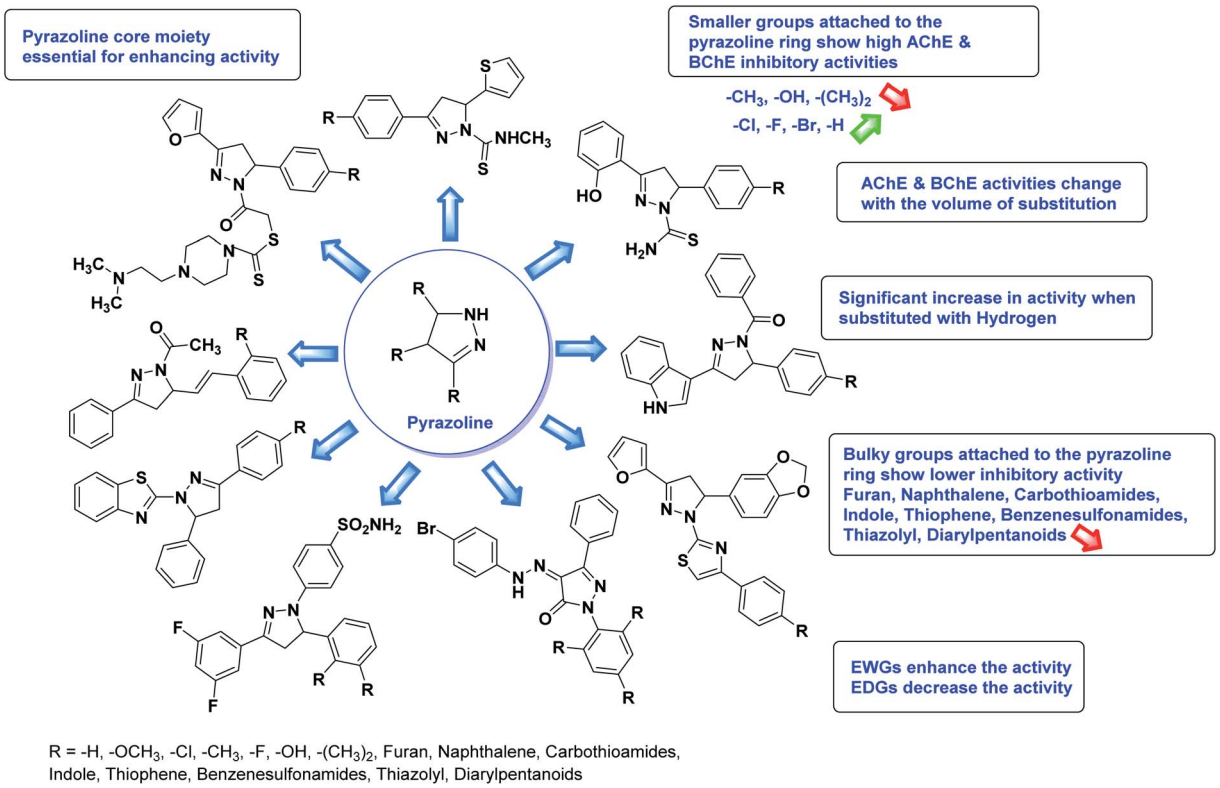

Fig. 14 SAR analysis of different pyrazoline derivatives as AChE and BChE inhibitors.

groups (–CH_3, –$(CH_3)_2$, *etc.*) reduce it. All the presented analogues thus far have shown moderate to good ChE inhibitory abilities with a minimal risk harmful side effect. Moreover, these analogs are cost-effective and easy to prepare in the laboratory, making them attractive for commercial development and marketing as drugs against cholinesterase.

Alinezhad *et al.* (2015) synthesized various 1,2,3-triazole linked acridone analogs and evaluated for their proficiency to inhibit AChE using rivastigmine as a drug. Most compounds ($IC_{50} \geq 100$ μM mL^{-1}) were inactive, although compound **115** was very potent ($IC_{50} = 7.31$ μM mL^{-1}) in comparison to rivastigmine ($IC_{50} = 11.07$ μM mL^{-1}). The SAR study showed that the substituents' electronic properties on acridone and 1,2,3-triazole rings impacts the anti-AChE activity since no activity was observed for compound **114** ($IC_{50} \geq 100$ μM mL^{-1}). Notably, the existence of 4-substituted chlorine on the benzyl group **115** plays a substantial role in the anti-AChE activity. Compound **115** was the best contender against AChE, highlighting the usefulness of methoxy and chlorine groups to generate effective interactions with the active site of the enzyme and is in agreement with factors outlined earlier that play a crucial role in inhibitory activity[206] (Table 5).

Munawar *et al.* (2015) synthesized a variety of escitalopram triazoles and assessed them for their AChE and BChE inhibitory abilities. Most of these revealed moderate activities, and four of these analogs showed potent BChE inhibitory ability ($IC_{50} =$ 4.52–9.52 μM) in comparison eserine ($IC_{50} = 0.85$ μM). The SAR showed that the escitalopram function was essential for the activity; 2-F **116** > 4-F **117** with optimum inhibition by ligands **116** and **117** that scored the lowest $IC_{50} = 4.52$ μM and 5.31 μM, respectively. The effect of substituent nature on the inhibition has been noted in the order of 2-F > 4-F > 4-OH-3-OCH_3 > 2-I > 3-Cl > 3-F. Consequently, the escitalopram triazoles have shown decent inhibitory activity against BChE and can be utilized as an essential entry point for further analysis of the possible use of these compounds in the process of drug discovery against neurodegenerative diseases[207] (Table 5).

Carvalho *et al.* (2016) reported the synthesis of 1,2,3-triazole-quinoline derivatives for use as selective dual binding site AChE inhibitors. All hybrids showed 0–55.7% growth inhibitory of hAChE at 100 μM level, but not as active as tacrine (92.8% growth inhibitory of hAChE at 100 μM) and donepezil (83.9% growth inhibitory of hAChE at 100 μM). Among these, products **118** (48.1% at 100 μM) and **119** (55.7% at 100 μM) demonstrated good hAChE inhibitory ability with IC_{50} values ranging between 114 and 104 μM, respectively. In contrast, compounds **118** (0.2% at 100 μM) and **119** (0% at 100 μM) proved inactive for hBChE enzyme[208] (Table 5).

Park *et al.* (2016) synthesized 1,2,3-triazole linked decursinol hybrids **120** and tested them for their inhibitory ability against ChE and BChE for AD. Compound **120** ($IC_{50} = 5.89$ μM against BChE) showed more efficient inhibitory ability against BChE than galantamine ($IC_{50} = 9.4$ μM). In addition, compound **120** exhibited no inhibitory capacity against AChE (IC_{50} value > 350 μM). Triazole-linked decursinol derivative **120** can be deemed as

Table 5 Chemical structures of triazole derivatives **114–148** and their IC_{50} values against cholinesterase enzymes

Compound no.	Chemical structure	IC_{50} values (μM) AChE	BChE	References
114	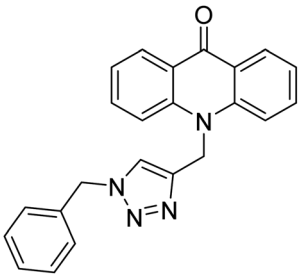	>100 μM mL^{-1}	—	206
115	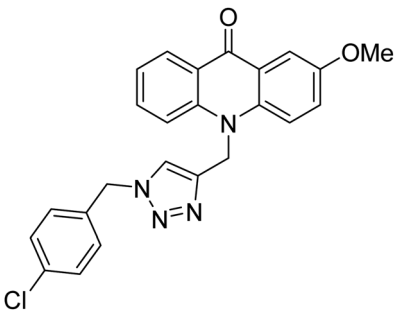	7.31 μM mL^{-1}	—	206
116	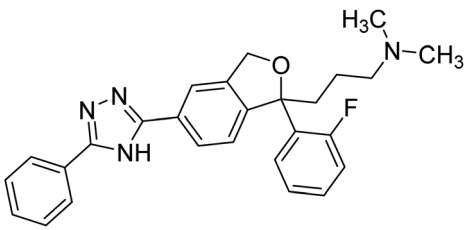	4.52	—	207
117	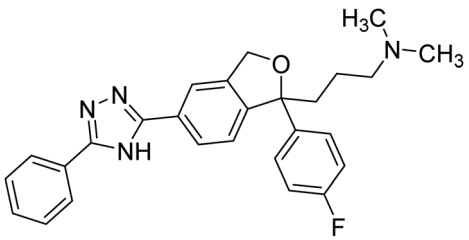	5.31	—	207
118	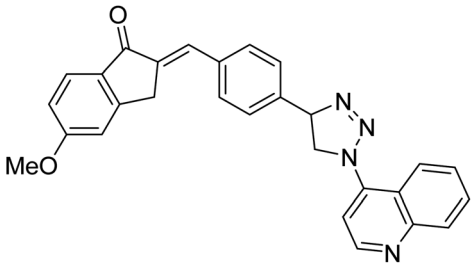	114	—	208
119	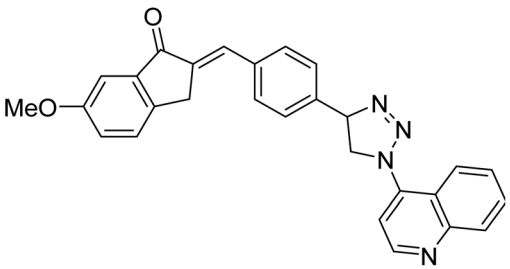	104	—	208

Table 5 (*Contd.*)

Compound no.	Chemical structure	IC_{50} values (μM) AChE	BChE	References
120	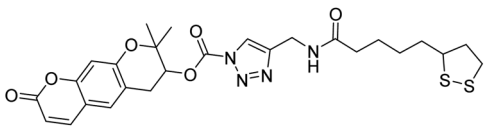	>350	5.98	209
121	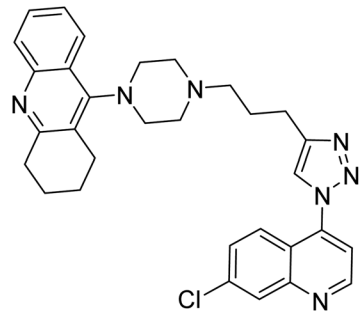	4.89	3.61	210
122	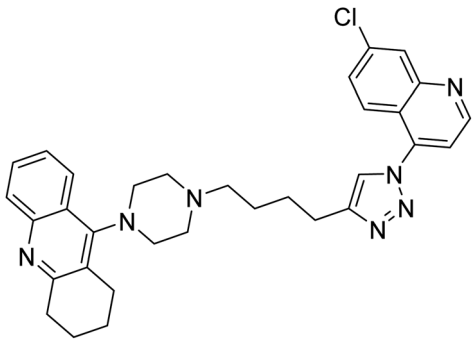	10	6.06	210
123	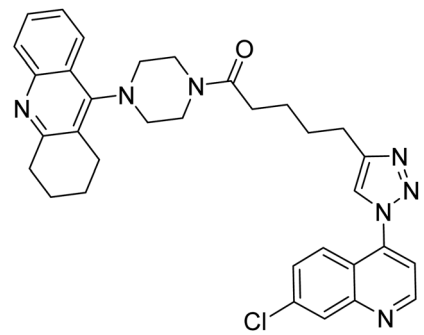	11.07	61.13	210
124	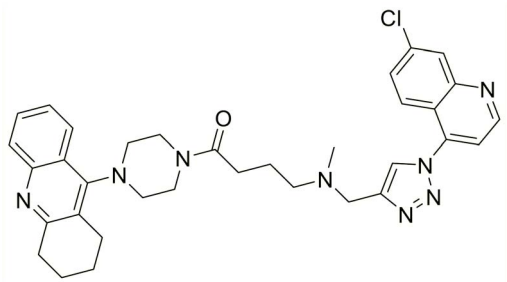	19.59	66.68	210

Table 5 (*Contd.*)

Compound no.	Chemical structure	IC_{50} values (μM) AChE	BChE	References
125	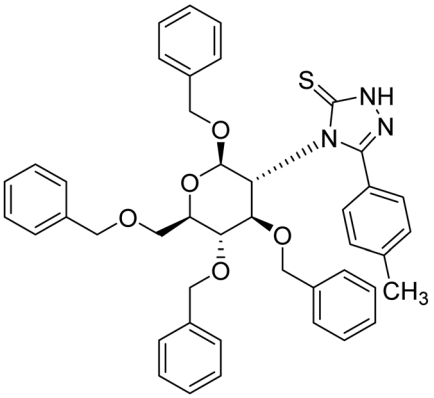	1.46 μg mL^{-1}	—	211
126	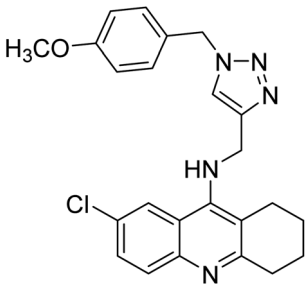	0.521	—	212
127	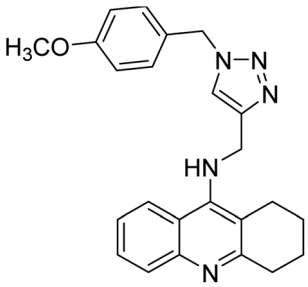	0.055	—	212
128	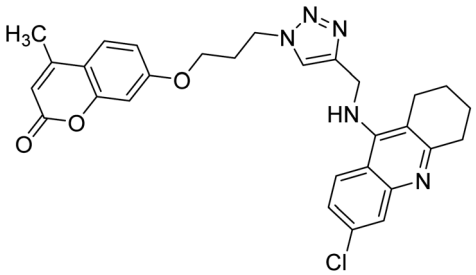	27	—	213
129	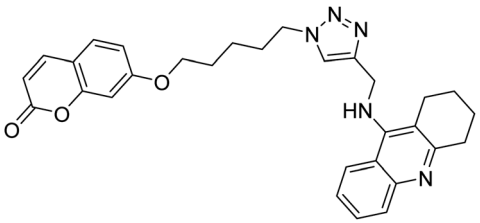	6	—	213

Table 5 (*Contd.*)

Compound no.	Chemical structure	IC_{50} values (μM) AChE	BChE	References
130	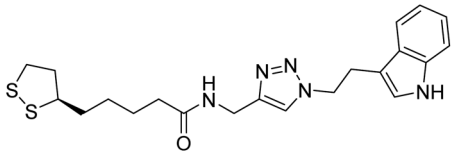	—	0.42	214
131	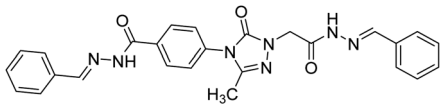	0.0876	—	215
132	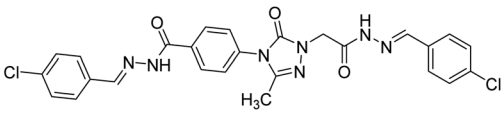	0.0574	—	215
133	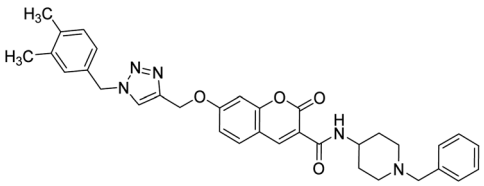	—	1.80	216
134	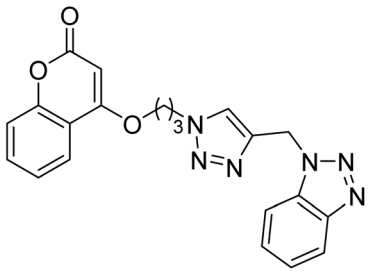	0.059	—	217
135	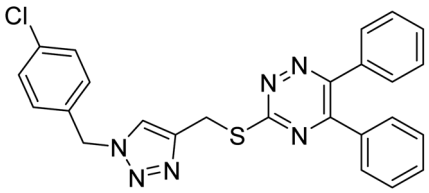	6.4	—	218
136	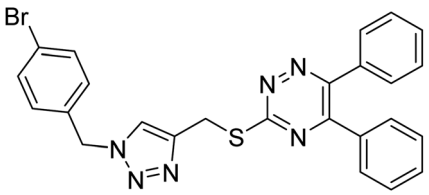	7.9	—	218
137	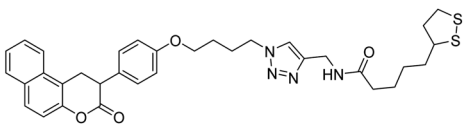	7.3	68.6	219

Table 5 (*Contd.*)

Compound no.	Chemical structure	IC_{50} values (μM) AChE	BChE	References
138	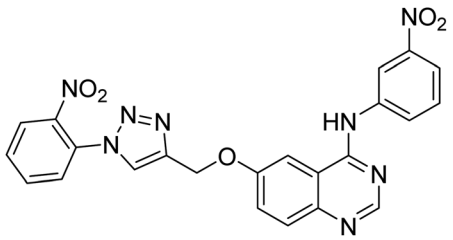	2.06	—	220
139	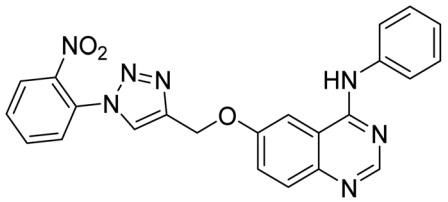	0.23	—	220
140	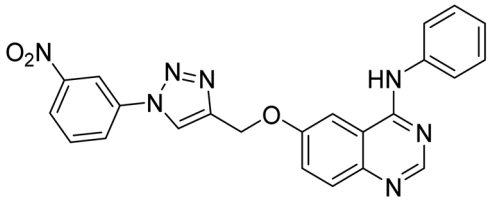	1.10	—	220
141	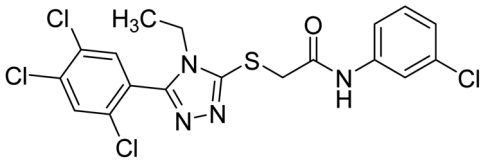	5.41	7.52	221
142	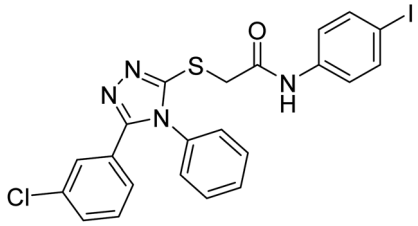	13.75	—	221
143	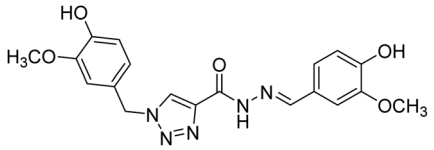	26.30	—	222
144	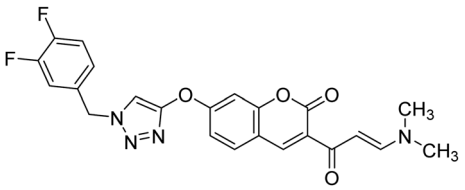	21.71	>100	223

Table 5 (*Contd.*)

Compound no.	Chemical structure	IC_{50} values (μM) AChE	BChE	References
145	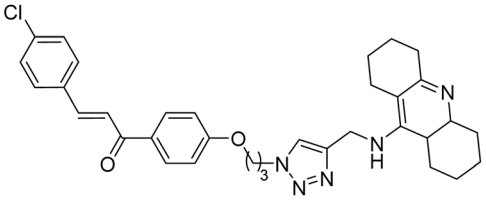	0.259	—	224
146	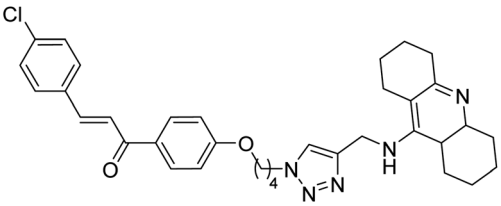	0.372	—	224
147	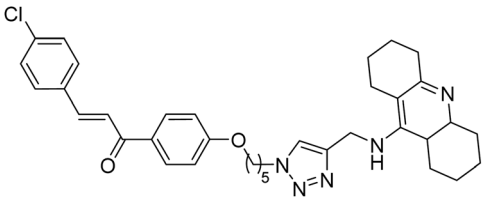	0.327	—	224
148	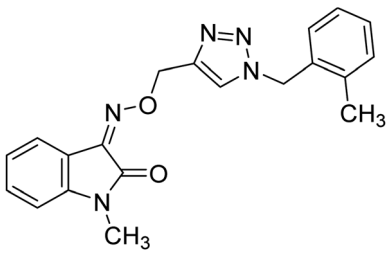	—	4.78	225

a new class inhibitor for BChE and can be employed to be a new drug contender to treat AD[209] (Table 5).

Liu *et al.* (2017) prepared tacrine-1,2,3-triazoles *via* a Cu(I)-catalyzed alkyne–azide 1,3-dipolar cycloaddition reaction. The compounds were assessed for their inhibition ability against AChE and BChE as prospective drug targets for AD. Among these, compound **121** displayed most potent and optimum inhibition against AChE and BChE with IC_{50} values of 4.89 μM and 3.61 μM, respectively. Besides, the inhibitory efficacy of **122**, **123**, and **124** produced IC_{50} values of 10, 11.07 and 19.59 μM against AChE, respectively. As for anti-BChE activity, IC_{50} value of **122** was 6.06 μM, followed by **123** (IC_{50} = 61.13 μM) and **124** (IC_{50} = 66.68 μM) were obtained. However, all compounds proved weaker inhibitors compared to tacrine. Further SARs and molecular modeling studies may offer invaluable insights to design and optimize better tacrine-triazole analogs with potential therapeutic uses for AD[210] (Table 5).

Liu *et al.* (2017) synthesized new C2-glycosyl triazoles and assessed them as ChE inhibitors. The AChE inhibitory abilities of the derivatives were tested using Ellman's method. Those that displayed over 85% inhibition were consequently evaluated for their IC_{50}. Compound **1** exhibited the best AChE inhibition ability with IC_{50} of 1.46 μg mL^{-1} (ref. 211) (Table 5).

Sharifzadeh *et al.* (2017) designed tacrine-1,2,3-triazole hybrids as dual ChE inhibitors. The majority of the synthesized compounds demonstrated good *in vitro* inhibitory abilities against both AChE and BChE. Amongst them, compound **126** proved the best potent anti-AChE derivative (IC_{50} = 0.521 μM) and compound **127** demonstrated the best anti-BChE activity (IC_{50} = 0.055 μM). Molecular modeling and kinetic investigations indicated that **148** and **149** bind concurrently to the peripheral anionic site (PAS) and catalytic sites (CS) of the AChE and BChE[212] (Table 5).

Akbarzadeh *et al.* (2019) synthesized tacrine-coumarin hybrids linked to 1,2,3-triazole and verified them as potent dual binding ChEIs for the treatment of AD. Amongst them, **128** was the best potent anti-AChE species (IC_{50} = 27 μM) and **129** exhibited the optimum anti-BChE activity (IC_{50} = 6 μM) exceeding that of tacrine (IC_{50} = 0.048 μM for AChE; 0.01 μM for

BChE) and donepezil (IC_{50} = 0.039 μM for AChE; 8.416 μM for BChE) as the reference drugs[213] (Table 5).

Park *et al.* (2019) synthesized tryptamine-triazole hybrid compounds *via* the click reaction. Their ChE inhibitory ability was assessed. Amongst the synthesized analogs, compound **130** displayed the top potent inhibitory ability (IC_{50} = 0.42 μM) for horse BChE and 1.96 μM for human BChE. From the molecular modeling investigation, derivative **130** was bound to the catalytic anionic site, anionic subsite, peripheral anionic subsite, acyl-binding pocket, and oxyanion hole of BChE by forming a hairpin or U-shaped structure. The Lineweaver–Burk plot of **130** against BChE suggested a mixed type of inhibition which matches well with the molecular modeling study[214] (Table 5).

Ozil *et al.* (2019) reported 1,2,4-triazole containing Schiff's bases and screened them for AChE and BChE activities. All compounds (IC_{50} = 0.0465–0.0966 μM for AChE, and IC_{50} = 0.0486–0.1253 μM for BChE) showed noteworthy potency against the two enzymes compared to neostigmine (IC_{50} = 0.136 μM for AChE and 0.084 μM for BChE). The SAR study showed that the aryl position substituent of the phenyl has a superior influence on AChE and BChE abilities than other groups, and EWGs as well as EDGs at the aryl position decrease the activity. The fact that only the phenyl group containing derivative **131** displayed the strongest inhibitory capacity may indicate that its overall geometry fosters strongest interactions with the enzyme's active site. A chlorine-containing analog **132** (0.0574 μM) substituted in the *p*-position appears to have an inhibitory value of 1.23 times less than **131**. The results obtained in this study show that compounds can potentially be used to produce strong inhibitors that target AChE and BChE enzymes. These newly synthesized compounds can also be used as drug precursors or building blocks in the preparation of more effective drug molecules[215] (Table 5).

Saeedi *et al.* (2019) synthesized 1,2,3-triazole-chromenone carboxamides and assessed their cholinesterase inhibitory ability. Amongst them, **133** showed the best BChE inhibitory activity (IC_{50} = 1.80 μM), though, it was not active against BChE. Noteworthy, **133** was appraised for its BACE1 inhibitory ability and the calculated IC_{50} = 21.13 μM confirmed its inhibitory activity[216] (Table 5).

Singh *et al.* (2020) synthesized triazole tethered coumarin-benzotriazole hybrids based on donepezil framework multi-functional agents for the treatment of AD. Amongst the prepared compounds, 134 displayed the top potent AChE inhibition (IC_{50} = 0.059 μM) with mixed type inhibition scenario. Therefore, hybrid 134 may act as potential lead for further construction of selective AChE inhibitors as multifunctional anti-Alzheimer's agents[217] (Table 5).

Edraki *et al.* (2020) synthesized a series of 5,6-diphenyl triazine-thio methyl triazole hybrid and assessed their ChE inhibitory activity, demonstrating that most of the derivatives displayed more selectivity against BChE than AChE. Compound **135** was determined as the top potent BChE inhibitor with an IC_{50} value of 6.4 μM, and **136** showed AChE inhibitory activity with 25.1% inhibition at 50 μM. Additionally, molecular docking investigations indicated that the thiazolidinediones function plays a key part in the inhibition mechanism by well-fitting into the enzyme binding pocket[218] (Table 5).

Foroumadi *et al.* (2020) synthesized 1,2,3-triazole-containing 3-phenylcoumarin-lipoic acid conjugates which showed promising AChE and BChE activity, with IC_{50} at the μM level. Compound **137** displayed excellent AChE (IC_{50} = 7.3 μM) and BChE (IC_{50} = 68.6 μM) activity, indicating that it may act as promising multi-functional agent for additional development[219] (Table 5).

Nguyen *et al.* (2020) synthesized a library of 12 quinazoline-triazole hybrids and tested them as AChE inhibitors to treat AD. The biological assay data confirmed the ability of several hybrid compounds to inhibit the AChE enzyme (IC_{50} range = 0.2–83.9 μM). To understand the high activity of these compounds, molecular docking simulations were carried out to get better insights into the mechanism of binding of these quinazoline-triazole hybrid compounds. As expected, compounds **138** (IC_{50} = 2.06 μM), **139** (IC_{50} = 0.23 μM) and **140** (IC_{50} = 1.10 μM) bind to both catalytic anionic site (CAS) and peripheral anionic site (PAS) in the active site of the AChE enzyme, suggesting that these compounds could act as dual binding site inhibitors. These compounds were not cytotoxic, and they also displayed appropriate physicochemical as well as pharmacokinetic profiles to be developed as new AD drug contenders[220] (Table 5).

Riaz *et al.* (2020) synthesized two groups of *N*-aryl derivatives of 2-(4-ethyl-5-(3-chlorophenyl)-4*H*-1,2,4-triazol-3-ylthio) acetamide and 2-(4-phenyl-5-(3-chlorophenyl)-4*H*-1,2,4-triazol-3-ylthio)acetamide. All the compounds were assessed for their inhibitory ability against AChE and BChE, where these analogs exhibited moderate to good activities against the investigated enzymes. Compounds **141** and **142** showed strong inhibitory potential (IC_{50} = 5.41 and 13.57 μM, respectively) against AChE while **141** showed strong inhibitory activity (IC_{50} = 7.52 μM) against BChE. The remaining compounds displayed good to moderate inhibitory abilities against the enzymes in the range of IC_{50} 14.29–43.94 μM for AChE and IC_{50} 21.59–41.54 μM for BChE[221] (Table 5).

Silva *et al.* (2020) synthesized a series of new triazole *N*-acylhydrazone hybrids and evaluated them for ChE inhibition. Compound **143** (IC_{50} = 26.30 μM) showed a potential profile of a multifunctional compound with the ability to inhibit AChE activity, though it was weaker than donepezil (IC_{50} = 0.026 μM). This compound also showed a good safety profile in the same neuronal model and *in silico* ADME parameters. Taken together, these results suggest that compound **143** could be considered as a lead compound for the development of further AD therapeutics[222] (Table 5).

Saeedi *et al.* (2020) synthesized a set of novel 1,2,3-triazole-chromenone carboxamide derivatives and assessed them for their ChE inhibitory activity. Most of the prepared products were not active at a concentration of 100 μM, though analog **144** was the top potent AChE inhibitor (IC_{50} = 21.71 μM). However, it was inactive toward BChE ($IC_{50} \geq 100$ μM). A kinetic study was undertaken to examine the mechanism of inhibition by **144** against BChE, revealing a mixed-type inhibition pattern based on graphical analysis of the reciprocal Lineweaver–Burk plot. Noteworthy, the butyrylcholinesterase inhibitor (BChEI) activity

depended strongly on the electronic property of functional group substituents and their locations on the Bz group attached to the 1,2,3-triazole ring. For instance, changing the location of the methyl from the 2- to the 3-position destroyed the AChE inhibitory activity. The presence of EWGs (–Cl, –F and –Br) on the terminal phenyl ring was favorable in the 3-position yet detrimental in the *o*- and *p*-positions[223] (Table 5).

Kumar *et al.* (2021) reported the preparation of 1*H*-1,2,3-triazole tethered tacrine-chalcone conjugates and measured their AChE inhibitory ability. *In vitro* AChE inhibition assay revealed three compounds, **145** (IC_{50} = 0.259 μM), **146** (IC_{50} = 0.372 μM) and **147** (IC_{50} = 0.327 μM), exceeding the activity of tacrine. The three active compounds **145–147** were further evaluated *in vitro* against AChE using the Ellman method with tacrine (IC_{50} = 0.375 μM) as a standard. Only compound **146** attained 50% inhibition at 10 μM concentration against the AChE enzyme. An IC_{50} value of 5.328 μM was obtained for compound **146**, indicating that these hybrid analogs are selective inhibitors of the AChE enzyme[224] (Table 5).

Mirfazli *et al.* (2021) prepared methylindolinone-1,2,3-triazole derivatives and assessed their *in vitro* ChE inhibitory activity. While most synthesized products exhibited weak AChE inhibitory activity, they showed moderate to good activity against BChE. The IC_{50} value for the anti-BChE activity of **148** was calculated as 4.78 μM which exceeded that of donepezil (5.19 μM). Based on the molecular docking assessment, compound **148** was found capable of binding at once to the peripheral and catalytic sites of BChE[225] (Table 5).

According to SAR analysis, the aforementioned triazole derivatives are potent AChE and BChE inhibitors (Fig. 15). In general, the activity is highly dependent on the electronic property of substituents and their locations on the moieties linked to the 1,2,3-triazole ring. The smaller groups attached to the triazole ring show higher AChE and BChE inhibitory abilities as compared to the bulky groups present on the rings. The electron withdrawing groups (–F, –Cl, –Br, –CN, –OH, *etc.*) may enhance the activity, depending on their positions, and electron-donating groups (–CH_3, –OCH_3, Et, *n*-Bu *etc.*) may decrease the activity accordingly. All the presented analogues thus far have shown good to excellent ChE inhibitory abilities with a low risk of harmful side effects. Moreover, new modifications may be introduced in the main scaffold to design novel and more potent such types of compounds.

Iqbal *et al.* (2012) reported a series of 2,5-disubstituted-1,3,4-thiadiazoles analogs and screened them for their AChE inhibition activity. Among the series, compound **149** showed excellent AChE inhibition (IC_{50} = 0.351 μM) due to the presence of the *m*-Cl group at the aryl ring[226] (Table 6).

Matysiak *et al.* (2012) synthesized a new series of (1,3,4-thiadiazol-2-yl)benzene-1,3-diol based compounds and investigated their potential AChE properties using the modified of Ellman's spectrophotometric method. Most of the compounds acted as AChE and BChE inhibitors *in vitro*, with IC_{50} values ranging from >500 to 0.053 μM and from >500 to 0.105 μM, respectively. The most potent compound **151** (IC_{50} = 0.053 μM) proved to be selective toward AChE, exhibiting selectivity ratios *versus* BChE of *ca.* 950. The kinetic studies showed that it is a mixed type of AChE inhibitor. Another compound, **150** (IC_{50} = 0.060 μM), was active against both enzymes with IC_{50} values in the low μM range, quite comparable to donepezil (IC_{50} = 0.02 μM) and neostigmine (IC_{50} = 0.05 μM)[227] (Table 6).

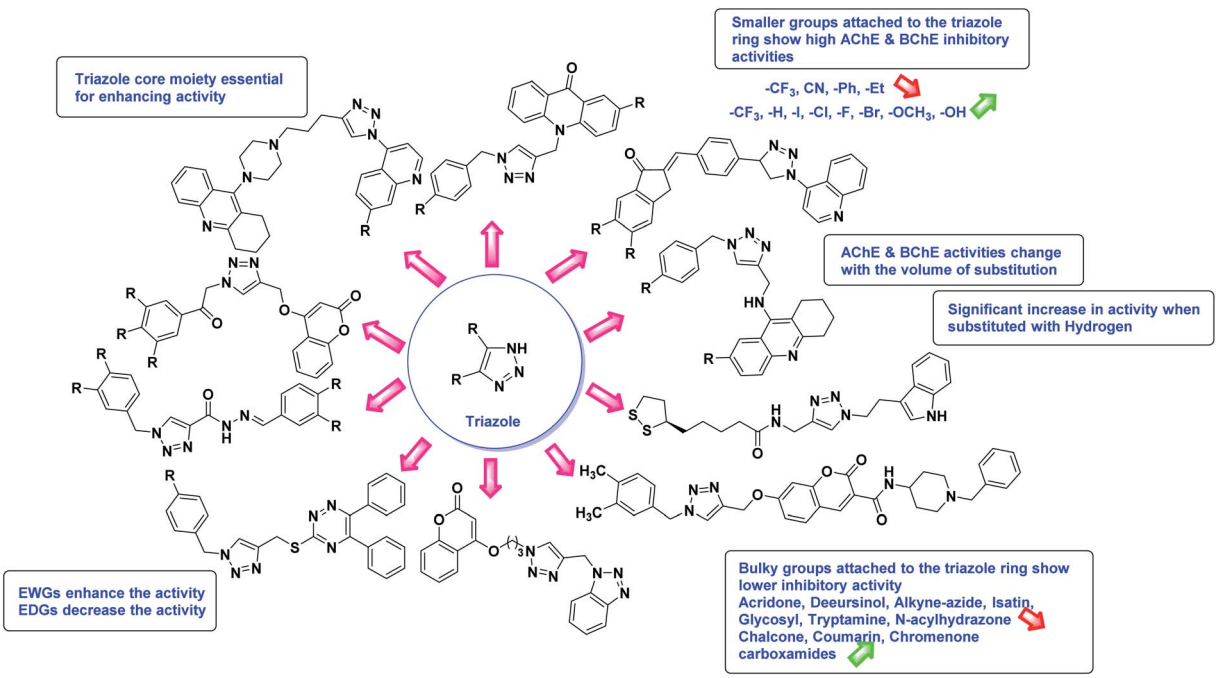

Fig. 15 SAR analysis of different triazole derivatives as AChE and BChE inhibitors.

Table 6 Chemical structures of thiadiazole derivatives **149–168** and their IC_{50} values against cholinesterase enzymes

Compound no.	Chemical structure	IC_{50} values (μM) AChE	BChE	References
149	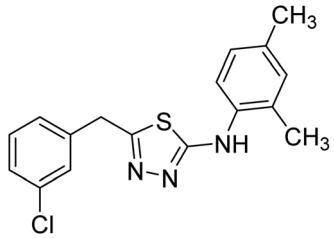	0.351	—	226
150	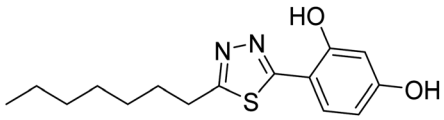	0.060	—	227
151	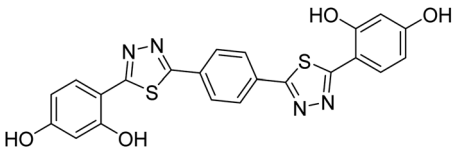	0.053	—	227
152	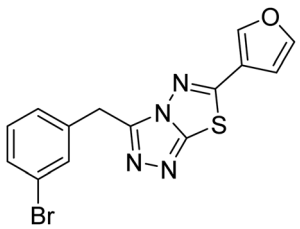	0.344	—	228
153	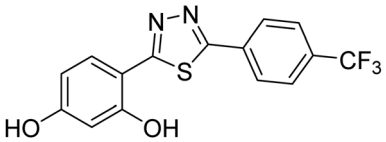	0.09	—	229
154	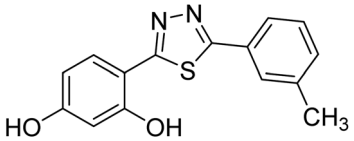	0.16	—	229
155	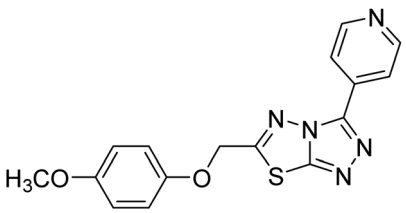	0.77	—	230
156	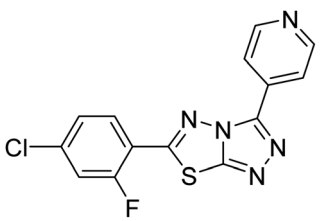	9.57	—	230

Table 6 (*Contd.*)

Compound no.	Chemical structure	IC_{50} values (μM) AChE	BChE	References
157	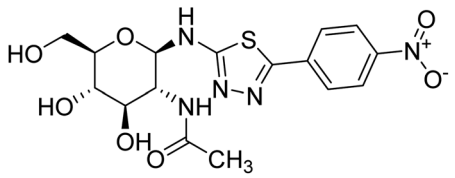	18.38	—	231
158	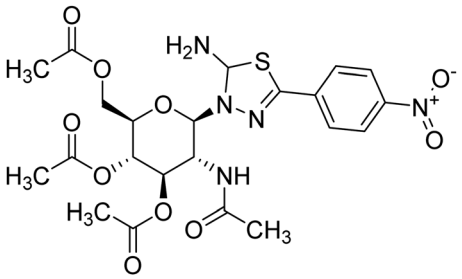	21.91	—	231
159	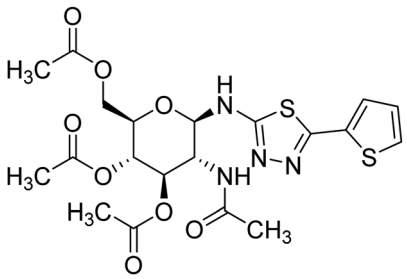	28.86	—	231
160	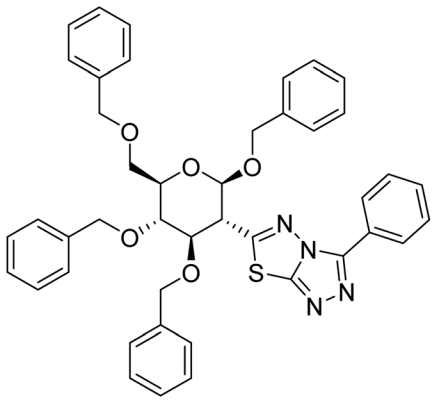	2.464	—	232
161	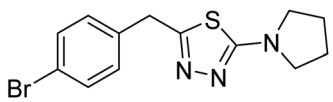	0.189	—	233
162	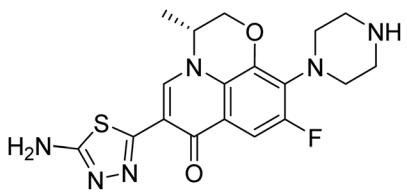	18.1 nM	—	234

Table 6 (*Contd.*)

Compound no.	Chemical structure	IC_{50} values (μM) AChE	BChE	References
163	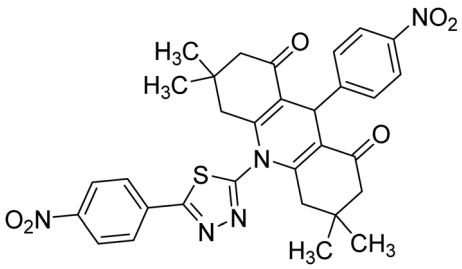	0.002	—	235
164	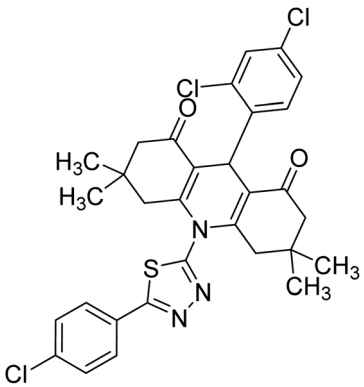	0.006	—	235
165	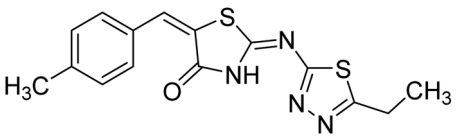	1.30	—	236
166	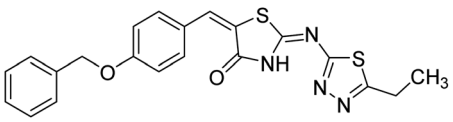	1.22	—	236
167	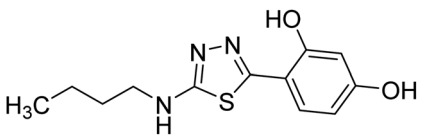	0.029	1.731	237
168	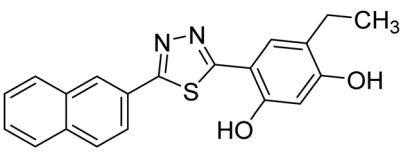	0.074	3.028	237

Seo *et al.* (2012) synthesized different 3,6-disubstituted 1,2,4-triazolo[3,4-*b*]1,3,4-thiadiazole analogs which were tested for their AChE inhibition activities. Neostigmine methyl sulfate with IC_{50} value of 69.1 μM and donepezil with IC_{50} value of 0.021 μM were used as reference drugs. Almost all compounds showed more activity than neostigmine methyl sulfate. The most active compound **152** with IC_{50} value of 0.344 μM showed comparable activity to that of donepezil. All other compounds showed IC_{50} values ranging from 1.78 to 78.21 μM (ref. 228) (Table 6).

Matysiak *et al.* (2013) synthesized a series of new 1,3,4-thiadiazole derivatives and evaluated them as AChE and BChE inhibitors. Some analogs showed promising inhibition of both enzymes *in vitro* in the μM range. Furthermore, the inhibitory potency of the compounds was stronger against AChE than BChE, where one analog was 1154-fold more active inhibiting AChE (IC_{50} = 0.17 μM) than BChE. The kinetic studies showed that one of the most active analogs **153** (IC_{50} = 0.09 μM, AChE) acted as a non-competitive AChE inhibitor and was characterized by a high selectivity index (300). The other derivative **154**

(IC_{50} = 0.16 μM) exhibited a mixed type of AChE inhibition. Docking simulations enabled the detection of key binding interactions of the compounds with AChE and revealed that they occupied mainly the catalytic active site. The scoring function for the novel compounds was similar or higher than that of the reference drug[229] (Table 6).

Iqbal *et al.* (2014) reported the preparation of 3,6-disubstituted-1,2,4-triazolo-[3,4-*b*]-1,3,4-thiadiazoles. The newly synthesized analogs were assessed for AChE and BChE inhibition. Almost all the compounds showed outstanding activities against AChE even superior to the reference drug. Compound **155** showed IC_{50} = 0.77 μM against AChE and **156** showed IC_{50} = 9.57 μM against BChE, rendering these derivatives useful candidates for the therapy of AD[230] (Table 6).

Liu *et al.* (2015) synthesized 4-substituted glycosyl-based thiadiazols and evaluated their AChE activity. The AChE inhibitory abilities of all the analogs were analyzed by Ellman's method. Amongst them, compound **157** displayed the best AChE-inhibition activity with IC_{50} of 18.38 μM and compounds **158**, **159** with 4-nitrophenyl and 2-thienyl substituent exhibited a moderate inhibition of AChE with IC_{50} = 21.91 μM and 28.86 μM, respectively. Compared with tacrine (IC_{50} = 0.26 μM), known as the first medication used for the treatment of AD, the above species offered promising inhibition activity against AChE, potentially useful in the treatment of AD[231] (Table 6).

Liu *et al.* (2017) prepared novel glycosyl containing 1,2,4-triazolo[3,4-*b*][1,3,4]thiadiazole compounds and evaluated their ChE inhibitory activity. The AChE inhibitory activity of the targeted compounds was screened by Ellman's method where the AChE extracts from *Electrophorus electricus* were used. The results indicated that all compounds had higher IC_{50} against AChE than the precursor D-glucosamine hydrochloride. The best compound **160** showed high activity with an IC_{50} of 2.464 μM against AChE[232] (Table 6).

Shi *et al.* (2017) prepared 5-benzyl-1,3,4-thiadiazole derivatives and tested their AChE inhibitory activity. Bioassay results revealed that compound **161** was the best anti-AChE analog and potential multi-target lead candidate against AD[233] (Table 6).

Saeed *et al.* (2019) synthesized a library of new 1,3,4-thiadiazole hybrids and measured their AChE enzyme inhibitory activity. The compounds demonstrated encouraging activities against AChE, particularly **162** (IC_{50} = 18.1 nM), which was the most promising analog in the library and considerably more active than the reference drug neostigmine methyl sulfate; (IC_{50} 2186.5 nM)[234] (Table 6).

Lotfi *et al.* (2020) synthesized new acridine derivatives containing substituted thiadiazol-2-amine moiety. Anticholinesterase (AChE) activity evaluation of the derivatives showed that all the derivatives are capable of inhibiting both enzymes and are highly selective towards AChE. Among them, the ability of **163** and **164** with respective IC_{50} values of 0.002 and 0.006 μM to inhibit AChE was higher than tacrine (IC_{50} = 0.016 μM)[235] (Table 6).

Aggarwal *et al.* (2021) synthesized thiazolidin-4-one analogs with thiadiazole derivatives in appreciable yield. The *in vitro* AChE inhibitory activity of these compounds was assessed using Ellman's method spectrophotometer and donepezil as a standard drug. Compounds **165** and **166** were found to be potent AChE enzyme inhibitors, with IC_{50} values of 1.30 and 1.22 μM, respectively. Finally, these significant results could pave the way for the development of new AChE inhibitors[236] (Table 6).

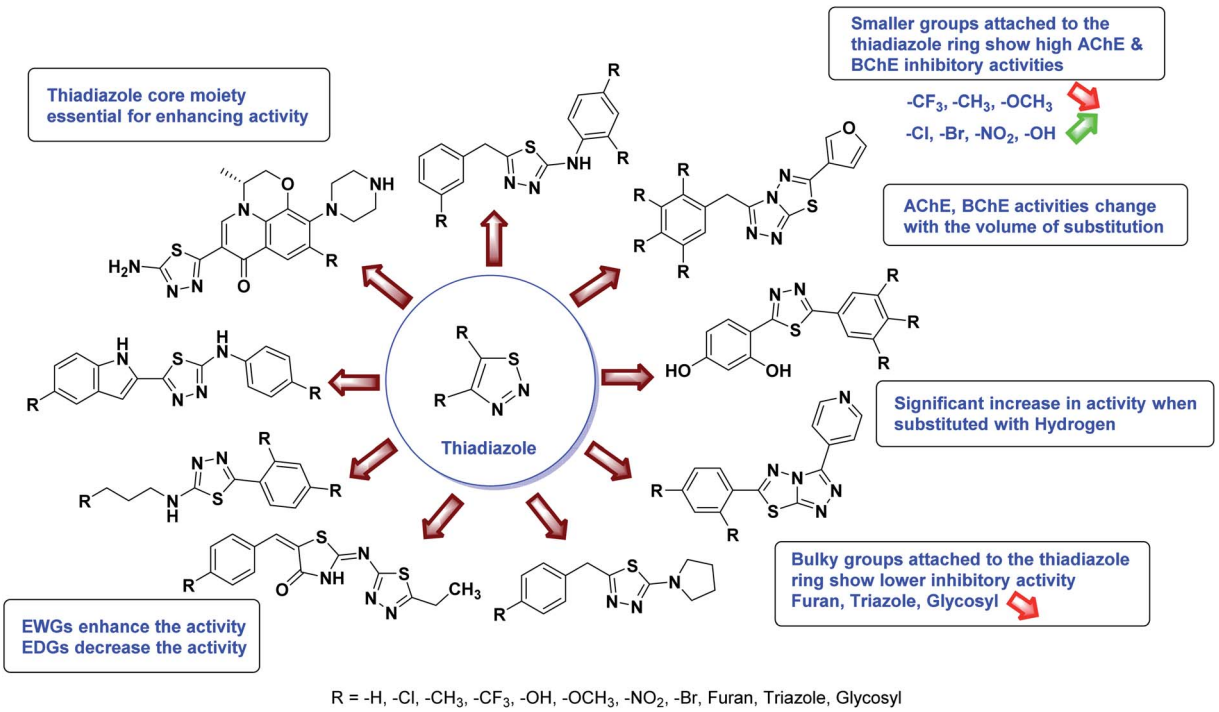

Fig. 16 SAR analysis of different thiadiazole derivatives as AChE and BChE inhibitors.

Table 7 Chemical structures of pyrrolidine derivatives **169–181** and their IC_{50} values against cholinesterase enzymes

Compound no.	Chemical structure	IC_{50} values (μM) AChE	BChE	References
169	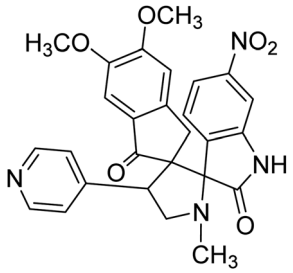	0.10 μmol L^{-1}	—	238
170	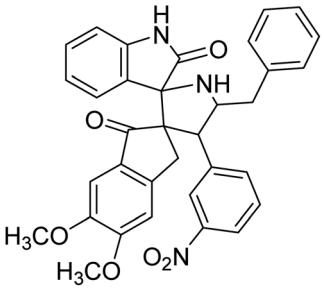	1.57	—	239
171	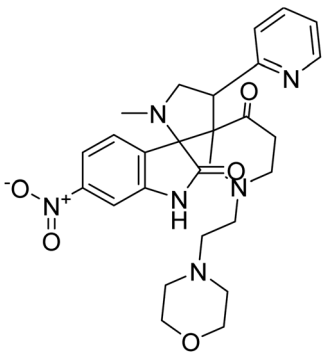	1.88	—	240
172	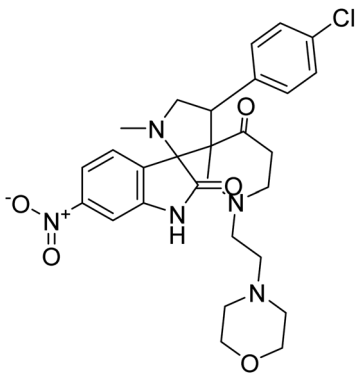	1.37	—	240
173	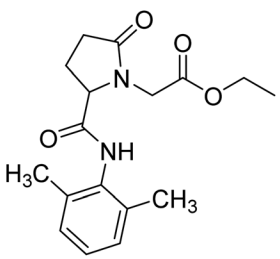	11.84 Pg g^{-1}	—	241

Table 7 (*Contd.*)

Compound no.	Chemical structure	IC_{50} values (μM) AChE	BChE	References
174	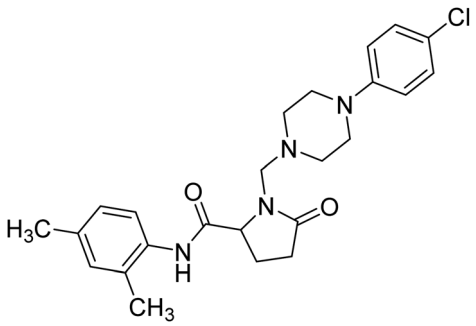	11.3 Pg g^{-1}	—	241
175	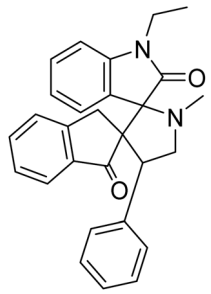	13.7	—	242
176	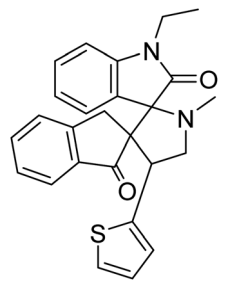	21.8	—	242
177	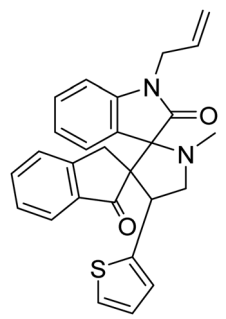	22.1	—	242
178	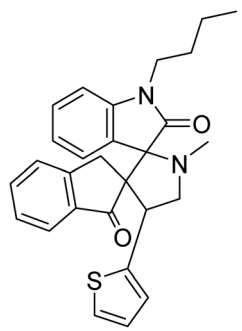	22.9	—	242

Table 7 (*Contd.*)

Compound no.	Chemical structure	IC_{50} values (μM) AChE	BChE	References
179	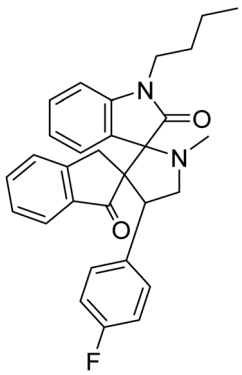	24.9	—	242
180	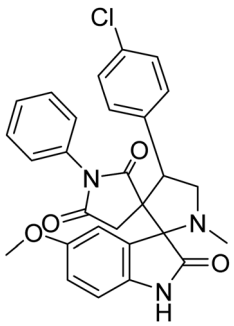	3.35	5.63	243
181	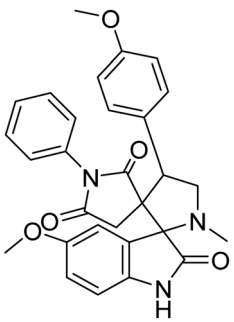	3.15	4.74	243

Matysiak *et al.* (2021) synthesized two series of novel 1,3,4-thiadiazole-resorcinol conjugates and evaluated them as ChE inhibitors. *N*-(Butyl- and *N*-chlorophenyl-5-amino-1,3,4-thiadiazol-2-yl)benzene-1,3-diols were identified as the most promising compounds of low nanomolar activity against AChE (IC_{50} = 29–76 nM) and moderate activity against BChE. The inhibition mechanism studies proved that the compounds are mixed-type inhibitors. IC_{50} values of the *N*-butyl thiadiazol and *N*-chloro thiadiazol derivatives are the most potent analogs against AChE and BChE, ranging from 0.029 to 0.085 μM and from 3.154 to 24.711 μM, respectively. The most potent compounds **167** has IC_{50} = 0.029 μM for AChE, 1.731 μM for BChE, **168** has IC_{50} = 0.074 μM for AChE, and 3.028 μM for BChE[237] (Table 6).

SAR studies of different oxadiazoles demonstrate that the different derivatives are active against AChE and BChE enzymes (Fig. 16). All the structural features are performing a significant role in the inhibitory activity, though, a slight variation in the activity of these analogs is due to variability in the nature and positions of substituents on aryl rings. The smaller groups attached to the thiadiazole ring show higher AChE and BChE inhibitory abilities as compared to the bulky groups present on the rings. The electron with-drawing groups (–F, –Cl, $–NO_2$, –OH, $–CF_3$ *etc.*) increase the activity and electron-donating groups ($–CH_3$, $–OCH_3$, *etc.*) decrease the activity. All the presented analogs thus far have shown good to excellent ChE inhibitory abilities with a low risk of toxic side effects. Furthermore, these species are inexpensive and easy to synthesize in the laboratory, making them

attractive for viable development and marketing as drugs against cholinesterase.

Lee *et al.* (2010) synthesized pyrrolidine analogs and examined these analogs as AChE inhibitors. Among the compounds, **169** ranked as the top potent inhibitors of the series. Compound **169** demonstrated effective inhibitory activity against the AChE enzyme with IC_{50} 0.10 μmol L^{-1}. Pyrrolidine analogs might be potential AChE agents for AD[238] (Table 7).

Kumar *et al.* (2015) synthesized a series of novel dimethoxyindanone embedded spiropyrrolidines in ionic liquid and were evaluated for their inhibitory abilities towards ChEs. Among the spiropyrrolidines, compound **170** exhibited the most potent activity with an IC_{50} value of 1.57 μM against AChE. Molecular docking simulation for the most active compound was employed to disclose its binding mechanism to the active site of the AChE receptor[239] (Table 7).

Murugaiyah *et al.* (2017) synthesized a library of piperidone grafted spiropyrrolidines and assessed the compounds for their AChE and BChE inhibitory abilities. Within the series, species **171** and **172** was more potent against AChE than the standard drugs with IC_{50} values of 1.88 and 1.37 μM, respectively. Molecular docking simulations for **172** revealed its appealing binding templates to the active site channel of AChE enzymes. These analogs are astonishing AChE inhibitors and may serve as prospective AD drugs[240] (Table 7).

Mohamed *et al.* (2018) prepared oxopyrrolidines and evaluated their effect on AD by measuring their inhibitory activity against AChE enzyme and amyloid β-42 protein. Most compounds showed decent inhibitory ability where compound **173** garnered the highest activity against AChE with IC_{50} value 1.84 ng g^{-1} tissue compared to the standard donepezil 3.34 ng g^{-1} tissue. Furthermore, compound **174** displayed the greatest activity against β-42 protein with IC_{50} value of 11.3 Pg g^{-1} tissue compared to 18.4 Pg g^{-1} tissue of donepezil[241] (Table 7).

Srour *et al.* (2019) synthesized regioselectively dispiro [indene-2,3′-pyrrolidine-2′,3″-indoline]-1,2″(3*H*)-diones and explored them as inhibitors of AChE and BChE enzymes; although no substantial inhibitory activity for the tested analogs were detected on AChE, analogs **175**, **176**, **177**, **178** and **179** proved best against BChE with IC_{50} = 13.7 μM, 21.8 μM, 22.1 μM, 22.9 μM and 24.9 μM respectively, compared to donepezil (IC_{50} = 0.72 μM). Compound **175** was determined to exhibit a mixed-type mode of inhibition[242] (Table 7).

Girgis *et al.* (2020) synthesized a set of dispiro[indoline-3,2″-pyrrolidine-3′,3″-pyrrolidines] in a regioselective manner using multi-component azomethine cycloaddition reaction of 3-(arylmethylidene)pyrrolidine-2,5-diones, isatins and sarcosine. Compounds **180** (IC_{50} = 3.35 μM for AChE, 5.63 μM for BChE) and **181** (IC_{50} = 3.15 μM for AChE, 4.74 μM for BChE) exhibited cholinesterase inhibitory abilities with promising inhibition of both AChE and BChE and were most selective towards AChE than BChE, showing consistent selectivity index trend to that donepezil (IC_{50} = 0.59 μM for AChE, 0.77 μM for BChE)[243] (Table 7).

SAR studies of pyrrolidine derivatives describe above indicate that the various analogous are potent against both AChE and BChE enzymes (Fig. 17). Limited SAR is establish based on

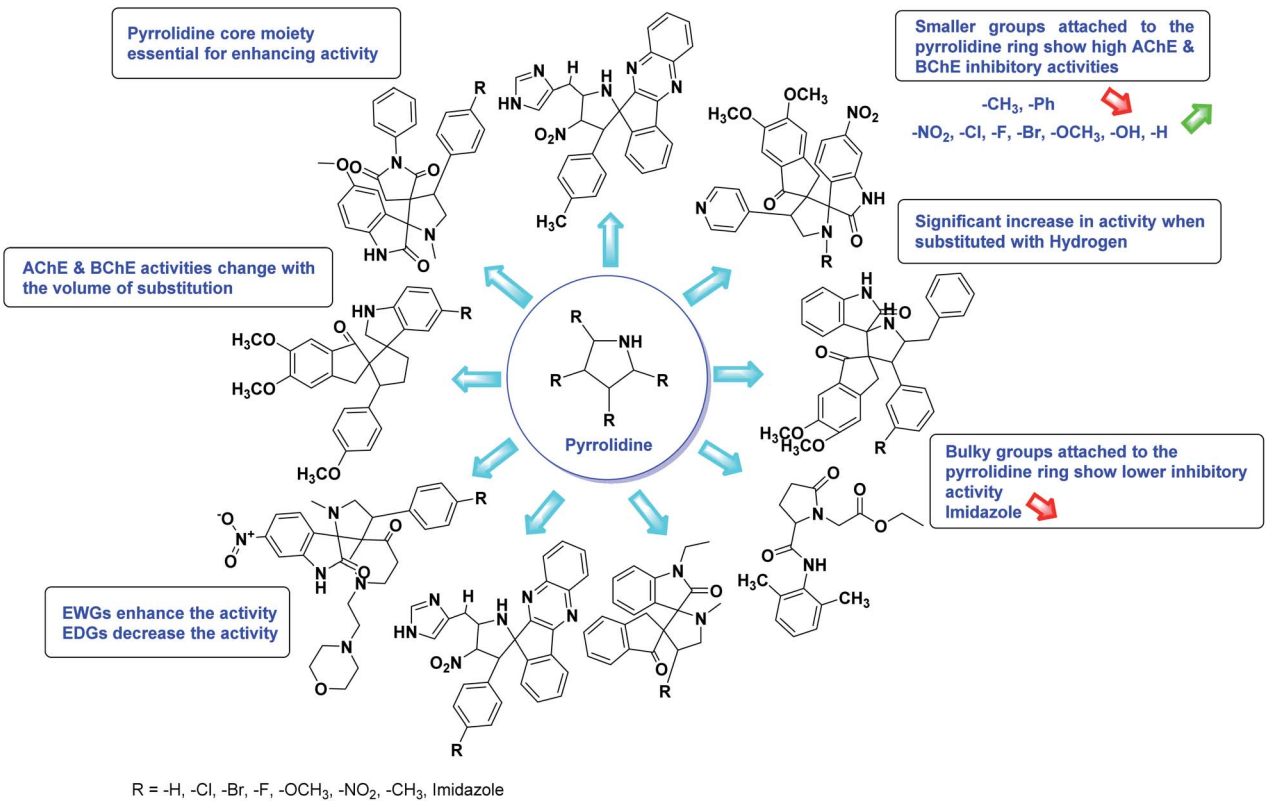

Fig. 17 SAR analysis of different pyrrolidine derivatives as AChE and BChE inhibitors.

the substitution pattern on the pyrrolidine motif and are accountable for influencing bioactivities. The smaller groups (–CH_3, –Ph, –NO_2, –Cl, –F, –Br, –OCH_3, –OH, –H, *etc.*) attached to the pyrrolidine ring promote higher AChE and BChE inhibitory abilities compared to the bulky (imidazole) groups present on the rings. All the analogs presented thus far have shown good ChE inhibitory abilities with minimum toxic side effects. Furthermore, these species are inexpensive and easy to synthesize in the laboratory, making them attractive for viable development and marketing as drugs against cholinesterase.

Rangappa *et al.* (2009) developed many lead compounds including piperidine derivatives to enhance the efficacy and reduce the general side effects of these AChE inhibitors. Donepezil is a regularly recommended AChE inhibitor having a piperidine ring in its structural composition. The group synthesized *cis*-2,6-dimethyl piperidine sulfonamides **182–187** in the presence of triethylamine using a nucleophilic substitution procedure between *cis*-2,6-dimethyl piperidine and alkyl/aryl sulfonyl chlorides and docked the products on the AChE enzyme. These piperidine sulfonamides were used to inverse scopolamine-induced memory loss in rats through *in vitro* AChE enzyme inhibition trials and *in vivo* antiamnesic studies. The SAR of the synthesized piperidine derivatives **182–187** based on *in vitro* findings indicated that adding a methyl group to sulfonyl-*cis*-2,6-dimethyl piperidine **182** inhibits AChE moderately, whereas adding an electronegative chlorine atom to positions 2 and 5 inhibits AChE. Inhibition was also suppressed by the electronegative NO_2 function at the *m*-position of the phenyl ring of **183** and the nitro group at the *ortho* position **184** of the phenyl ring (IC_{50} = 186, 192, 200 and 195, 185, 180 nM, respectively). The nitro group at the *p*-position of the phenyl ring **185** is detrimental to activity (IC_{50} = 120, 1150, and 1210 nM). Also, having a chlorine atom at the *p*-position of the phenyl group **186** reduces inhibitory activity (IC_{50} = 325, 318, and 312 nM) when compared to *ortho*, *meta* substitution of chlorine atoms as in **187**. Alkyl substitution at the *para* position (methyl and *tert*-butyl) inhibits AChE (IC_{50} = 362, 368, 365, 463, 458, and 450 nM, respectively)[244] (Table 8).

Rehman *et al.* (2014) synthesized *N*′-[(alkyl/aryl)sulfonyl]-1-(phenylsulfonyl)piperidine-4-carbohydrazide analogs using ethyl piperidine-4-carboxylate to generate 2-(phenylsulfonyl) piperidine-4-carbohydrazide **188** *N*′-[(alkyl/aryl)sulfonyl] piperidine-4-carbohydrazide **189**, and 4-(bromomethyl)-*N*′-(1-(phenylsulfonyl)piperidine-4-carbonyl) benzenesulfonohydrazide **190**. The structures were confirmed using IR, ^{1}H-NMR, and EI-MS spectra, and they were all examined for their capacity to inhibit the enzymes AChE and BChE. The interactions of these chemicals with the human proteins AChE and BChE were studied using molecular docking. The binding mechanisms of the inhibitors under investigation were identified and compared to anti-enzymatic IC_{50} values using an automated docking program (AutoDock). Both studies determined that the compounds are potentially effective AChE and BChE inhibitors[245] (Table 8).

Brahmachari *et al.* (2015) used a diastereoselective one-pot multicomponent approach to synthesize a range of densely functionalized piperidine scaffolds under eco-friendly conditions. The piperidines were tested *in vitro* for inhibitory activity against AChE, and *in silico* studies were carried out for all analogs using molecular docking, pharmacophore mapping, and QSAR investigation to better appreciate the structural topographies mandatory for interaction with the AChE enzyme and the main active site residues implicated in intermolecular interactions. Nitration, halogenation, or 3,4-methylenedioxy-substitution at the benzene ring linked to the 2- and 6-carbons of the 1,2,5,6-tetrahydropyridine nucleus significantly improved the AChE inhibitory effect of compounds **191–198**. The IC_{50} values of the reported analogs **191** (IC_{50} = 0.71 μM), **192** (IC_{50} = 0.26 μM), **193** (IC_{50} = 0.88 μM), **194** (IC_{50} = 0.05 μM), **195** (IC_{50} = 0.02 μM), **196** (IC_{50} = 0.13 μM), **197** (IC_{50} = 0.17 μM) and **198** (IC_{50} = 0.01 μM) showed that these derivatives are more potent than the standard galantamine (IC_{50} = 0.09 μM). According to docking studies, the inhibitors fit neatly in the active sites. Researchers will be able to better grasp how to alter scaffolds for improved therapeutic effectiveness against AD based on *in silico* tests[246] (Table 8).

According to Tiwari *et al.* (2015), the creation of multi-target directed ligands (MTDLs) has emerged as a potential strategy for addressing the complex etiology of AD. Using this approach, a novel set of *N*′-(4-benzylpiperidin-/piperazin-/benzhydrylpiperazin-1-yl)alkylamine derivatives were designed, synthesized, and physiologically assessed as inhibitors of cholinesterase (ChEs), amyloid-beta (Aβ) self-aggregation, and radical scavenging activity. According to *in vitro* experiments, the majority of the compounds produced inhibited AChE and BChE with IC_{50} values in the low nanomolar range and were more powerful than the reference drug donepezil in this regard. With IC_{50} values of 6.83 nM and 2.13 nM, respectively, inhibitors **199** and **200** significantly suppressed AChE, while compound **200** was shown to be exceptionally selective for AChE (38-fold). Furthermore, both the kinetic analysis of AChE inhibition and the docking study revealed that **200** binds to both the catalytic active site and the peripheral anionic site of AChE. Additionally, at 25 μM, these compounds reduced self-induced $A\beta_{1-42}$ aggregation with percentage inhibition ranging from 54 to 89%, with compound **200** offering the highest inhibition (88.81%). The ORAC of the compounds with methoxy and hydroxy groups ranged from 2.2 to 4.4 times that of Trolox. Furthermore, ADMET tests demonstrated that all compounds have sufficient drug-like properties. These findings suggest that **200** could be a promising lead chemical for the development of future Alzheimer's therapies or their AChE inhibiting activity[247] (Table 8).

Kumar *et al.* (2015) disseminated a study aiming to discover, manufacture, and test novel AChE/BChE inhibitors. A series of 4-thiazolidinone and piperidine substituted arecoline compounds with inhibitory action against AChE and BChE was revealed, and the chemical structures of all compounds were validated using IR, ^{1}H NMR, ^{13}C NMR and mass spectroscopy. Only a few of the compounds generated demonstrated substantial activity for AChE over BChE at micromolar doses according to the cholinesterase inhibition studies. Compound **201** inhibits AChE the most, with IC_{50} values of 6.62 μM for AChE and 13.78 μM for BChE, which are similar to the normal

Table 8 Chemical structures of piperidine derivatives **182–202** and their IC_{50} values against cholinesterase enzymes

Compound no.	Chemical structure	IC_{50} values (μM) AChE	BChE	References
182	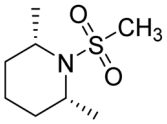	186 nM	—	244
183	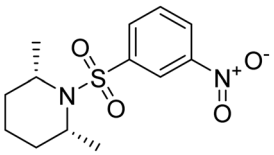	192 nM	—	244
184	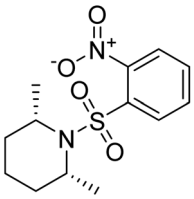	200 nM	—	244
185	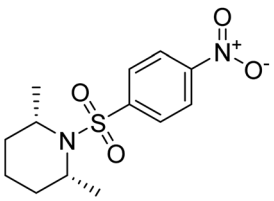	120 nM	—	244
186	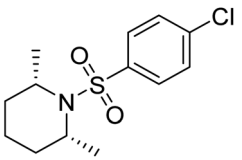	325 nM	—	244
187	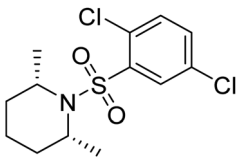	362 nM	—	244
188	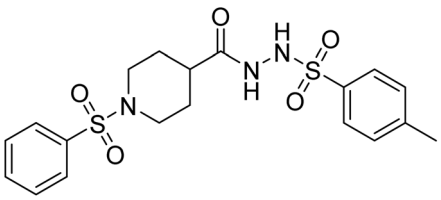	157	—	245
189	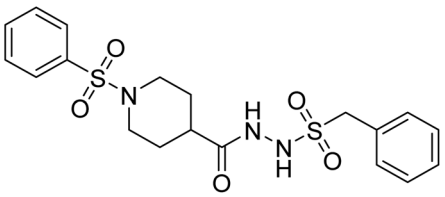	219	—	245

Table 8 (*Contd.*)

Compound no.	Chemical structure	IC_{50} values (μM) AChE	BChE	References
190	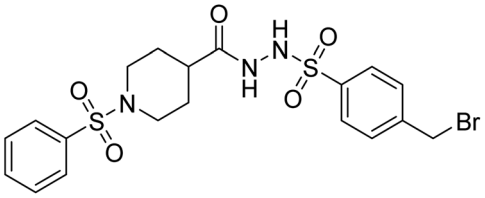	145	—	245
191	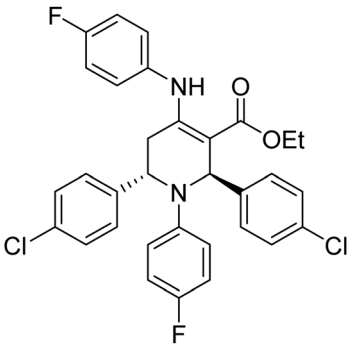	0.71	—	246
192	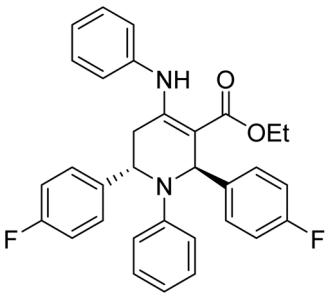	0.26	—	246
193	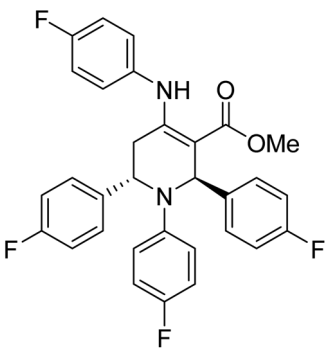	0.88	—	246
194	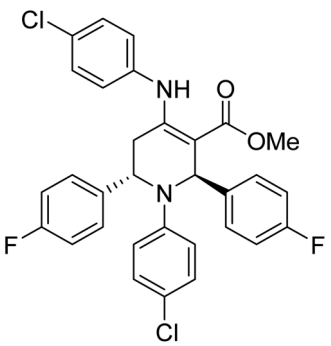	0.05	—	246

Table 8 (*Contd.*)

Compound no.	Chemical structure	IC_{50} values (μM) AChE	BChE	References
195	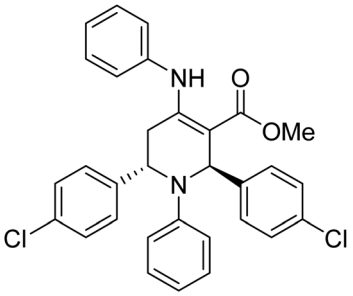	0.02	—	246
196	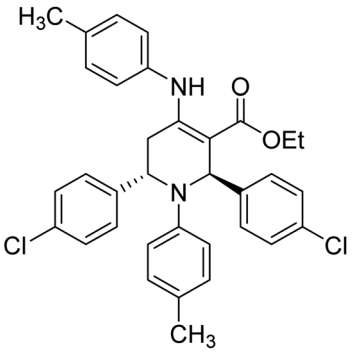	0.13	—	246
197	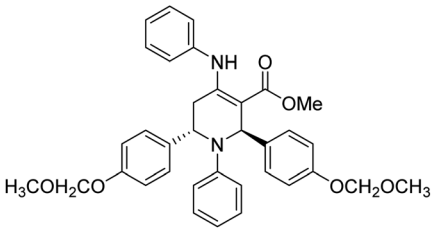	0.17	—	246
198	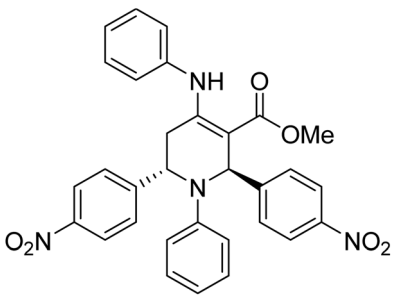	0.01	—	246
199	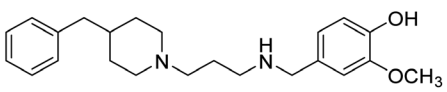	6.83 nM	—	247
200	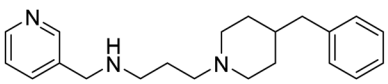	2.13 nM	—	247
201	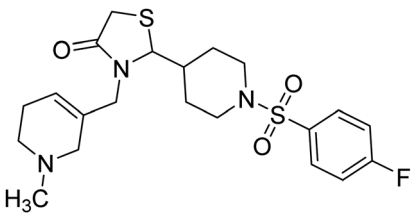	6.62	13.78	248

Table 8 (*Contd.*)

Compound no.	Chemical structure	IC_{50} values (μM) AChE	BChE	References
202	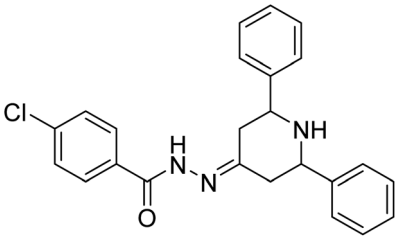	—	35.30	249

neostigmine's IC_{50} values of 2.05 μM for AChE and 3.64 μM for BChE[248] (Table 8).

Emre *et al.* (2016) presented hydrazones and piperidines as suitable substrates for drug development. The objective of their study was to prepare benzoyl hydrazones from 2,6-diphenylpiperidin-4-one and ethyl 4-oxopiperidine-1-carboxylate. The antioxidant, anticholinesterase, and anti-cancer activities of the synthesized compounds were investigated. Anticholinesterase activity was measured using the enzyme BChE. Compound **202** (IC_{50} = 35.30 μM) inhibited BChE more efficiently than galantamine (IC_{50} = 46.03 μM), pointing to **202** as a more suitable BChE inhibitor. The docking method was also used to determine the BChE inhibitory mechanism of analog **202**. A molecular docking investigation revealed that analog **202** connected to the BChE enzyme more efficiently than AChE owing to its orientations and various sorts of interactions with the enzyme[249] (Table 8).

SAR studies of piperidine explore that the various derivatives are potent against AChE and BChE enzymes (Fig. 18). All the structural features are performing a significant role in the inhibitory activity, though, a slight variation in the activity of these analogs is due to variability in the nature and positions of substituents on aryl rings. The smaller groups (–F, –Cl, $–NO_2$, –OH, Br, –I, $–CH_3$) attached to the piperidine ring show higher AChE and BChE inhibitory abilities as compared to the bulky (sulfonamide) groups present on the rings. The electron withdrawing groups (–F, –Cl, $–NO_2$, –OH, $–CF_3$ *etc.*) increase the activity and electron-donating groups ($–CH_3$, $–OCH_3$, *etc.*) decrease the activity. All the presented analogs thus far have shown good to excellent ChE inhibitory abilities with a low risk of toxic side effects. Furthermore, these analogs are less toxic and easy to synthesize in the laboratory, making them attractive for viable development and marketing as drugs against cholinesterase.

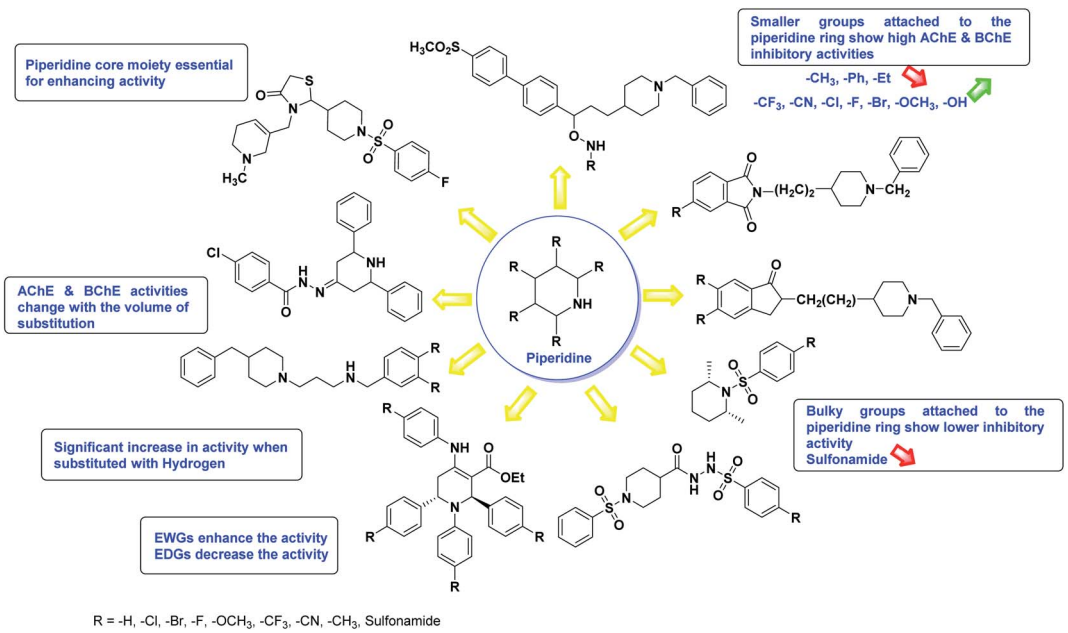

Fig. 18 SAR analysis of different piperidine derivatives as AChE and BChE inhibitors.

Table 9 Chemical structures of piperazine derivatives **203–220** and their IC_{50} values against cholinesterase enzymes

Compound no.	Chemical structure	IC_{50} values (μM) AChE	BChE	References
203	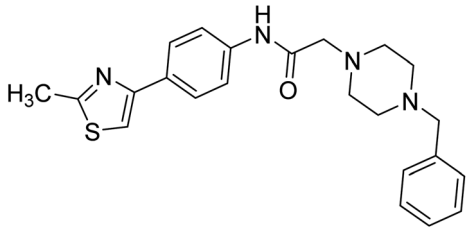	0.11	—	250
204	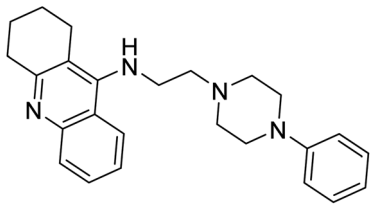	2 nM	—	251
205	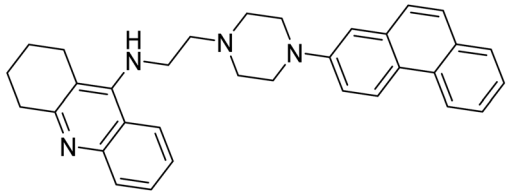	260 nM	—	251
206	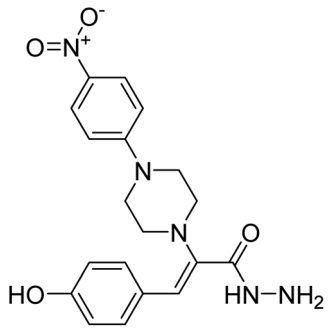	29.5	—	252
207	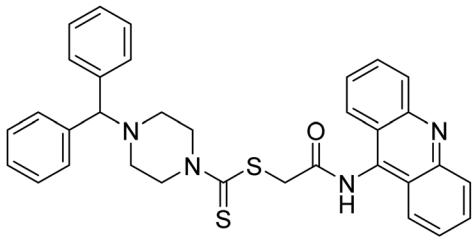	0.092	—	253
208	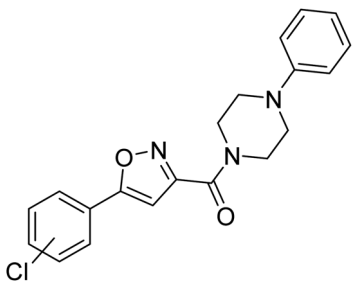	51.66	—	254

Table 9 (*Contd.*)

Compound no.	Chemical structure	IC_{50} values (μM) AChE	BChE	References
209	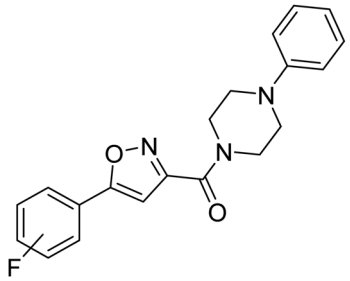	79.12	—	254
210	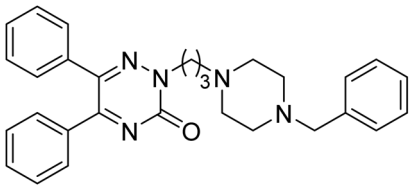	0.6	—	255
211	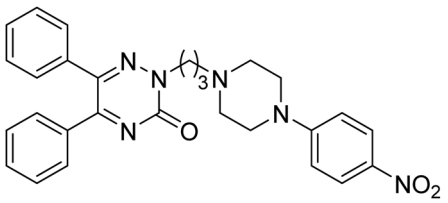	0.5	—	255
212	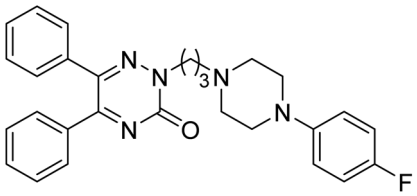	0.4	—	255
213	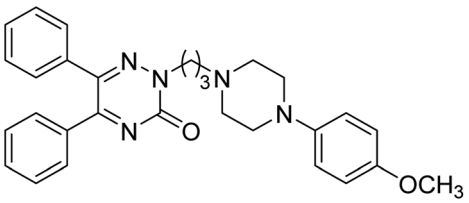	0.3	—	255
214	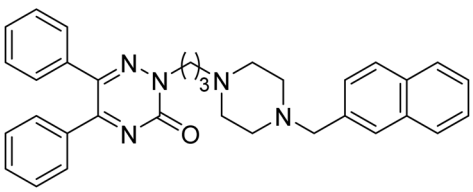	0.2	—	255
215	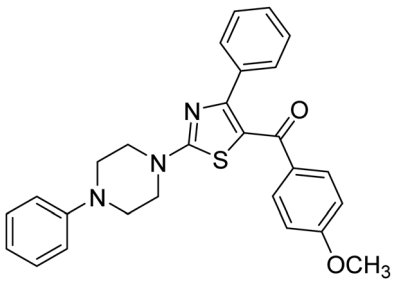	0.268	—	256

Table 9 (*Contd.*)

Compound no.	Chemical structure	IC_{50} values (μM) AChE	BChE	References
216	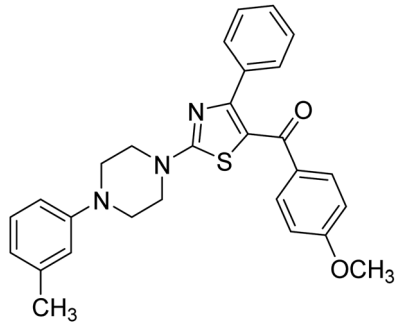	0.286	—	256
217	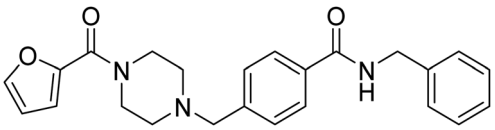	289.61	—	257
218	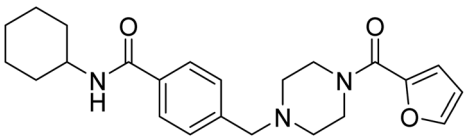	252.36	—	257
219	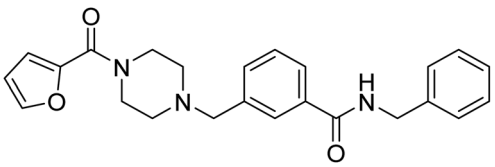	412.71	—	257
220	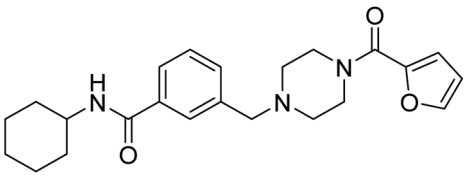	54.81	—	257

Kaplanckl *et al.* (2013) described a process for making novel 2-(4-substituted piperazine-1-yl)-*N*-[4-(2-methylthiazol-4-yl) phenyl]acetamide derivatives which were subsequently tested for anticholinesterase activity on AChE and BChE enzymes using Ellman's approach. The structures of all compounds were deduced based on IR, ^{1}H-NMR, ^{13}C-NMR, and MS spectral data, as well as elemental analysis measurements. The most powerful compounds against AChE at 0.1 μM concentration were **203** which showed 89.70% inhibition rates, respectively, in the described assay. Furthermore, the IC_{50} value of compound **203** was revealed to be 0.011 μM, whereas the IC_{50} value of the reference drug donepezil was 0.054 μM. The IC_{50} values of compounds, on the other hand, are in the range of 6.34–8.42 μM. The molecules which were comparable to donepezil, also have AChE inhibitory action. The chemical **203** has the same inhibitory efficacy as the reference drug because it contains a 2-pyridyl moiety in the fourth position of the piperazine ring. Compound **203**, which included a 4-benzylpiperazine fragment, also demonstrated a five-fold lower IC_{50} (0.11 μM) than donepezil. There is no evident inhibitory effect of the compounds generated on BChE[250] (Table 9).

According to Hamulakova *et al.* (2014) the potential of synthetic piperidine derivatives as novel AChE and BChE inhibitors with nanomolar inhibitory activity was investigated using a new series of substituted tacrine/acridine and tacrine/tacrine dimers with aliphatic or alkylene-thiourea linkers. The most potent AChE inhibitor was found to be homodimeric tacrine derivative **204**, which had an IC_{50} value of 2 nM, indicating a 250-fold higher activity rate than tacrine and 7500-fold higher activity rate than the study's standard, 7-MEOTA. Dual site binding is evident in the generated compounds with two tacrines or tacrine and acridine as terminal moieties, signifying a second binding site. According to the IC_{50} values obtained throughout the study, all compounds had an inhibitory effect

on both AChE and BChE. Among the synthesized derivatives **204** and **205** displayed the highest levels of nanomolar AChE inhibition. The findings reveal that combining terminal acridine or tacrine units with alkylene-piperazine or alkylene-thiourea linkers is highly successful. Inhibitors of both mono and dual binding sites are present in ligands **204** and **205**. A study of inhibitory efficacy within the series revealed the importance of linker length. The solitary ethylene unit in **204** provides only medium-nanomolar activity, but the two ethylene units in **205** ensure low-nanomolar inhibitory action (260 nM). This demonstrates that the length of molecule **204** is insufficient to simultaneously reach both enzyme binding sites. The tacrine derivatives **204** and **205**, which have an ethylene unit attached to them, have a low, even sub-nanomolar effectiveness (for BChE: 0.4–20 nM), which is superior to tacrine itself. In this family of compounds, the presence of another aromatic rings on the opposite side of the molecules is a crucial factor that promotes binding (Bn or THA). Finally, a comparison of AChE/BChE selectivity within the series shows that compound **205** (despite its low activity) is the most selective for AChE, whereas compound **204** is the most selective for BChE[251] (Table 9).

Ozkay *et al.* (2017) established a procedure for evaluating the anticholinesterase effects of different hydrazone derivatives. A sequence of eleven new *N*-(2,4-disubstitutedbenzylidene)-2-(4-nitrophenyl-piperazin-1-yl)acetohydrazide analogs were prepared by reacting 2-[4-(4-nitrophenyl)piperazin-1-yl] acetohydrazide with aromatic aldehydes. The inhibitory efficacy of compounds against AChE and BChE was tested and assessed using a modified version of Ellman's spectrophotometric approach. The most active derivative of the compounds studied was found to be compound **206**. The drug galantamine was used as a reference drug. All the compounds had lower anticholinesterase potency than the reference drug. Only compound **206**, which had a hydroxyl substituent at the *para* position, inhibited AChE, with an IC_{50} of 29.5 μM (ref. 252) (Table 9).

Ozkay *et al.* (2018) discussed a study in which they synthesized 2-(9-acridinylamino)-2-oxoethyl piperazine/piperidine/morpholinecarbodithioate analogs to investigate anticholinesterase activity. All the compounds exhibited unique and encouraging anti-BChE activity. The first class of compounds inhibit BChE with IC_{50} values ranging from 0.014 to 2.097 μM. Piperazine derivatives including 2-dimethylaminoethyl, 3-dimethylaminopropyl, 2-hydroxyethyl, 4-chlorophenyl, 4-(trifluoromethyl)benzyl and 4-methylbenzyl exhibited higher inhibitory activity against BChE than the other compounds in the group. Additionally, it inhibited BChE 15.4-fold better than the positive control, donepezil (IC_{50} = 1.419 μM), and the highest active chemical, **207** (IC_{50} = 0.092 μM)[253] (Table 9).

Akbarzadeh *et al.* (2019) outlined a technique for developing, synthesizing, and testing a novel family of arylisoxazole-phenylpiperazines against AChE and BChE. [5-(2-Chlorophenyl)-1,2-oxazol-3-yl](4-phenylpiperazin-1-yl) methanone **208** was determined to be the most potent AChE inhibitor, with an IC_{50} of 21.85 μM. It should be noted that most of the compounds synthesized exhibited little anti-BChE activity, with the most active being [5-(2-fluorophenyl)-1,2-oxazol-3-yl](4-phenylpiperazin-1-yl)methanone **208** (IC_{50} = 51.66 μM). Additionally, kinetic studies of the inhibitory activity of compounds **208** and **209** on AChE and BChE indicated that they bind to both the catalytic site (CS) and the peripheral anionic site (PAS) of AChE and BChE. Additionally, docking analysis demonstrated that compound **208** formed favorable contacts with amino acid residues in the active and peripheral anionic sites. Finally, compound **208** had a negligible neuroprotective effect against Aβ-induced neurotoxicity in PC12 cells[254] (Table 9).

Tripathi *et al.* (2019) reported the synthesis of several piperazine-tethered biphenyl-3-oxo-1,2,4-triazine analogs. In comparison to donepezil (AChE, IC_{50} = 0.1 μM), compound **210** demonstrated substantial non-competitive inhibitory activity against AChE (IC_{50} = 0.2 μM). In *in vivo* behavioural studies, compound **210** significantly improved cognitive dysfunctions in scopolamine-induced amnesia animal models. *Ex vivo* tests also demonstrated that compound **210** suppressed AChE and repaired the oxidative damage caused by scopolamine. The PAS and active catalytic site (CAS) residues of AChE displayed a reciprocal binding affinity and active site interactions, according to docking and dynamics simulations of **210**. The compound **210** with a propyl (n = 3) linker have potential AChE inhibitory action. Compound **210**, which contains a phenylpiperazine moiety, was found to have satisfactory AChE inhibitory activity (IC_{50} = 0.6 μM). Notably, EWG (nitro, **211**; and fluoro, **212**) and electron-releasing (methoxy, **213**) substituents increased AChE inhibition at the *p*-position of the phenylpiperazine ring (**211**, IC_{50} = 0.5 μM; **212**, IC_{50} = 0.4 μM; **213**, IC_{50} = 0.3 μM). Compound **213**, which contains a 4-methoxyphenyl group, inhibited AChE more effectively than compounds **211** and **212**. The OCH_3 group's non-polar properties, which interacted with AChE's hydrophobic pocket, may have improved AChE inhibitory potential. In a study of compounds with various electron-withdrawing groups, analog **211** with a fluoro atom demonstrated somewhat greater inhibitory capability against AChE than compound **212** with a nitro group. The increased inhibitory effectiveness might be explained by the fluorine's high electronegativity, which changes the molecule's lipophilicity. Of all the derivatives tested, compound **214**, which contains 3 carbon atoms linked to the benzylpiperazine end group, exhibited the most potent inhibition of AChE (IC_{50} = 0.2 μM). Because of the engagement of the Bz group at the bottom of the enzyme gorge and improved interaction with AChE CAS residues, the AChE inhibitory activity of compound **214** matched that of donepezil (IC_{50} = 0.01 μM). The ability of all the produced species to inhibit BChE was then tested, but none of them showed any discernible effect. Because two aromatic amino acids have been replaced with smaller aliphatic amino acids, BChE has a wider gorge than AChE[255] (Table 9).

Yurttaş *et al.* (2019) described a method for synthesizing [2-(4-(2,3,4-substituted phenyl)piperazin-1-yl)-4-phenylthiazol-5-yl][3,4-substituted phenyl]methanone derivatives **297** and investigated their anticholinesterase properties. The molecular interactions as well as the kinetic mode were examined. The Ellman approach was used to look at how AChE and BChE enzymes

were inhibited. The activity of 44 compounds was assessed on AChE and BChE enzymes at doses of 103 and 104 μM. The inhibitory dosage for six compounds on AChE varied from 0.268 μM to 2.104 μM. Compound **215** with the 4-methoxy group (IC_{50} = 0.268 μM) and compound **216** with the 4-methoxy and 3-methyl substituents had the greatest AChE inhibitory action (IC_{50} = 0.286 μM). Hydrogen bonding with Arg296 and Ar interactions with Trp286 were also investigated[256] (Table 9).

Abbasi *et al.* (2020) described a technique for synthesizing and testing multifunctional compounds **217–220** against BChE. The BChE enzyme has been shown to be inhibited by two of these compounds **217** and **219**. Assessment of the hemolytic activity potential of **218** indicated that it possesses low toxicity level. An approach previously published for the BChE. Enzyme was used to measure the activity of the enzyme inhibitor. The data reveal that several of the chemicals have potential inhibitory capacity against this enzyme. Though the observed activity is related to the combined effect of all functionalities embedded in a molecule's entire framework, the effects of different entities in these four molecules, such as furoyl, piperazine, and benzamide functionalities, were examined to establish a brief SAR. *N*-Cyclohexyl-4-[4-(2-furoyl)-1-piperazinyl]methyl-benzamide **218** and *N*-cyclohexyl-3-[4-(2-furoyl)-1-piperazinyl] methyl-benzamide were the most effective inhibitors of BChE enzyme **220**. The other two compounds, **217** and **219**, remained the least efficient due to their higher IC_{50} values. Eserine was utilized as the reference drug, attaining IC_{50} value of 0.85 μM. The difference between these compounds can be seen in the *N*-substituted groups such as aralkyl/aryl and the location of the methylene group on the benzamide moiety, as shown in the structures. In compounds **218** and **220**, the cyclohexyl group is linked to the nitrogen of the benzamide functionality, but in compounds **217** and **219**, a benzyl group is attached to the amide nitrogen. In molecules **217** and **218**, the methylene group is perpendicular to the benzamide moiety, but in molecules **219** and **220**, it is in the third position. When compared to the reference drug, eserine, which has an IC_{50} of 0.85 μM, the addition of methylene at the third position of the benzamide moiety reduces the IC_{50} from 252.36 μM in **218** to 54.81 μM in **220**. Compounds **217** and **219** both had an evident impact due to the existence of a methylene group in *p*-position to the benzamide, as indicated by the IC_{50} of compound **217** (289.61 μM), which exhibited stronger enzyme inhibition than **219**, which had an inhibitory potential of 412.71 μM. Eserine was utilized as a positive control for cholinesterase enzymes. The inhibitory potential could be improved even further by replacing a substituted cycloalkyl or straight chain alkyl group for the cycloalkyl group. Compounds **218** and **220**, as a result, might be viable novel therapeutic candidates for inhibiting the BChE enzyme[257] (Table 9).

SAR studies of piperazine analogs demonstrate that the reported derivatives are active against AChE and BChE enzymes (Fig. 19). All the structural features are performing a significant role in the inhibitory activity, though, a slight variation in the activity of these analogs is due to variability in the nature and positions of substituents on aryl rings. The smaller groups (–CH_3, –Ph, –Et, –CF_3, –CN, –Cl, –F, –Br, –OCH_3, –OH) attached to the piperazine ring show higher AChE and BChE inhibitory abilities as compared to the bulky groups (furan, urea, thiazole) present on the rings. All the presented analogs thus far have shown excellent ChE inhibitory abilities with minimum toxic side effects. Moreover, these analogs are easy to synthesize in the laboratory, making them appealing for viable development and marketing as drugs against cholinesterase.

Szymanski *et al.* (2012) present a method for synthesizing and testing 4-fluorobenzoic acid and 2,3-dihydro-1*H*-cyclopenta[*b*]quinoline derivatives for AChE and BChE inhibition. The compounds were made by condensing amino derivatives of 2,3-dihydro-1*H*-cyclopenta[*b*]quinoline and 4-fluorobenzoic acid. The Ellman spectrophotometric method was used to conduct biological testing for cholinesterase inhibition. Compounds **222** (IC_{50} = 10.80 μM for AChE; 4.70 μM for BChE) and **224** (IC_{50} = 153 μM for AChE; 559 μM for BChE) proved less active than tacrine (IC_{50} = 0.016 μM for AChE; 0.0026 μM for BChE). The activity of compounds **223** (IC_{50} = 5.83 μM for AChE; 14.00 μM for BChE), **226** (IC_{50} = 5.20 μM for AChE; 699 μM for BChE), and **227** (IC_{50} = 5.48 μM for AChE; 744 μM for BChE), on the other hand, is comparable to that of tacrine. Compounds **221** (IC_{50} = 1.07 μM for AChE; 4.59 μM for BChE), **224** (IC_{50} = 0.49 μM for AChE; 5.91 μM for BChE), and **225** (IC_{50} = 2.77 μM for AChE; 717 μM for BChE) were shown to be more effective in deactivating AChE than tacrine. When compared to tacrine, all the generated compounds displayed better selectivity for AChE than BChE, except for compound **221**. This compound was like tacrine in terms of AChE selectivity, although it was more selective for BChE[258] (Table 10).

Najafi *et al.* (2016) reported a collection of acridine-chromenone and quinoline-chromenones and evaluated them for AD. 7-(4-(6-Chloro-2,3-dihydro-1*H*-cyclopenta[*b*]quinolin-9-ylamino)phenoxy)-4-methyl-2*H*-chromen-2-one **228** had the most anti-AChE inhibitory action (IC_{50} = 16.17 μM) compared to rivastigmine (IC_{50} = 11.07 μM). It is worth noting that kinetic studies and molecular modelling demonstrated that **228** interacted with both the catalytic active site and the peripheral anionic site of AChE simultaneously. The anti-AChE activity of **228** was the greatest (IC_{50} = 16.17 μM), while the rest of these compounds were only moderately effective in suppressing AChE. This compound has a 4-methylchromenone group as a peripheral site interaction unit and a quinoline structure as a catalytic site binding unit. Based on kinetic studies and molecular modelling, analog **228** has enough span to bind to both the CAS and the PAS of AChE as a dual binding inhibitor. In the PAS, the 4-methylchromenone group of **228** showed parallel π–π stacking with Trp279 at the gorge's mouth, but in the CAS, parallel π–π stacking with Trp84 was seen at the gorge's bottom. The neuroprotective effect was low as compared to quercetin[259] (Table 10).

Liu *et al.* (2017) developed a novel class of multitarget drugs that bind to AChE, BChE and monoamino oxidase (MAO) A and B. Novel 3,4-dihydro-2(1*H*)-quinoline-*O*-alkylamine compounds were prepared using a conjunctive technique combining the JMC49 (MAO-B inhibitor) and donepezil. The study described the synthesis of a novel family of 3,4-dihydro-2-(1*H*)-quinoline-*O*-alkylamine derivatives that can be used to treat AD. According

to both kinetic and molecular modelling studies, the most promising compound **229** exhibited powerful and balanced inhibitory effects against AChE, BChE, hMAO-A and hMAO-B. With IC_{50} values of 0.56 μM and 2.3 μM, compound **229** exhibited the highest inhibitory action against AChE and BChE and showed even better inhibitory effectiveness against hMAO-A (IC_{50} = 0.3 μM) and hMAO-B (IC_{50} = 1.4 μM). The kinetic study showed that **229** inhibited AChE in a mixed-type manner and that it could bind to both the CAS and the PAS, which was consistent with the molecular modelling studies. Furthermore, their findings showed that the compound could cross the blood–brain barrier (BBB) *in vitro* and adhered to Lipinski's rule of five. The findings of this study imply that **229** might be a potential multi-target lead chemical for further development into advanced AD therapy[260] (Table 10).

Sarrafi *et al.* (2017) described a procedure for developing and manufacturing cholinesterase inhibitors, which consisted of polyfunctionalized tacrine-derived compounds, most notably 5-amino-2-phenyl-4*H*-pyrano[2,3-*b*] quinoline-3-carboxylates. *In vitro* inhibition studies against AChE and BChE established that most compounds were efficient AChE inhibitors, with the potential for BChE inhibition remaining. The most potent compound against AChE/BChE was compound **230**, which bears a 4-(3-bromophenyl) moiety (IC_{50} = 0.069 μM and 1.35 μM, respectively). The anti-AChE activity of **230** was 5 times that of tacrine. Furthermore, the promising chemical **230** demonstrated lower cytotoxicity in HepG2 cells when compared to tacrine. According to the SAR study, a chloro/bromo atom at the *o*- or *m*-position of the 4-phenyl ring can enhance anticholinesterase activity. With respect to modification of substituents on the 4-phenyl ring, while electron releasing and EWG are not favorable for *para*-position, electron withdrawing groups such as chloro and bromo located at the *ortho* or *meta* positions may improve the cholinesterase inhibition potential[261] (Table 10).

Iqbal *et al.* (2018) synthesized a series of quinoline carboxylic acids and investigated their inhibitory capabilities against monoamine oxidase and cholinesterase *in vitro* to identify novel and efficient Parkinson's disease inhibitors. The strongest inhibitors were subjected to molecular docking and *in silico* studies to uncover the likely binding mechanisms in the active site of monoamine oxidase enzymes. To measure the compounds' drug-likeness, molecular properties were also assessed. The examined compounds were shown to be particularly active against monoamine oxidase (A and B), with IC_{50} values of 0.51 and 0.51 μM for both isoforms of MAO, respectively. The tested compounds displayed a significant and completely specific inhibitory action on AChE, with IC_{50} values ranging from 4.36 to 89.24 μM (AChE). Quinoline **231** was shown to be the most powerful inhibitor of AChE among the compounds examined, with an IC_{50} value of 4.36 μM. Docking experiments confirmed strong binding site interactions with the inhibitors. Such quinolines hold promise as potential agents to treat neurodegenerative illnesses although they will require additional pharmacophore tweaking to boost their binding affinities. Given the importance of this target in PD pathogenesis, compound **232** might be a promising new chemical entity for the creation of multi-target directed ligands[262] (Table 10).

According to Iqbal *et al.* (2018) cholinesterases (ChEs) play an important role in cholinergic transmission control. By restoring ACh levels in the brain, inhibition of ChEs is believed to embody a novel and potentially therapeutic target for neurodegenerative illnesses like AD. To increase the chemical diversity of cholinesterase inhibitors, a variety of quinoline chalcones derivatives were tested against AChE and BChE isoenzymes. These were discovered to exhibit strong anti-AChE and anti-BChE activity. Homology models were used to conduct molecular docking experiments on both AChE and BChE isoenzymes with the objective of establishing the likely binding mechanisms of the strongest inhibitor in the series. To analyze the pharmacological similarity of newly studied compounds, they employed *in silico* ADME assessment. The ADME results for compounds **233** (IC_{50} = 0.032 for AChE and 0.90 μM for BChE) and **234** (IC_{50} = 2.99 for AChE and 0.11 μM for BChE) were positive, indicating that these derivatives will have high oral bioavailability and projected to be more potent than donepezil (IC_{50} = 0.02 for AChE and 0.23 μM for BChE). Because of their favorable ADME profiles, the investigated analogs are expected to be a safer class of cholinesterase inhibitors[263] (Table 10).

Chen *et al.* (2019) presented the development, production, and testing of a variety of new multifunctional quinoline-ferulic acid hybrids with cholinesterase inhibitory characteristics. Both AChE and BChE were inhibited by most of the compounds. The most effective inhibitor of AChE and BChE was determined to be **235** (AChE IC_{50} = 0.62 μM; BChE IC_{50} = 0.10 μM). According to molecular docking and dynamic modelling, the generated compounds connect to the target by simultaneously interacting with the catalytic active site (CAS) and the peripheral anionic site (PAS) of both AChE and BChE. The U-shaped conformation of **235** coupled to BChE was preferred over the linear conformation of **235** bound to AChE. According to cell-based experiments, compound **235** exhibit moderate neuroprotective effects against H_2O_2-induced oxidative damage in PC12 cells. Furthermore, **235** had lesser hepatotoxicity than tacrine, suggesting that it might be a safer alternative to treat AD[264] (Table 10).

Brum *et al.* (2019) developed and evaluated quinoline-piperonal hybrids as prospective AD therapies. Theoretical examination of the compounds' pharmacokinetic and toxicological attributes revealed that they have excellent oral bioavailability and can pass the blood–brain barrier to reach their target. Three compounds were shown to exhibit inhibitory action against acetyl- and butyrylcholinesterase in the Ellman's test, with one analog capable of deactivating both enzymes. Further molecular docking studies of the 6 analogs developed aided in clarifying the primary interactions that might be accountable for the detected inhibitory effects. The existence of aromatic rings in the quinolines resemble the base structure of tacrine (IC_{50} = 0.0414 μM) allows enables π–π interactions with the amino acids present in the active site, while the guanyl hydrazone is able of interacting with the CAS of AChE *via* the guanidine function. In comparison to rivastigmine, compound

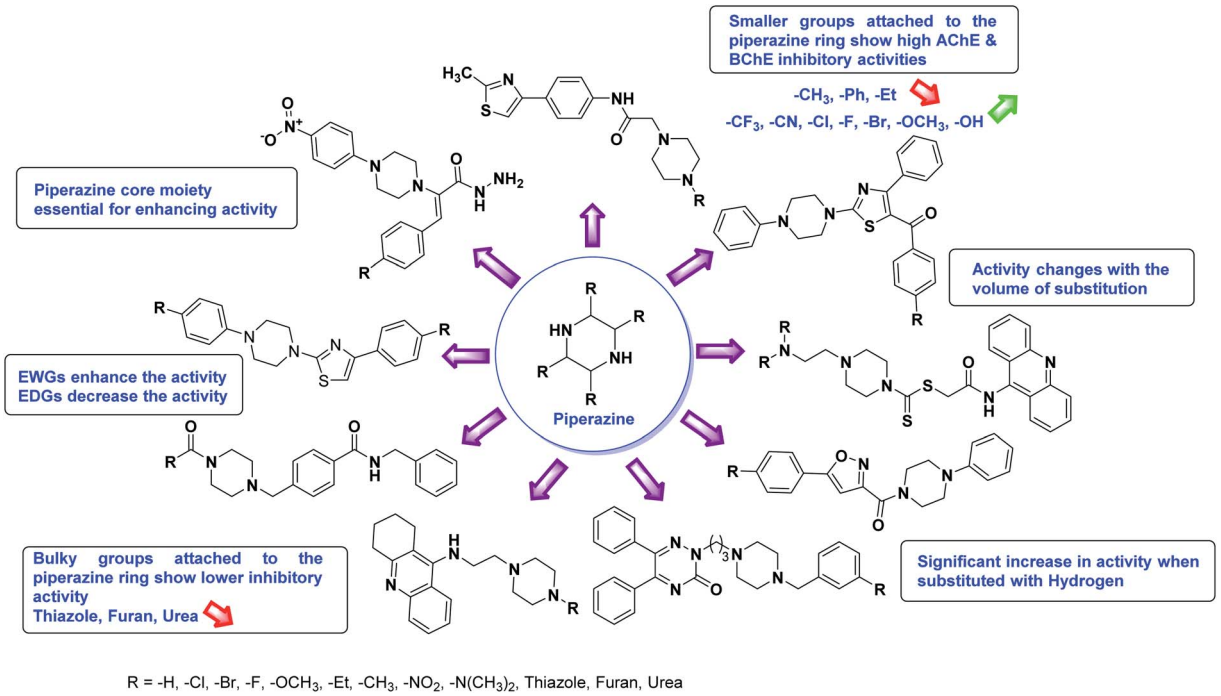

Fig. 19 SAR analysis of different piperazine derivatives as AChE and BChE inhibitors.

236 (IC_{50} = 32.06 μM) showed promise as AChE inhibitors[265] (Table 10).

Kouznetsov *et al.* (2019) reported the preparation of triazolyl-quinoline hybrids and described their modest inhibitory action against commercial AChE from *Electrophorus electricus* (electric-eel AChE) (IC_{50} = 27.7 g mL^{-1}) and low anti-ChE activity on *S. frugiperda* larval homogenate (IC_{50} = 68.4 g mL^{-1}). Molecular docking simulations revealed that hybrid **237** binds to the enzyme's catalytic active site (CAS) and the rim of the cavity, operating as a mixed (competitive and noncompetitive) inhibitor like methomyl. Triazolyl-quinolines **238** and **239** act as non-competitive inhibitors of AChE by binding around the periphery of the enzyme cavity[266] (Table 10).

Bazine *et al.* (2020) employed the Kabachnik–Fields reaction to develop and synthesize a series of novel amino phosphonate derivatives with quinoline moiety. The derivatives **240** (IC_{50} = 28.42 μM), **241** (IC_{50} = 38.39 μM), **242** (IC_{50} = 52.55 μM), and **243** (IC_{50} = 55.23 μM) demonstrated the highest inhibitory activity against AChE when compared to galantamine standard (IC_{50} = 21.81 μM). All tested compounds showed strong anti-BChE activity when compared to galantamine standard (IC_{50} = 120.93 μM)[267] (Table 10).

Garlapati *et al.* (2020) prepared several novel tacrine analogues and evaluated them for cholinesterase inhibitory activity. Most synthesized compounds showed inhibitory action against AChE and BChE enzymes *in vitro*. With IC_{50} values of 0.65, 1.32 and 0.85, 1.65 and 0.92, 1.91 μM against AChE and BChE, compounds **244**, **245** and **246**, which have a larger saturated carboxylic ring tethered to the pyridine group and 3,4-dihydroxy, 3,4,5-trimethoxy substituents on the aryl ring attached at the stereogenic centre, have shown identical potency to tacrine. Tacrine's IC_{50} values against AChE and BChE were 0.47 and 0.65 μM, respectively, while donepezil had IC_{50} values of 0.71 and 0.31 μM respectively. All the analogs had hydrogen bond interactions with the binding site, according to docking experiments[268] (Table 10).

Garlapati *et al.* (2021) prepared a new family of AChE and BChE inhibitors based on the structure of tacrine using a multicomponent Friedlander reaction between 2-amino-benzonitrile and cycloalkanones. The Ellman technique was used to test their inhibitory ability against AChE and BChE. When compared to the standard tacrine and rivastigmine, which had IC_{50} values of 0.23, 0.47 μM for AChE and 0.31, 0.65 μM for BChE, respectively, compounds **247** and **248**, which contained piperazine containing acetamide and butyrylamide chains, had IC_{50} values of 0.71, 0.04 μM for AChE, 1.01, 0.03 μM for BChE, 0.52, 0.03 μM for AChE, and 0.73, 0.04 μM for BChE, respectively. As a result, these five membered-ring novel tacrine analogs have emerged as possible cholinesterase inhibitors that might one day be employed as Alzheimer's anti-drugs. Docking studies on all the compounds demonstrated tight hydrogen bond interactions inside the binding area. With IC_{50} values of 0.97 and 1.74 μM, the unsubstituted compound **247** (n = 3 and n' = 1), which has a five-membered 'C' ring and a two-carbon linker, has demonstrated significant activity against AChE and BChE. These findings pointed to a larger nonpolar area in the binding pocket that might accommodate the larger cycloalkyl ring. The inhibitory action of the preceding species found active *in vitro* on AChE and BChE in the brain was investigated *in vivo*. To further understand the binding interactions inside the active site of cholinesterases, the compounds were also subjected to molecular docking investigations. Except for a few compounds,

Table 10 Chemical structures of quinoline derivatives **221–248** and their IC_{50} values against cholinesterase enzymes

Compound no.	Chemical structure	IC_{50} values (μM) AChE	BChE	References
221	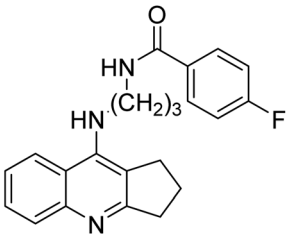	1.07	4.59	258
222	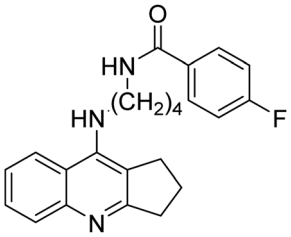	10.80	4.70	258
223	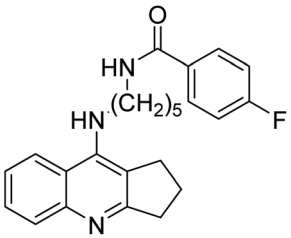	5.83	14.00	258
224	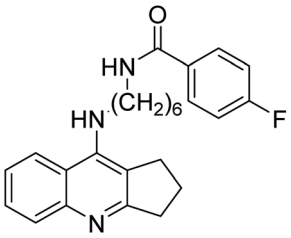	0.49	5.91	258
225	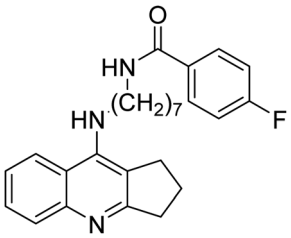	2.77	717	258
226	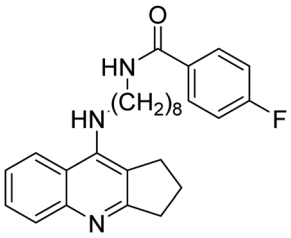	5.20	699	258

Table 10 (*Contd.*)

Compound no.	Chemical structure	IC_{50} values (μM) AChE	BChE	References
227	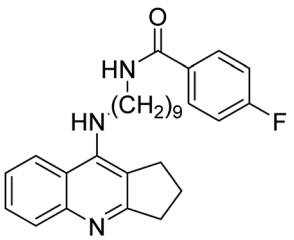	5.48	744	258
228	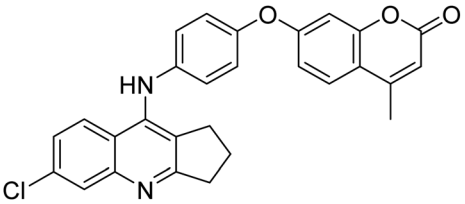	16.17	—	259
229	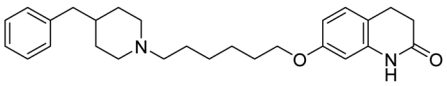	0.56	2.3	260
230	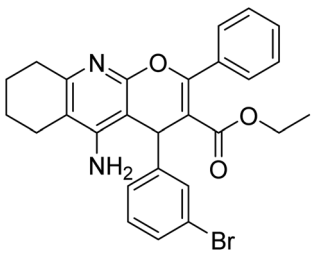	0.069	1.35	261
231	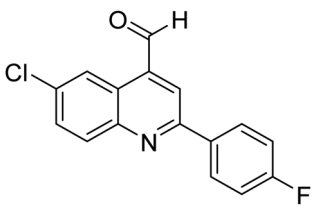	4.36	—	262
232	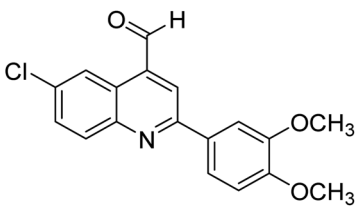	7.10	—	262
233	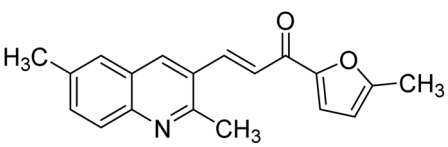	0.032	0.90	263
234	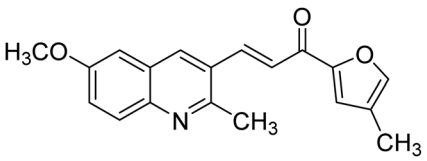	2.99	0.11	263

Table 10 (*Contd.*)

Compound no.	Chemical structure	IC_{50} values (μM) AChE	BChE	References
235	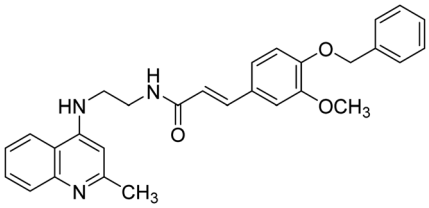	0.62	0.10	264
236	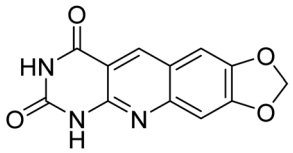	32.06	—	265
237	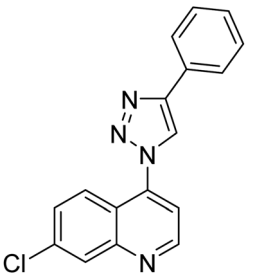	10.24	—	266
238	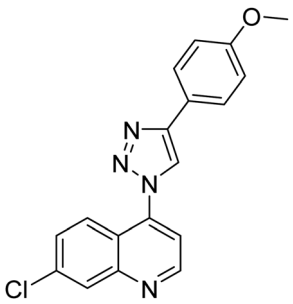	11.89	—	266
239	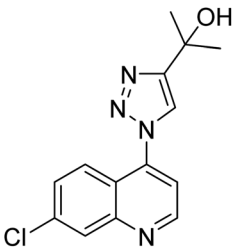	17.74	—	266
240	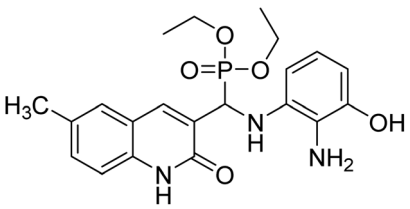	28.42	—	267

Table 10 (*Contd.*)

Compound no.	Chemical structure	IC_{50} values (μM) AChE	BChE	References
241	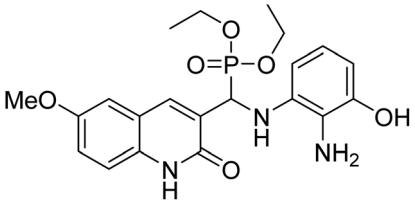	38.39	—	267
242	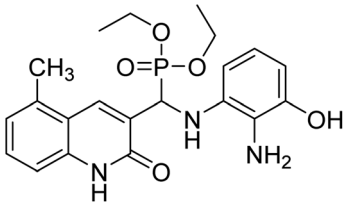	52.55	—	267
243	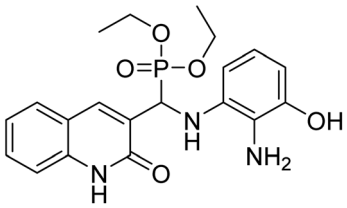	55.23	—	267
244	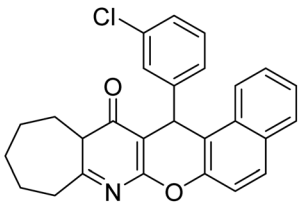	0.65	1.32	268
245	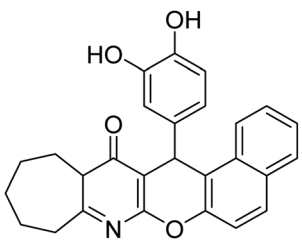	0.85	1.65	268
246	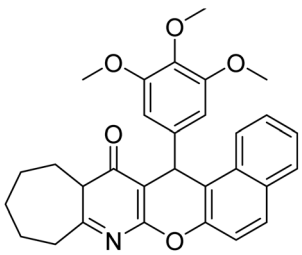	0.92	1.91	268
247	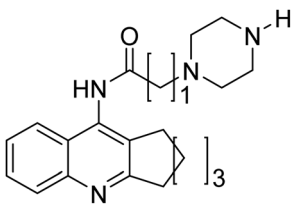	0.71	0.04	269

Table 10 (*Contd.*)

Compound no.	Chemical structure	IC_{50} values (μM) AChE	BChE	References
248	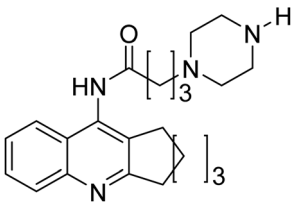	1.01	0.03	269

docking tests revealed that the developed molecules interacted with the nicotinic receptor *via* at least two hydrogen bond interactions[269] (Table 10).

The SAR studies of the aforementioned quinolines demonstrate that the various analogs are active AChE and BChE inhibitors (Fig. 20). All the structural features are performing a significant role in the inhibitory activity, though, a slight variation in the activity of these analogs is due to variability in the nature and positions of substituents on aryl rings. The smaller groups (–$N(CH_3)_2$, –CH_3, –Ph, –Et, –CF_3, –Cl, –F, –Br, –OCH_3, –OH, *etc.*) attached to the quinoline ring show higher AChE and BChE inhibitory abilities compared to the bulky groups (tacrine, furan urea, *etc.*) present on the rings. All the presented analogs thus far have shown good to excellent ChE inhibitory abilities with a minimum toxic side effect. Furthermore, these are easy to synthesize in the laboratory, making them attractive for viable development and marketing as drugs against cholinesterase.

Rao *et al.* (2011) created a novel class of 2,4-disubstituted pyrimidines and investigated them as dual cholinesterase and amyloid-β (Aβ)-aggregation inhibitors. *In vitro*, the most potent AChE inhibitor was determined to be *N*-(naphth-1-ylmethyl)-2-(pyrrolidin-1-yl)pyrimidin-4-amine **249** (IC_{50} = 5.5 μM). The most effective and selective BChE inhibitor was discovered to be 2-(4-methylpiperidin-1-yl)-*N*-(naphth-1-ylmethyl)pyrimidin-4-amine **250**, which was roughly 5.7 times more potent than the commercially available, authorized reference drug galantamine (BChE; IC_{50} = 12.6 μM). Furthermore, *N*-benzyl-2-(4-methylpiperazin-1-yl)pyrimidin-4-amine **251**, a specific AChE inhibitor, effectively reduced hAChE-induced $Aβ_{1–40}$ fibril

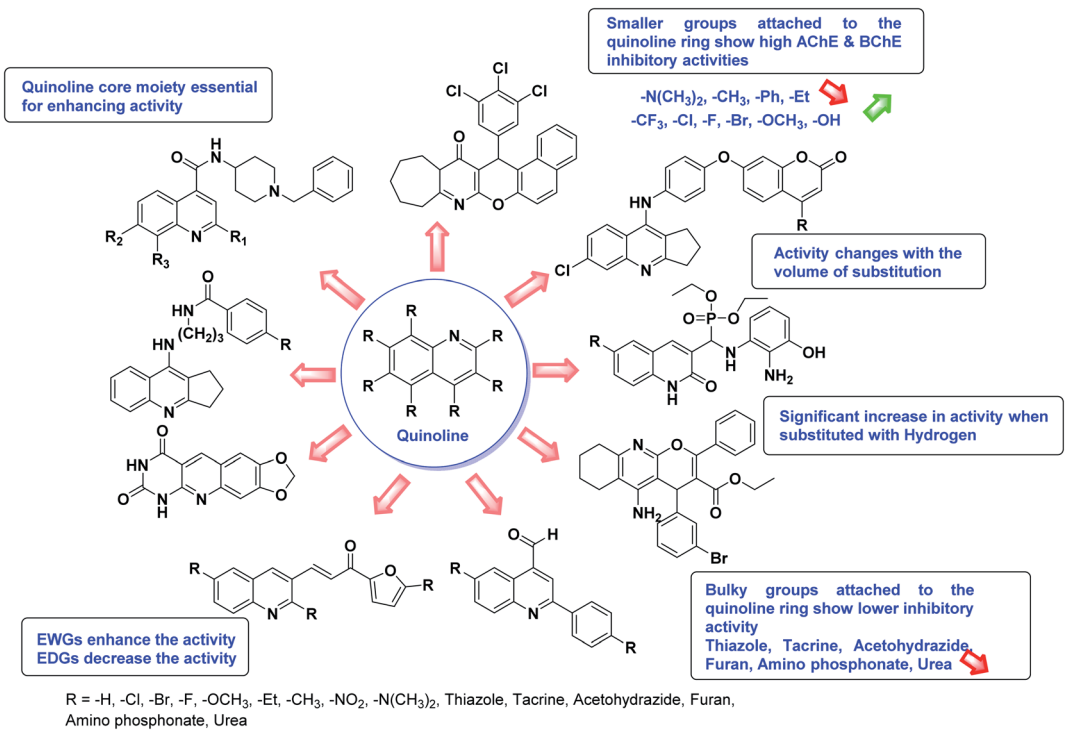

Fig. 20 SAR analysis of different quinoline derivatives as AChE and BChE inhibitors.

Table 11 Chemical structures of pyrimidine derivatives **249–262** and their IC_{50} values against cholinesterase enzymes

Compound no.	Chemical structure	IC_{50} values (μM) AChE	BChE	References
249	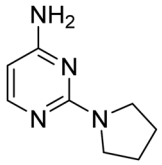	5.5	56.9	270
250	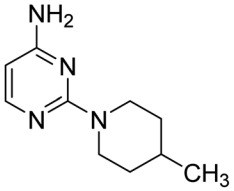	8.7	26.4	270
251	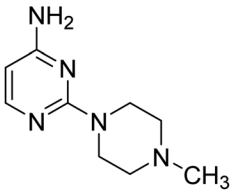	7.9	2.2	270
252	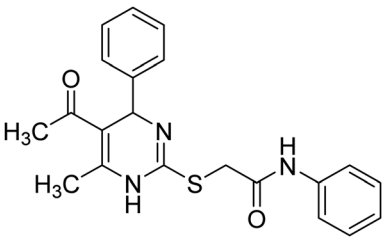	0.17	2.37	271
253	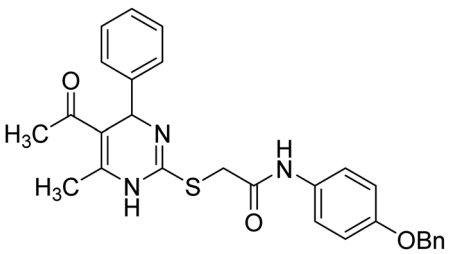	0.39	5.69	271
254	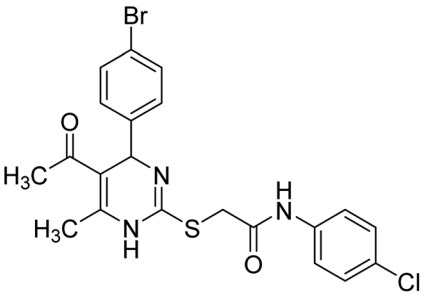	2.01	—	271

Table 11 (*Contd.*)

Compound no.	Chemical structure	IC_{50} values (μM) AChE	BChE	References
255	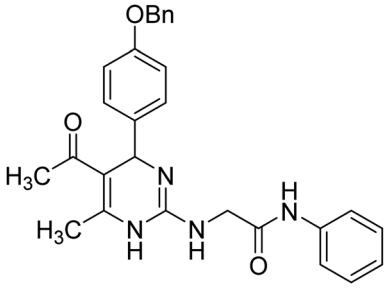	—	30	271
256	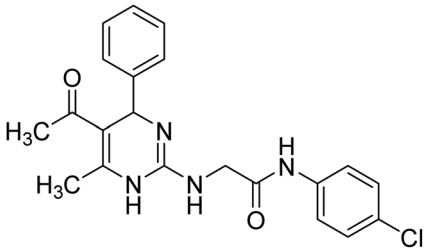	2.01	—	271
257	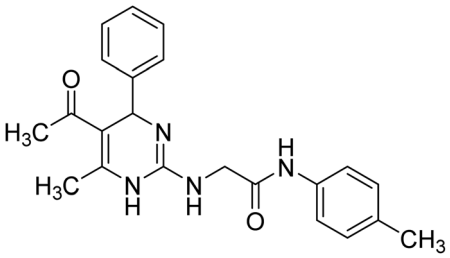	15.01	—	271
258	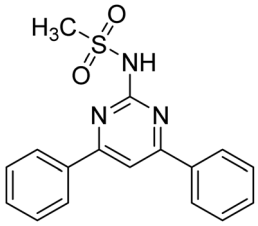	143.73	144.81	272
259	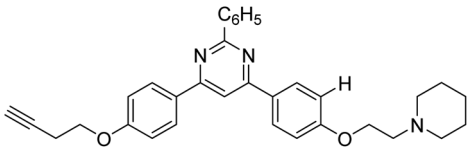	2.84	—	273
260	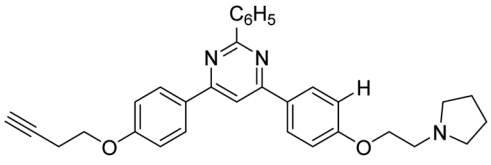	2.19	—	273

Table 11 (*Contd.*)

Compound no.	Chemical structure	IC_{50} values (μM) AChE	BChE	References
261	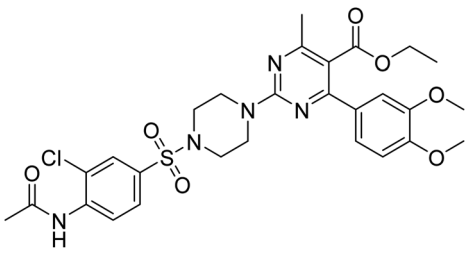	47.33 nM	159.43 nM	274
262	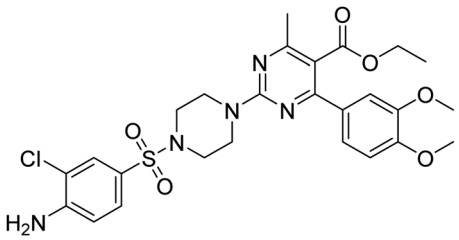	51.36 nM	153.3 nM	274

aggregation (59% inhibition). Furthermore, molecular modelling studies revealed that a central pyrimidine ring can be employed as a template for generating dual inhibitors of cholinesterase and AChE-induced Aβ aggregation, allowing for the targeting of a variety of pathogenic pathways in AD. ChE inhibition against AChE was enhanced by the addition of a five-membered heterocycloalkyl C-2 group, such as pyrrolidine **251** (AChE $IC_{50} = 8.7$ μM; BChE $IC_{50} = 26.4$ μM). The ChE inhibitory potency was lowered when the C-2 five-membered pyrrolidine was replaced with a six-membered ring. On the other hand, the addition of a C-2 4-methylpiperidine **250** increased BChE inhibitory potency and selectivity. Compound **250** had a 5.7-fold higher BChE inhibition ($IC_{50} = 2.2$ μM) and selectivity (S.I. = 11.7) than the reference drug galantamine (BChE $IC_{50} = 12.6$ μM; S.I. = 0.27) and was much more potent than donepezil (BChE $IC_{50} = 3.6$ μM), relative to **250** (AChE $IC_{50} = 25.8$ μM)[270] (Table 11).

Based on the pharmacological relevance of the dihydropyrimidine (DHPM) scaffold, Rashid *et al.* (2016) synthesized substituted DHPMs coupled with an acetamide linker to substituted aromatic anilines and tested their effectiveness as AChE and BChE inhibitors. Among the 4-dihydropyrimidine-2-thione and 2-amino-1,4-dihyropyrimidines series, compounds **355** and **356** having the highest IC_{50} values of 0.17 and 0.39 μM, respectively, inhibited AChE effectively. BChE inhibition was seen at higher doses (2.37–56.32 μM). The compounds were tested for AChE (*Electrophorus electricus*) and BChE inhibition using Ellman's approach (equine serum). The most efficient ChE inhibitor was identified to be compound **252**, which has a 14-fold selectivity for AChE. (IC_{50} values for AChE 0.17 μM and BChE 2.37 μM). With an IC_{50} of AChE 0.39 μM and BChE $IC_{50} = 5.69$ μM, S.I = 15, compound **253**, which includes a benzyloxy phenyl ring, is likewise more selective against AChE. Compound **254** demonstrated significant AChE activity with IC_{50} values of 2.01 μM. **255**, on the other hand, had a low inhibitory effect on BChE, with an IC_{50} of 30 μM (S.I. = 15). With an IC_{50} of 1.07 μM (S.I. = 17), the 4-benzoxypehnyl derivative **256**, which belongs to the 2-amino-1,4-dihyropyrimidine family, is the strongest and selective AChE inhibitor. The 4-chloro substituted derivative **256** demonstrated strong AChE activity with an IC_{50} of 2.01 μM and a substitution pattern on the aniline ring. The IC_{50} value of the compounds in 2-amino-1,4-dihyropyrimidine series for BChE inhibition is seen over a greater concentration range (15.01–38.53 μM) than for AChE inhibition. Compound **257** has emerged as the most potent BChE inhibitor in this series, with an IC_{50} of 15.01 μM (ref. 271) (Table 11).

Khan *et al.* (2017) synthesized novel pyrimidine-based sulfonamides with fair to excellent yield (54–86%) in short period of time under microwave conditions. Structurally, these heterocycles have a core pyrimidine ring with a phenyl group and pyrimidine groups with sulfonamide functions. The capacity of these compounds to suppress the enzymes AChE and BChE, which are key in AD therapy, was investigated. When compared to the reference drug eserine, the IC_{50} values of the synthesized compounds varied from 3.73 μM to 57.36 μM for AChE and 4.81 μM to 111.61 μM for BChE. Among the compounds tested, compound **258** with a $-CH_3$ group was shown to be the most effective against both enzymes (AChE, $IC_{50} = 143.73$ μM; BChE, $IC_{50} = 144.81$ μM). Molecular docking and QSAR studies were also conducted on the synthesized molecules. The goal of the molecular modelling work on sulfonamide **258** was to anticipate how it would bind to the active sites of the relevant enzyme. This study presents

a straightforward approach for generating compounds with high yields and a fast response time that are helpful against AD[272] (Table 11).

Kumar *et al.* (2020) investigated AD as a complicated neurological ailment in which single-targeted treatments failed to reduce or reverse disease progression. In recent years, multi-target medicines have been explored as a therapeutic strategy for the successful treatment of AD. A variety of (4-(pent-4-yn-1-yloxy)phenyl)-2-phenylpyrimidine analogs have been examined for their effects on AChE enzyme. The bulk of the synthesized compounds were discovered to be effective AChE inhibitor, with IC_{50} values in the low micromolar range. Analogs **259** and **260** were the most effective inhibitors of AChE enzyme. The former inhibited AChE with IC_{50} value of 2.84 μM, respectively. The AChE enzyme was likewise inhibited by **260**, with IC_{50} value of 2.19 μM. Consequently, **259** and **260** may be employed as lead compounds in the design of more effective AD treatments[273] (Table 11).

According to Kumar *et al.* (2021) AD is a complicated neurological condition characterised by impaired behavioural and cognitive functions. Multitarget-directed ligand (MTDL) approaches are a potential drug development paradigm that might lead to new AD therapy alternatives. A series of new MTDLs phenylsulfonyl-pyrimidine carboxylate derivatives were designed and synthesized for the treatment of AD. To investigate the likely binding affinity of the prepared pyrimidines, a molecular docking study was done, and the findings revealed a significant interaction with the active sites of AChE and BChE. The synthesized compounds show moderate to excellent *in vitro* enzyme inhibitory activity against AChE and BChE at nanomolar (nM) doses. The drug **262** inhibited AchE non-competitively with K_i 14 nM in an enzyme kinetics study. The hybrids generated demonstrated moderate to good *in vitro* inhibitory effectiveness against AchE and BchE at nanomolar doses. **261** and **262** substances inhibited AchE and BChE, respectively, with IC_{50} values of 47.33, 51.36 nM and IC_{50} 159.43, 153.3 nM, respectively. Compounds **261** and **262** had the strongest AChE inhibitory action, which can be attributable to the presence of electron-donating dimethoxy and chloro groups, which enhance AChE binding affinity. These derivatives were able to attach to both the CAS and PAS of AChE at the same time[274] (Table 11).

SAR studies of pyrimidines demonstrate that the various derivatives are potent against AChE and BChE enzymes (Fig. 21). All the structural features perform significant role in the inhibitory activity, though, the observed variation in the activity of these analogs is due to variability in the nature and positions of substituents on aryl rings. The smaller groups ($-CH_3$, –Et, –Ph, $-OCH_3$, $-CF_3$, $-NH_2$, –CN, *etc.*) attached to the pyrimidine ring show higher AChE and BChE inhibitory abilities as compared to the bulky group (sulfonamide) present on the rings. All the presented analogs thus far have shown to excellent ChE inhibitory abilities with a low risk of toxic side effects. Furthermore, these species are inexpensive and easy to synthesize in the laboratory, making them attractive for viable development and marketing as drugs against cholinesterase.

A series of new cyanopyridine–triazine hybrids were synthesized and assessed by Hoda *et al.* (2016) as multitarget agents. These molecules were created with the aid of computational tools and synthesized utilizing a feasible and efficient synthetic approach. The inhibitory potencies of the triazines against cholinesterases were investigated. Compounds **263** and **264** showed high inhibitory action against AChE, as well as good inhibition selectivity towards AChE over BChE, with IC_{50} values of 0.059 and 0.080 μM, respectively. According to molecular modelling, these compounds interacted with AChE's catalytic active site (CAS) and peripheral anionic site (PAS) simultaneously. The mixed type inhibition mode of compound **263** in

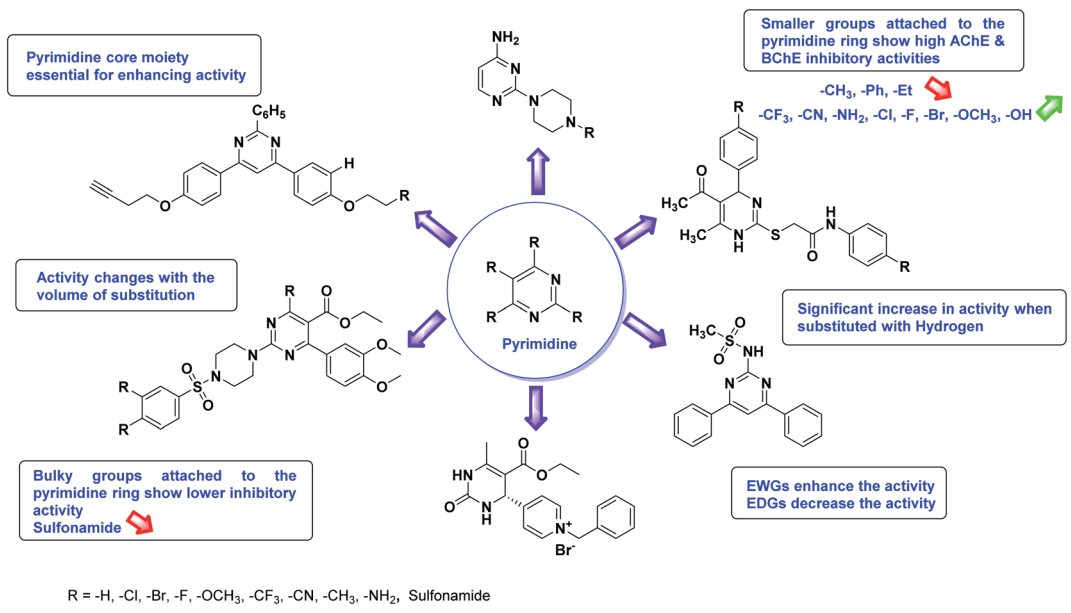

Fig. 21 SAR analysis of different pyrimidine derivatives as AChE and BChE inhibitors.

kinetic studies further confirmed the dual binding nature. Furthermore, an *in silico* analysis of the absorption, distribution, metabolism, and excretion (ADME) profiles of the best compounds **263** and **264** revealed that they had drug-like properties. Overall, these cyanopyridine–triazine hybrids seem to be a decent candidate for further pharmacological investigation in the treatment of AD. Ellman's approach was utilized to evaluate the inhibitory activity of synthesized compounds against AChE (from *Electrophorus electricus*) and BChE (from horse serum) with donepezil (IC_{50} = 0.038 μM for AChE; 3.14 μM for BChE) and tacrine (IC_{50} = 0.13 μM for AChE; 0.054 μM for BChE) acting as positive controls. To improve the inhibitory effect of the generated compounds on ChEs, substituents with varied electronic properties were added to the core triazine scaffold. Compounds with 3-(trifluoromethyl) aniline connected to the triazine moiety inhibited AChE more efficiently than those with 2-fluoro and 3-chloro-4-fluoro substituents, *i.e.* **265** (IC_{50} = 1.412 μM) and **266** (IC_{50} = 1.701 μM), respectively. Within the subgroup of triazines containing 3-(trifluoromethyl) aniline, the inhibitory effect against AChE improved as the electron withdrawing properties of the 5-(substituted) aniline moiety increased. Compound **263**, which included 3-chloro-4-fluoroanaline, showed the highest inhibitory potency (IC_{50} = 0.059 μM). Furthermore, substituting cyclopropylamine for the modified aniline group in compound **267** resulted in a 9-fold drop-in inhibitory activity (IC_{50} = 0.528 μM), compared to the most powerful compound **263**. All the target compounds demonstrated a greater selectivity for AChE than for BChE, with the best derivative **263** having a 61-fold selectivity ratio. In addition, the inhibitory efficacy of **263** was shown to be comparable to conventional donepezil (IC_{50} = 0.038 μM) and superior to tacrine (IC_{50} = 0.038 μM). Additionally, docking experiments involving cholinesterases were carried out to better understand their method of action[275] (Table 12).

According to Boga *et al.* (2019), 1,3-diaryltriazenes are useful linkers for diverse pharmacological applications. In their investigation, the diazonium salt of sulfanylamide and substituted aryl amines were used to synthesize a series of 1,3-diaryltriazene sulfonamides. Most of the 1,3-diaryltriazene sulfonamides in the present series showed high activity against both cholinesterases, AChE and BChE. All chemicals, except for **268** and **269**, showed stronger BChE inhibitory activity than AChE inhibition activity. With % inhibition values of 84.48, 85.01 and 93.67, the compounds **268**, **270** and **271** inhibited AChE more efficiently than the standard drug galantamine. The compounds **269**, **272**, **273** and **274** were moderate inhibitors of this enzyme, with % inhibition values ranging from 55.35 to 69.60. With 98.47 and 97.00% inhibition, compounds **271** and **274** reduced BChE activity the highest at 200 μM. Because the AChE and BChE enzymes are associated to neurodegenerative diseases and their inhibition is important for various sorts of brain problems, these 1,3-diaryltriazene sulfonamides could serve as useful in *in vivo* research[276] (Table 12).

Supuran *et al.* (2020) investigated novel triazine benzenesulfonamides containing aromatic amines, dimethylamine, morpholine, and piperidine as substituents on the 1,3,5-triazine moiety. They compounds were investigated as AChE, BChE, and tyrosinase inhibitors. Compounds **275**, **276** and **277** demonstrated inhibitory activity against AChE with % inhibition values >90. Most of the synthesized compounds also successfully inhibited BChE, with inhibitory potencies >90%. The most potent AChE inhibitors were compounds **275**, **276** and **277** with % inhibition values of 96.37, 91.10 and 93.19, respectively, exceeding the standard medicine galantamine. The bulk of the generated compounds, on the other hand, effectively inhibited the BChE enzyme. On the % inhibition scale, several of the remaining compounds **275**, **276**, **277** and **278** exhibited % inhibition values of 87.44, 88.76, 89.21 and 88.48, respectively, which were quite comparable in values to the standard drug. The three compounds have anticholinesterase activity, suggesting that they may be produced and used as effective cholinesterase inhibitors[277] (Table 12).

SAR studies of triazines demonstrate that the different derivatives are active as AChE and BChE inhibitors (Fig. 22). All the structural features are performing a significant role in the inhibitory activity, though, a slight variation in the activity of these analogs is due to variability in the nature and positions of substituents on aromatic rings. The smaller groups (–Ph, –Me, –Et, –OMe, $–CF_3$, –OH, Cl, –Br, –CN, *etc.*) attached to the triazine ring show higher AChE and BChE inhibitory abilities as compared to the bulky groups present on the rings. All the presented analogs thus far have shown excellent ChE inhibitory abilities with less toxic side effects. Moreover, these analogs are easy to synthesize in the laboratory, making them attractive for viable development and marketing as drugs against cholinesterase.

Alptüzün (2016) used a series of pyridinium salts with alkylphenyl groups at position 1 and hydrazone structure at the 4^{th} position of the pyridinium ring to inhibit both AChE and BChE enzymes. The inhibitory activity of cholinesterase was measured using Ellman's colorimetric method (ChE). All the compounds displayed considerable AChE and BChE inhibitory activity when compared to galantamine, the reference drug, and some of them had exceptional anti-AChE activity. The series of title compounds with a benzofuran aromatic ring had the highest inhibitory action on both AChE and BChE enzymes. With an IC_{50} value of 0.23 μM, 1-(3-phenylpropyl)pyridinium bromide **280** was the most effective molecule against AChE (hAChE), whereas 4-[2-(1-(benzofuran-2-yl)ethylidene) hydrazinyl]-1-phenethylpyridinium bromide **279**, with an IC_{50} of 0.95 μM, was the most effective compound against BChE. Pyridinium ions **279** and **280** were also found to be more active than galantamine (AChE (hAChE) IC_{50} 0.43 μM; BChE IC_{50} 14.92 μM). Compound **280**, which demonstrated the highest inhibitory action against AChE, was the subject of molecular docking investigations. Several hydrazone-containing pyridinium salts were tested for their ability to inhibit cholinesterase. All compounds demonstrated inhibitory activity ranging from excellent to moderate on both AChE and BChE enzymes. In the title compounds, the length of the side chain and its hydrophobic feature appear to be important for AChE activity. The scaffold of benzofuran-pyridiniumhydrazone can be utilized as a starting point for further study and a template for further structural adjustments[278] (Table 13).

Table 12 Chemical structures of triazine derivatives **263–278** and their IC_{50} values against cholinesterase enzymes

Compound no.	Chemical structure	IC_{50} values (μM) AChE	BChE	References
263	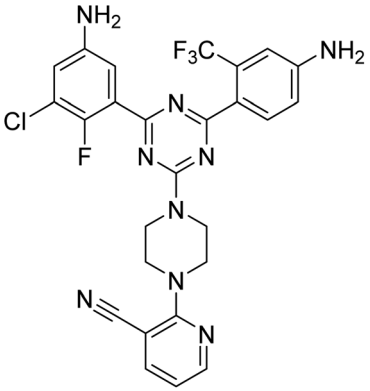	0.059	—	275
264	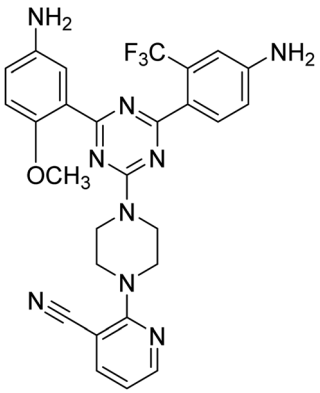	0.080	—	275
265	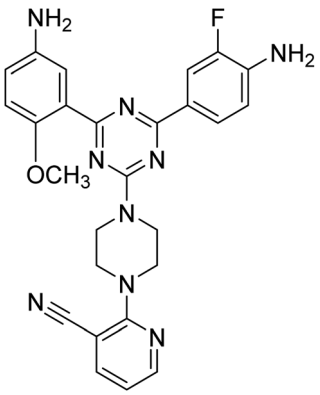	1.412	—	275
266	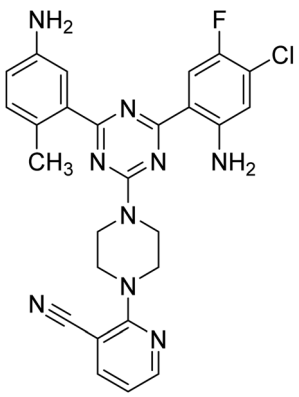	1.701	—	275

Table 12 (*Contd.*)

Compound no.	Chemical structure	IC_{50} values (μM) AChE	BChE	References
267	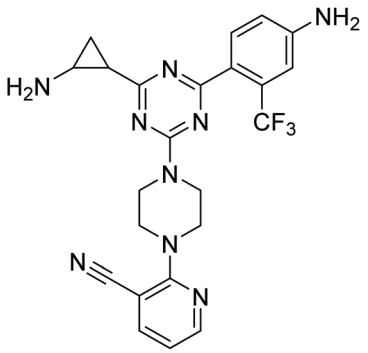	0.528	—	275
268	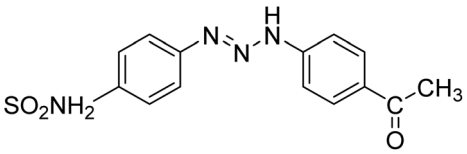	84.48	—	276
269	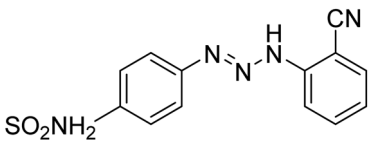	69.60	—	276
270	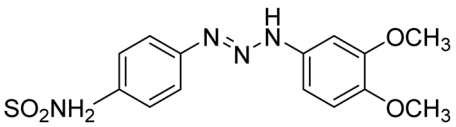	85.01	—	276
271	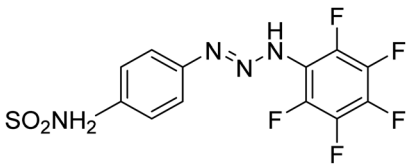	93.67	—	276
272	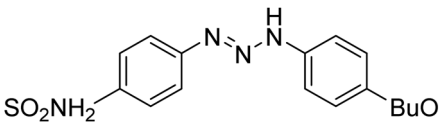	98.47	—	276
273	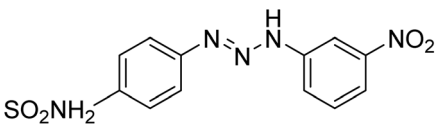	55.35	—	276
274	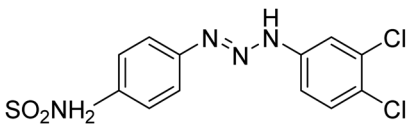	97.00	—	276
275	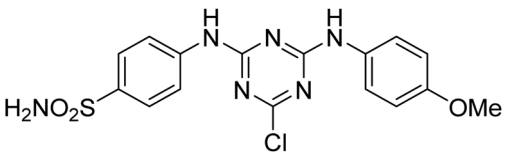	96.37	—	277

Table 12 (*Contd.*)

Compound no.	Chemical structure	IC_{50} values (μM) AChE	BChE	References
276	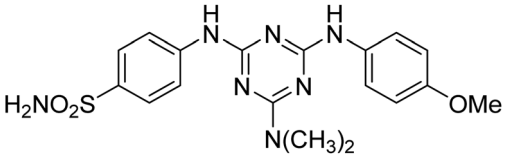	91.10	—	277
277	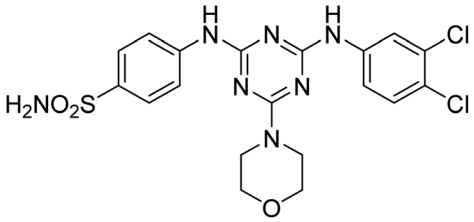	93.19	—	277
278	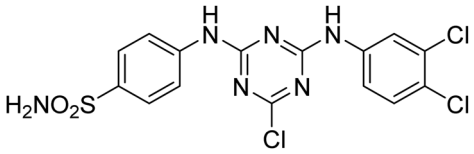	88.48	—	277

Bergamini *et al.* (2017) developed and synthesized a novel class of pyridine compounds with carbamic or amidic functions that can inhibit cholinesterase. The molecules feature two aromatic ends connected by a flexible alkyl chain of variable length. AChE and hAChE, as well as BChE and hBChE, were used to evaluate the produced compounds. Compound **281** was the best inhibitor of hAChE (IC_{50} 0.153 nM), whereas compound **282** was the most effective inhibitor of hBChE (IC_{50} 0.828 nM). According to molecular docking study, **281** may bind AChE through interacting with both CAS and PAS, confirming a mixed-type inhibition mechanism. The most active compounds against EeAChE were **281** and **282**, which had K_i values of 38.6 nM and 52.8 nM, respectively. Further research on the human isoforms of AChE and BChE revealed that, despite some differences in enzyme source, both carbamate and amide derivatives were effective inhibitors of hChE, with **283** being the most potent inhibitor of hAChE (IC_{50} 153 nM) and **284** being the best inhibitor of hBChE (IC_{50} 828 nM). Molecular docking experiments on hAChE (co-crystallized with donepezil, PDB code 4EY7) provided more insight on the most powerful ChEI in the series' method of interaction. The study found that **281** may form a variety of connections with the amino acids of the CAS area *via* the benzyl group and protonated amine nitrogens, whereas the 2,6-dichloro-pyridine moiety can contact Trp286 inside the PAS. In the amyloid self-aggregation experiment, **281**, the most potent hAChEI in this investigation, inhibited Aβ42 self-aggregation by 26.5% at 50 nM. This compound was also less toxic to T67 and HeLa cells, with IC_{50} values of 24.1 and 20.8 nM, respectively. Finally, it appears that **281** has a high inhibitory efficacy against hAChE, as well as a high selectivity against hBChE and the ability to prevent Aβ42 self-aggregation. These findings, together with the low toxicity and strong projected BBB permeability properties, make this chemical a promising candidate for the creation of novel multifactorial cholinesterase inhibitors that might help cure AD[279] (Table 13).

According to Amini *et al.* (2018), BChE inhibitors have emerged as a viable target for AD therapy. A class of dual binding site BChE inhibitors was designed and synthesized using 2,3,4,9-tetrahydro-1*H*-carbazole linked benzyl pyridine moieties. In an *in vitro* investigation, all the prepared compounds were found to be selective and potent BChE inhibitors. The most potent BChE inhibitor with mixed-type inhibition was compound **285** (IC_{50} 0.088 μM). According to docking studies, **285** is a BChE inhibitor with two binding sites. Furthermore, **285** pharmacokinetic characteristics were in accordance with Lipinski's rule. In addition, **285** is neuroprotective and inhibits the enzyme β-secretase (BACE1). This compound may also inhibit AChE-induced and self-induced Aβ peptide aggregation at doses of 100 μM and 10 μM. The findings suggest that selective BChE inhibitors hold therapeutic promise in the treatment of AD. Because intact BChE compensates for the loss of AChE activity as AD progresses, they may have therapeutic use in the treatment of the condition. According to molecular modelling studies, compound **285** had strong interactions with BChE's choline binding site, peripheral binding site, and catalytic site. It was long enough to contact the acyl pocket as well. BACE1 inhibitory and neuroprotective effects were also found in compound **285**. The pharmacokinetic properties of **285** were also confirmed using Lipinski rules of 5. In summary, the study has discovered new highly selective BChE inhibitors with therapeutic promise for AD therapy[280] (Table 13).

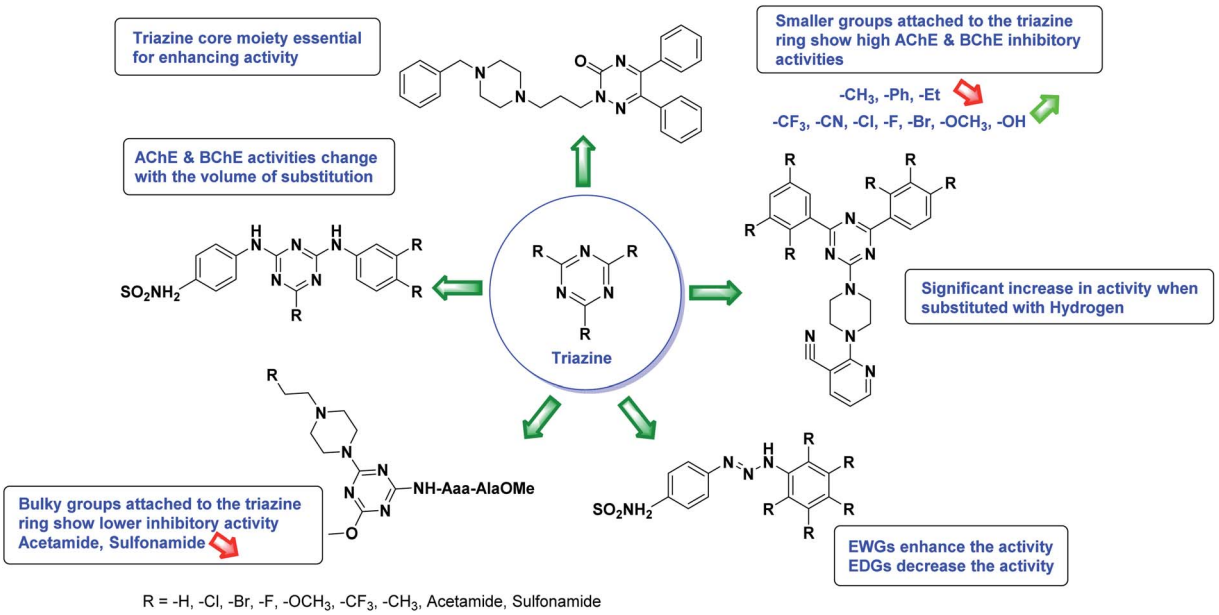

Fig. 22 SAR analysis of different triazine derivatives as AChE and BChE inhibitors.

Shirsat *et al.* (2018) synthesized and characterized new 4-aminopyridine analogs using analytical methods such as UV, IR, NMR, elemental analysis, and assessed their inhibitory character on AChE activity using molecular docking studies and Ellman's spectrophotometric method for enzyme kinetics. The antiamnesic and cognition-enhancing properties of the synthesized analogues were then evaluated using a passive avoidance test. The AChE inhibitory activity of all produced analogs was measured using the Ellman spectrophotometric technique. The inhibitory concentration of produced analogs (IC_{50}) for inhibiting AChE was calculated using Graph Pad Prism. The IC_{50} values for all the analogs ranged from moderate to excellent. Compounds **286** and **287** produced IC_{50} values of 6.32 μM and 5.58 μM, respectively, compared to rivastigmine (6.15 μM). The most active compounds **286** and **287** inhibited AChE in a non-competitive manner (K_i = 11.23 and 6.44, respectively). The non-competitive inhibition is attributed to a probable contact of the analog with the peripheral anionic site (PAS) of AChE and docking investigations have supported this. *In vitro* studies of the synthesized analogs revealed that compounds **286** and **287** had the highest activity when compared to the standard drug rivastigmine, whereas enzyme kinetic studies demonstrated a non-competitive inhibition of AChE, which was attributed to a possible interaction of the analogs with AChE's peripheral anionic site (PAS) and confirmed by molecular docking studies. The hydroxyl group of one of these compounds' phenyl rings was observed forming an H-bond with Tyr-70 in docking studies, and Tyr-70 appears to play a dual role in the active centre: (a) its hydroxyl appears to maintain the functional orientation of Phe-288 and Tyr-70 by hydrogen bonding, and (b) its aromatic moiety appears to maintain the functional orientation of the anionic subsite Trp-84. Compounds **286** and **287** were discovered as the most potent species in an AChE inhibition and passive avoidance test, which could lead to the discovery of new cognition enhancers soon[281] (Table 13).

The SAR studies of the aforementioned pyridines demonstrate that the different derivatives are potent as AChE and BChE inhibitors (Fig. 23). All the structural features are performing a significant role in the inhibitory activity, though, a slight variation in the activity of these analogs is due to variability in the nature and positions of substituents on aryl rings. The smaller groups (–CH_3, –OCH_3, –CF_3, –F, –Cl, –NO_2, –OH, *etc.*) attached to the pyridine ring show higher AChE and BChE inhibitory abilities as compared to the bulky group (benzofuran) present on the rings. All the presented analogs thus far have shown good to excellent ChE inhibitory abilities with a low risk of toxic side effects. Furthermore, these species are inexpensive and easy to synthesize in the laboratory, making them attractive for viable development and marketing as drugs against cholinesterase.

Sultana *et al.* (2017) described using the *N*1-substitution of the 2,3-dihydroquinazolin-4(1*H*)-one nucleus to make AChE inhibitors that were effective. A set of *N*-alkylated/benzylated quinazoline derivatives were made and evaluated to see if they could inhibit cholinesterases. *N*-Alkylation improved the activity of a series of compounds previously described (*N*-unsubstituted). All the substances inhibited both enzymes in the micromolar to submicromolar range. According to the SAR of the synthesized derivatives, *N*-benzylated compounds have higher activity than *N*-alkylated compounds. The *N*-benzylated compounds **288** and **289** were found to be extremely effective against AChE, with IC_{50} values in the micromolar range (0.8 μM and 0.6 μM, respectively). According to ADMET computational projections, all the substances exhibited good pharmacokinetic properties and no AMES toxicity or carcinogenicity. Furthermore, all the chemicals were expected to be absorbed and cross the blood–brain barrier in humans. Generally, the prepared

Table 13 Chemical structures of pyridine derivatives **279–287** and their IC_{50} values against cholinesterase enzymes

Compound no.	Chemical structure	IC_{50} values (μM) AChE	BChE	References
279	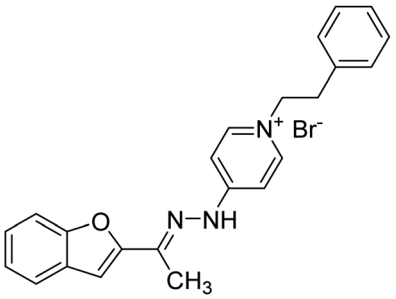	0.95	—	278
280	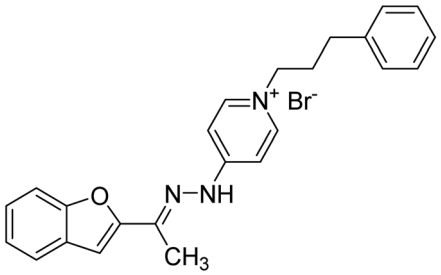	0.23	—	278
281	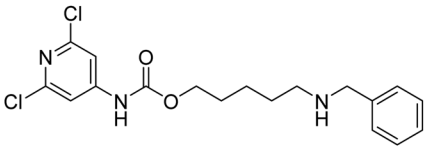	0.153 nM	38.6 nM	279
282	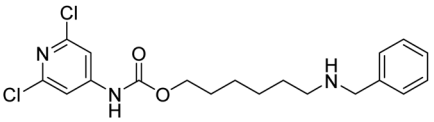	52.8 nM	0.828 nM	279
283	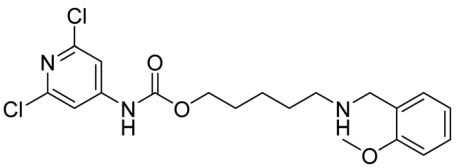	—	153 nM	279
284	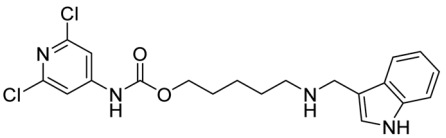	—	828 nM	279
285	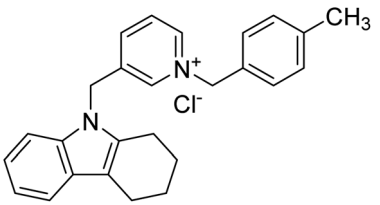	—	0.088	280
286	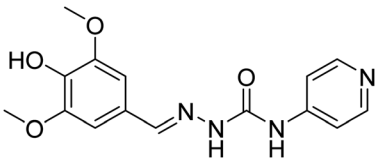	6.32	—	281

Table 13 (*Contd.*)

Compound no.	Chemical structure	IC_{50} values (μM) AChE	BChE	References
287	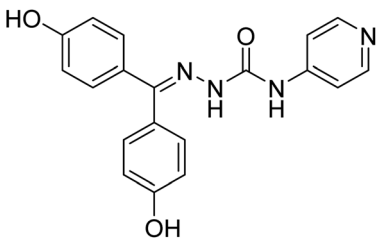	5.58	—	281

compounds have paved the path for the development of new cholinesterase inhibitors[282] (Table 14).

Rao *et al.* (2017) created and appraised a series of 2,4-disubstituted quinazoline analogs as a new type of AD multi-targeting therapy (AD). The results of the biological assays show that several quinazoline derivatives can inhibit both AChE and BChE enzymes (IC_{50} range 1.6–30.5 μM). Compound **290** was reported to be a dual cholinesterase inhibitor (AChE IC_{50} = 14.3 μM; BChE IC_{50} = 8.3 μM) that also inhibited Aβ aggregation (Aβ40 IC_{50} = 2.3 μM). A 2,4-disubstituted quinazoline ring can be utilized as a template for generating multi-targeting drugs to treat AD, according to these thorough SAR investigations. Compound **290** demonstrated a 4.7-fold increase in AChE potency and a 1.4-fold rise in BChE potency when compared to the pyrimidine derivative previously disclosed (AChE IC_{50} = 9.90 μM; BChE IC_{50} = 11.40 μM)[283] (Table 14).

Sarfraz *et al.* (2017) developed and evaluated several cholinesterase inhibitors based on 2,3-dihydroquinazolin-4(1*H*)-one analogs. *In vitro* experiments demonstrated that all compounds were active against both AChE and BChE enzymes, where analogs with a longer alkyl chain at the C-2 position displayed stronger inhibitory activity than galantamine. Bromo derivatives were also more active than their non-substituted counterparts and nitro derivatives. Dihydroquinazolinone **291** proved a potent cholinesterase (AChE/BChE) inhibitor with a higher selectivity for BChE, with IC_{50} values of 4.8 μM for AChE and 11.1 μM for BChE. Synthetically, the reaction of 2-aminobenzamide with butyrylchloride produces quinazolinone, which is subsequently brominated to generate inhibitor **291** (ref. 284) (Table 14).

SAR studies of quinazoline demonstrate that the different derivatives are potent AChE and BChE inhibitors (Fig. 24). All

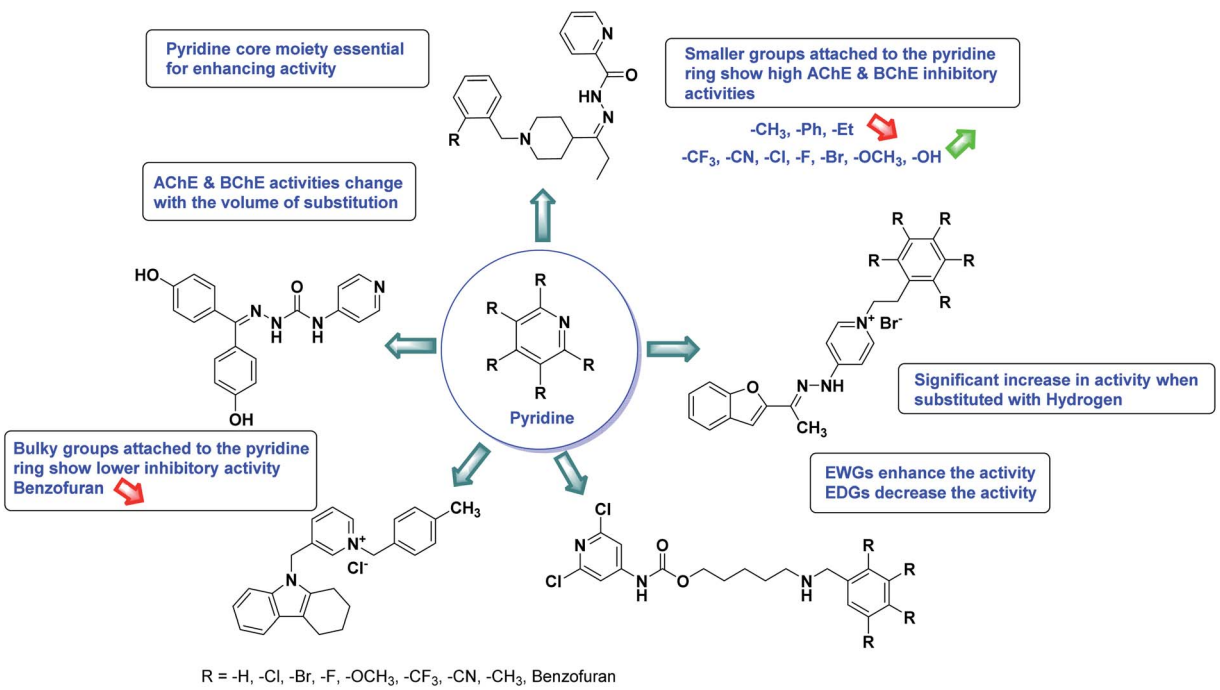

Fig. 23 SAR analysis of different pyridine derivatives as AChE and BChE inhibitors.

Table 14 Chemical structures of quinazoline derivatives **288–291** and their IC_{50} values against cholinesterase enzymes

Compound no.	Chemical structure	IC_{50} values (μM) AChE	IC_{50} values (μM) BChE	References
288	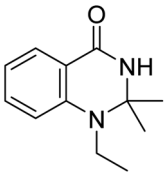	0.8	—	282
289	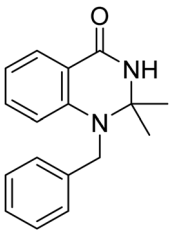	0.6	—	282
290	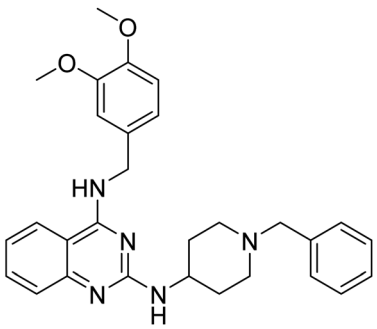	14.3	8.3	283
291	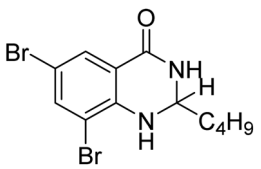	4.8	11.1	284

the structural features are performing a significant role in the inhibitory activity, though, a slight variation in the activity of these analogs is due to variability in the nature and positions of substituents on aryl rings. The smaller groups (–F, –Cl, $–NO_2$, –OH, $–CH_3$, $–OCH_3$, $–CF_3$ *etc.*) attached to the quinazoline ring show higher AChE and BChE inhibitory abilities as compared to the bulky group (triazole) present on the rings. All the presented analogs thus far have shown good to excellent ChE inhibitory abilities with a low risk of toxic side effects. Furthermore, these species are inexpensive and easy to synthesize in the laboratory, making them attractive for viable development and marketing as drugs against cholinesterase.

Gulcin *et al.* (2017) designed and synthesized a series of new 1-(4-(3-(aryl)acryloyl)phenyl)-1*H*-pyrrole-2,5-diones and screened them for ChE inhibitory activities. All the target compounds exhibited AChE inhibiting activity with IC_{50} values in the range of 139.43–244.70 nM. Chalcone-imide derivatives effectively inhibited AChE enzyme with K_i values in the range of 70.470–229.42 nM. All the synthesized chalcone-imide derivatives showed similar inhibition profile against AChE. Compound **292**, which showed the weakest AChE inhibition, had two times AChE inhibition effects than that of tacrine. The best inhibition for AChE enzyme was determined by compound **293** with K_i value of 70.470 nM (ref. 285) (Table 15).

Mughal *et al.* (2017) reported a series of 3-oxoaurones and 3-thioaurones. All the synthetic compounds were screened for their inhibitory potential against *in vitro* AChE and BChE enzymes. The results showed that compounds **294** (IC_{50} = 1.26 μM), **295** (IC_{50} = 0.98 μM) and **296** (IC_{50} = 6.39 μM) showed AChE inhibition activities whereas, compounds whereas **295** (IC_{50} = 1.02 μM) and **297** (IC_{50} = 5.27 μM) against BChE. Noteworthy, the compound **295** was found to be the potent dual inhibitor of AChE (IC_{50} = 0.98 μM) and BChE (IC_{50} = 1.02 μM) as compared to the standard donepezil (IC_{50} = 0.09 μM for AChE; 0.13 μM for BChE). Furthermore, compound **294** (IC_{50} = 1.26 μM) found to have considerable selective activity against AChE and may serve as lead compound for the development of powerful inhibitor for AChE. Overall, it is concluded from the

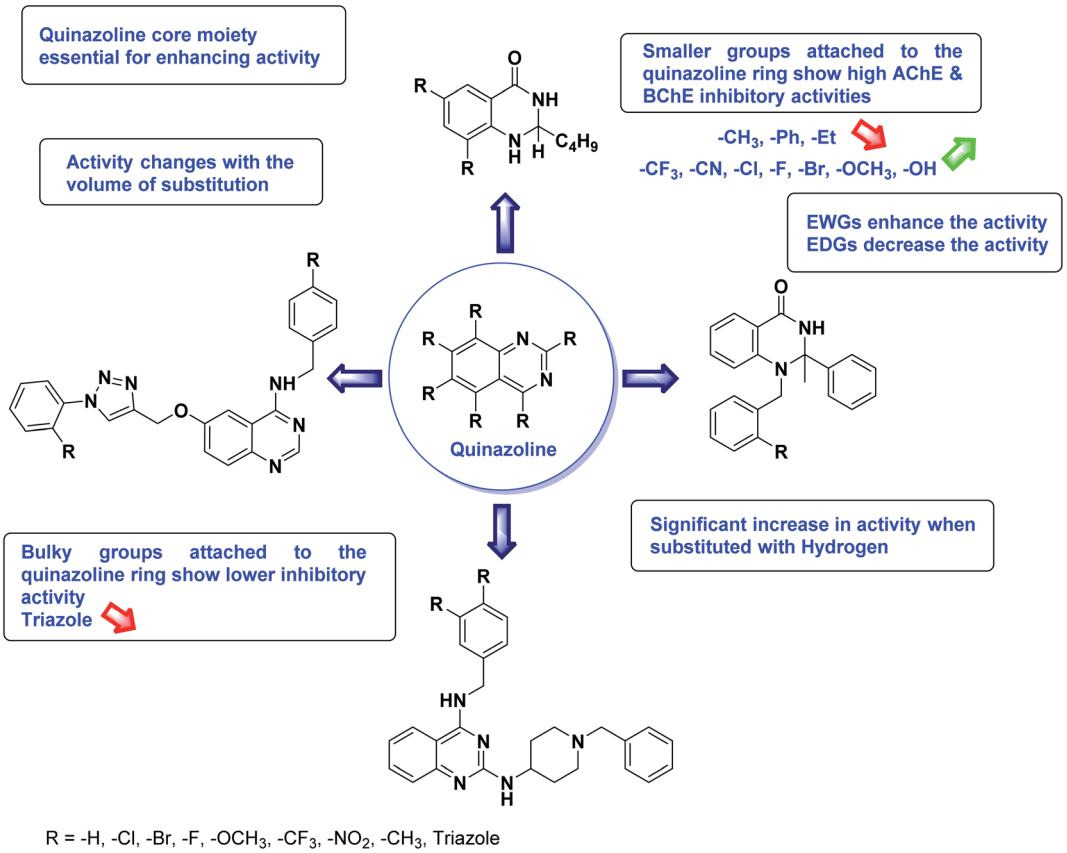

Fig. 24 SAR analysis of different quinazolines derivatives as AChE and BChE inhibitors.

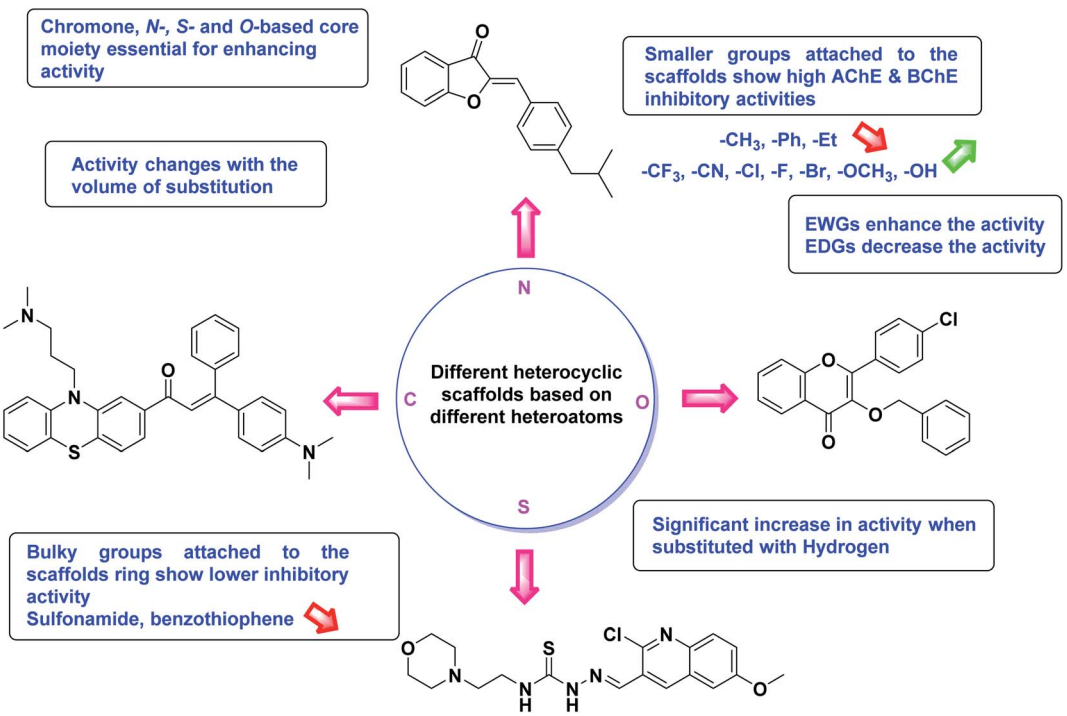

Fig. 25 SAR analysis of different *N*, *O* and *S* based heterocycles as AChE and BChE inhibitors.

Table 15 Chemical structures of different *N*, *O* and *S* based heterocycles **292–323** and their IC_{50} values against cholinesterase enzymes

Compound no.	Chemical structure	IC_{50} values (μM) AChE	BChE	References
292	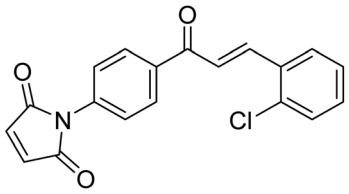	210.56	—	285
293	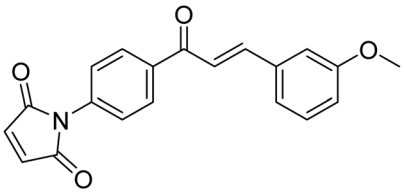	70.470	—	285
294	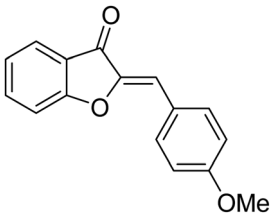	1.26	—	19
295	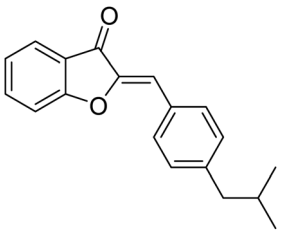	0.98	1.02	19
296	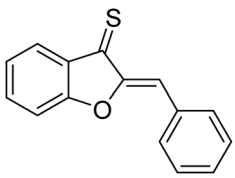	6.39	—	19
297	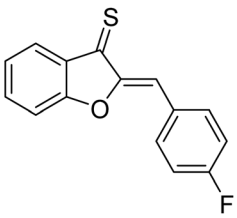	5.27	—	19
298	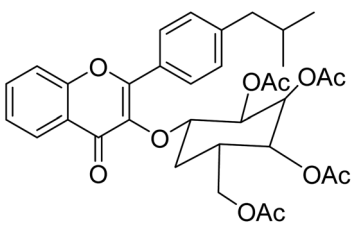	2.05	5.42	18

Table 15 (*Contd.*)

Compound no.	Chemical structure	IC_{50} values (μM) AChE	BChE	References
299	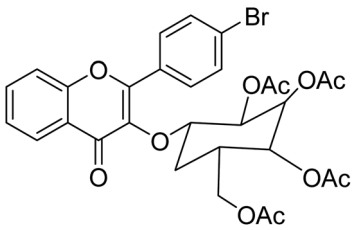	10.2	3.12	18
300	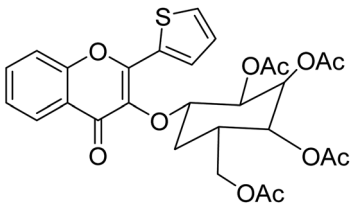	18.52	25.51	18
301	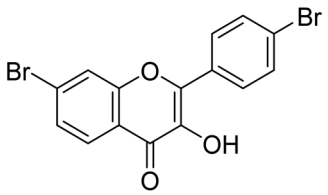	2.01	1.40	13
302	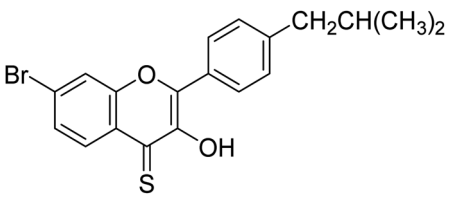	0.08	0.12	13
303	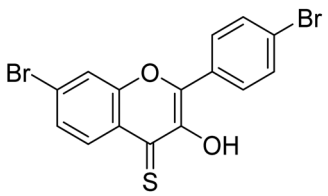	0.07	0.15	13
304	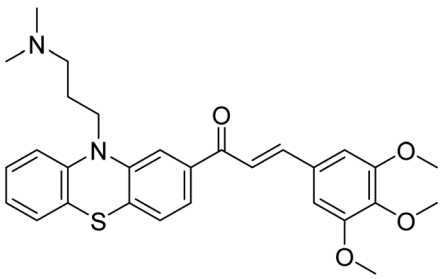	3.63	—	286
305	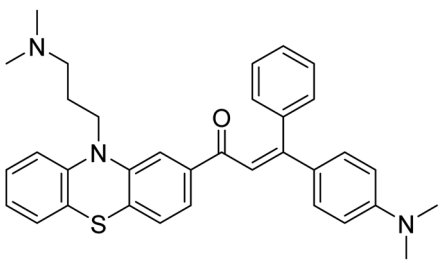	1.10	—	286

Table 15 (*Contd.*)

Compound no.	Chemical structure	IC_{50} values (μM) AChE	BChE	References
306	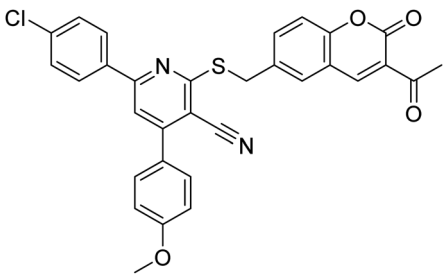	324 nM	—	287
307	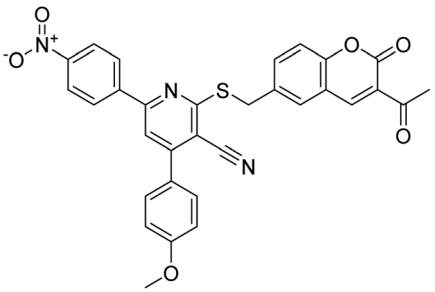	226 nM	—	287
308	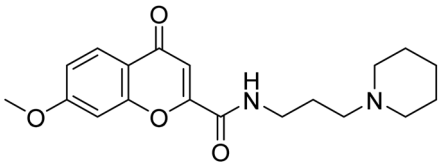	0.09	27.91	288
309	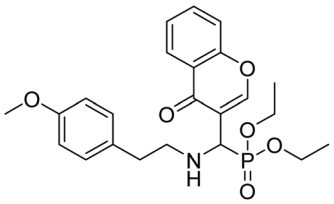	0.103	—	289
310	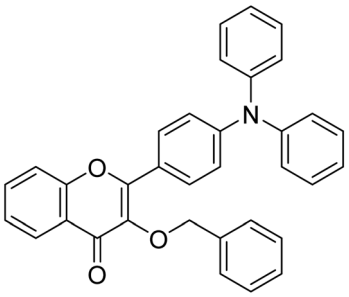	0.05	0.09	21
311	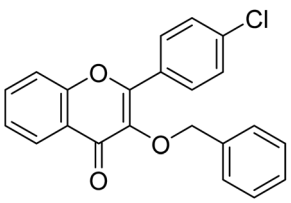	0.07	—	21

Table 15 (*Contd.*)

Compound no.	Chemical structure	IC_{50} values (μM) AChE	BChE	References
312	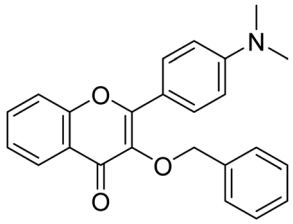	0.08	—	21
313	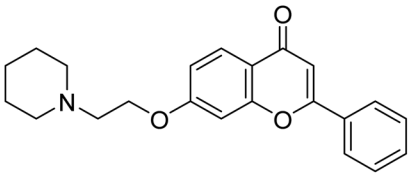	1.29 μmol L^{-1}	—	290
314	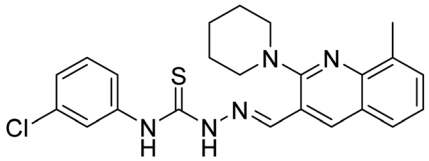	9.68	11.59	291
315	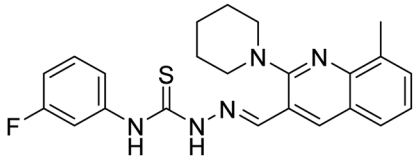	15.8	—	291
316	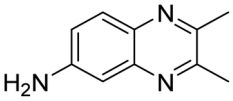	0.077	—	292
317	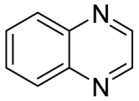	40.64	—	292
318	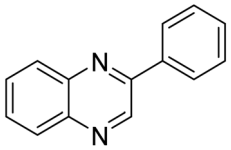	14.91	—	292
319	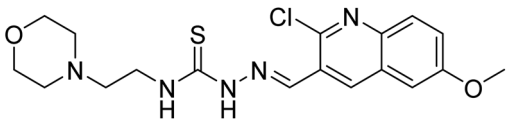	0.12	—	293
320	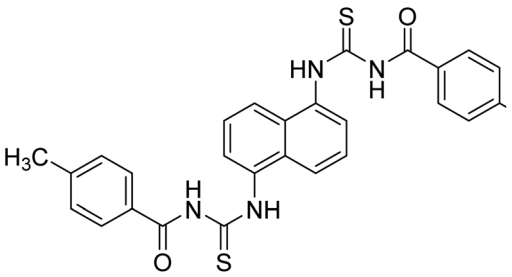	0.1761	—	294

Table 15 (*Contd.*)

Compound no.	Chemical structure	IC_{50} values (μM) AChE	BChE	References
321	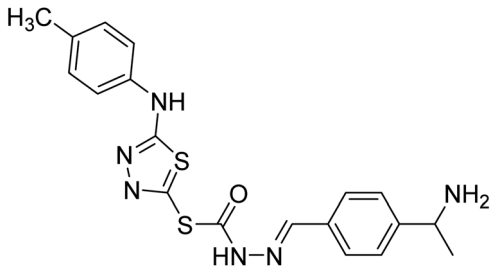	3.63	56.01	295
322	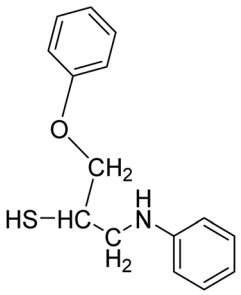	52.50	—	296
323	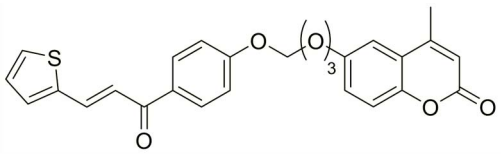	0.42	—	297

study that 3-oxoaurones are appeared to be more potent as compared to 3-thioaurones. The replacement of oxygen with sulfur caused decreased in the activities such compounds **294** (IC_{50} = 1.26 μM for AChE) and **295** (IC_{50} = 0.98 μM for AChE; 1.02 μM for BChE) when transformed their thio derivatives (IC_{50} = 0.00 μM for AChE; 0.10 μM for BChE) and (IC_{50} = 0.00 μM for AChE; 0.00 μM for BChE) they completely lost the AChE activity. These compounds may serve as a lead-candidates in near future for the development of new drugs to treat AD[19] (Table 15).

Mughal *et al.* (2018) designed and synthesized 3-*O*-flavonol glycosides, which were evaluated for inhibition potential against ChE enzymes. The results displayed that most of the derivatives were potent inhibitors of AChE and BChE with varying degree of IC_{50} values (IC_{50} = 0.205 to 102.91 μM for AChE; 0.13to 49.83 μM for BChE). Donepezil was used as standard (IC_{50} = 0.09 μM for AChE; 0.13 μM for BChE). Among the series, the compound **298** was found to be the most active dual inhibitor (IC_{50} = 02.05 μM for AChE and 05.42 μM for BChE) having isobutyl at *p*-position. The next most potent dual inhibitor is compound **299** (IC_{50} = 10.20 μM for AChE and 03.12 μM for BChE) with bromo group at *p*-position of the phenyl ring. Moreover, sulfur containing ring, for example compound **300**, makes strong interaction with active pockets of AChE (IC_{50} = 18.52 μM) rather than BChE (IC_{50} = 25.51 μM). These compounds could be used for the development of new drugs for the cure of AD[18] (Table 15).

Similarly, Mughal *et al.* (2019) reported a series of substituted flavonols and 4-thioflavonols potent as ChE inhibitors. Therein, the results unveiled that these derivatives were potent selective inhibitors of acetylcholinesterase (AChE), except the compound **301** (IC_{50} = 2.01 μM for AChE; 1.40 μM for BChE) which was selective inhibitor of butyrylcholinesterase (BChE), with varying degree of IC_{50} values. Remarkably, the compounds **302** (IC_{50} = 0.08 μM for AChE; 0.12 μM for BChE) and **303** (IC_{50} = 0.07 μM for AChE; 0.15 μM for BChE) have been found the most potent dual inhibitors of ChE amongst the series with IC_{50} values even less than the standard drug donepezil (IC_{50} = 0.09 μM for AChE; 0.13 μM for BChE)[13] (Table 15).

Thai *et al.* (2020) synthesized a series of *N*-substituted-4-phenothiazine-chalcones and tested them for AChE inhibitory activity. All the synthesized target analogs showed IC_{50} values in the range of 186.21 to 1.10 μM for AChE. Among all the synthesized compounds, two substances **304** (IC_{50} = 3.63 μM for AChE) and **305** (IC_{50} = 1.10 μM for AChE) exhibited the most potent AChE inhibitory activity as compared to the standard galanthamine (IC_{50} = 1.26 μM for AChE). These synthesized compounds could be used as AChE inhibitors to cure the AD[286] (Table 15).

Mekky *et al.* (2020) explored a new series of nicotinonitrile-coumarin hybrids as potent AChE inhibitors. The *in vitro* AChE inhibitory activity was examined for the new nicotinonitrile-coumarin hybrid molecules, when compared with donepezil as a standard drug with IC_{50} of 14 nM. Coumarin derivative, linked to 6-(4-nitrophenyl)-4-phenylnicotinonitrile, showed more effective inhibitory activity than the reference donepezil with IC_{50} of 13 nM. Compounds **306** and **307**, with *p*-Cl and *p*-NO_2 linked to 6-aryl moiety, respectively, exhibited the best AChE inhibitory activities with IC_{50} of 324 and 226 nM, respectively[287] (Table 15).

Lomlim *et al.* (2020) designed and synthesized chromone-2-carboxamido-alkylamine derivatives and evaluated their ChE inhibitory activities. The compounds exhibited potent AChE inhibitory activities at micromolar range (IC_{50} = 0.09–9.16 μM) and demonstrated weak BChE inhibitory activities (IC_{50} = 12.09–44.56 μM). Compound **308** (IC_{50} = 0.09 μM) was the most potent AChE inhibitor in this series; it showed higher activity than the clinical used drug tacrine (IC_{50} = 0.13 μM for AChE) and weak BChE inhibitor (IC_{50} = 27.91 μM) as compared to the tacrine (IC_{50} = 0.01 μM for AChE). Chromone-2-carboxamidoalkylamines can be promising lead compounds for development of anti-Alzheimer's agents[288] (Table 15).

Jadhav *et al.* (2020) synthesized a series of *N*-substituted α-aminophosphonates-bearing chromone moiety evaluated for ChE activities. Inhibitory activity against AChE ranged between 0.103 and 5.781 μM, whereas for BChE, activities ranged between 8.619 and 18.789 μM. The results showed that among the different synthesized analogs, strongest AChE inhibition was found for the compound containing aliphatic amine analogs, while in case of BChE, aromatic amines showed better activity as compared to aliphatic amines. Compound **309** was found to be the most potent inhibitor of AChE with an IC_{50} value of 0.103 μM and inhibited AChE through mixed-type inhibition. Compound **309** was 2-folds more potent than tacrine (IC_{50} = 0.289 μM), 35-folds potent than galantamine (IC_{50} = 3.643 μM) and 50-folds potent than rivastigmine (IC_{50} = 5.207 μM)[289] (Table 15).

Mughal *et al.* (2020) explored 3-benzyloxyflavones as the potent ChE inhibitors. The findings showed that all the synthesized target compounds were dual inhibitors of AChE and BChE enzymes with varying IC_{50} values. In comparison, they are more active against AChE than BChE. Fascinatingly, amongst the series, the compound **310** was identified as the most active inhibitor of both AChE (IC_{50} = 0.05 μM) and BChE (IC_{50} = 0.09 μM) relative to the standard donepezil (IC_{50} = 0.09 μM for AChE; 0.13 μM for BChE). Moreover, the compounds **311** (IC_{50} = 0.07 μM) and **312** (IC_{50} = 0.08 μM) exhibited the highest selective inhibition against AChE as compared to the standard[21] (Table 15).

Liu *et al.* (2020) designed and prepared a series of new flavone derivatives containing 6 or 7-substituted tertiary amine side chain and evaluated those compounds against AChE and BChE inhibition. The results indicated that the alteration of aromatic ring connecting to chromone scaffold markedly changed biological activity. Compared with flavones, the inhibitory activity of 2-naphthyl chromone, 2-anthryl-chromone derivatives against AChE significantly decreased, while that of 2-biphenyl chromone derivatives with 7-substituted tertiary amine side chain is better than relative flavones derivatives. Among the newly synthesized compounds, compound **313** was potent in AChE inhibition (IC_{50} = 1.29 μmol L^{-1}) with high selectivity for AChE over BChE (selectivity ratio: 27.96)[290] (Table 15).

Khan *et al.* (2021) synthesized a library of quinoline thiosemicarbazones endowed with a piperidine moiety by a microwave-assisted method. The *in vitro* ChE assay results revealed several compounds as potential inhibitors of AChE (IC_{50} = 15.8 to 62.3 μM) and BChE (IC_{50} = 11.59 to 60.02 μM) enzymes. Among all the synthesized compounds, five compounds exhibited IC_{50} values less than 20 μM. Moreover, compound **314** emerged as the most potent dual inhibitor of AChE and BChE with IC_{50} values of 9.68 and 11.59 μM, respectively as compared the standard donepezil (IC_{50} = 2.98 μM for AChE; 7.21 μM for BChE). Moreover, compound **315** appeared to be the selective inhibitor of AChE with an IC_{50} value of 15.8 μM. Despite several clinically approved drugs and development of anti-Alzheimer's heterocyclic structural leads, the treatment of AD requires safer hybrid therapeutics with characteristic structural and biochemical properties[291] (Table 15).

Lomlim *et al.* (2021) designed and synthesized quinoxaline-based derivatives and evaluated them as novel AChE inhibitors. The results showed that all compounds exhibited potent AChE and BChE inhibitory activities with IC_{50} values of 0.077 to 50.080 μM and 14.91 to 60.95 μM, respectively. Compound **316** (IC_{50} = 0.077 μM) displayed the highest AChE inhibitor activity and the compounds **317**, IC_{50} = 40.64 μM and **318**, (IC_{50} = 14.91 μM) resulted in elevated butyrylcholinesterase inhibitory activity as compared to tacrine (IC_{50} = 0.107 μM for AChE; 0.00066 μM for BChE) and galanthamine (IC_{50} = 0.59 μM for AChE; 11.55 μM for BChE). Therefore, the quinoxaline analogs could offer the lead for the newly developed candidates as potent AChE inhibitors[292] (Table 15).

Munir *et al.* (2021) synthesized a series of quinoline-thiosemicarbazones and evaluated their AChE inhibitory activity. All the tested hybrid derivatives were found completely selective towards AChE and showed inhibition in the range of 0.12–60.9 μM. *In vitro* inhibitory results revealed compound **319** as a promising and lead inhibitor with an IC_{50} value of 0.12 μM, a 5-fold higher potency than standard drug (galanthamine; IC_{50} = 0.62 μM). The synergistic effect of electron-rich (methoxy) group and ethylmorpholine moiety in quinolinethiosemicarbazone conjugates contributes significantly to improving the inhibition level[293] (Table 15).

Bahadur *et al.* (2021) synthesized a new series of bis-thioureas and screened them for AChE inhibition activity. The results of AChE inhibition assay were found to be active in inhibiting the target enzyme with different IC_{50} values. The synthesized compounds showed AChE inhibition in the range of IC_{50} = 0.176 to 25.2063 μM. Among all derivatives, the **4g** showed highly potent inhibition potential against AChE enzyme with IC_{50} value of 0.1761 μM, which is several times better than the reference inhibitor neostigmine methylsulfate IC_{50} = 2.469 μM. The pharmacokinetic studies guided those compounds

possess good lead-like properties with little toxicity and hence be used as a ChE inhibitors in near future for the cure of AD[294] (Table 15).

Recently, Cevik *et al.* (2022) reported some new substituted thiazolylhydrazine analogs and evaluated their inhibitory effects against AChE and BChE enzymes. According to the enzyme inhibition results, the target compounds showed selectivity against BChE. Among all synthesized derivatives, compound **321** was found to be the most potent dual AChE and BChE inhibitor with an IC_{50} value of 3.63 and 56.01 μM, respectively as compared to the standard donepezil (IC_{50} = 98.86 μM for AChE; 78.95 μM for BChE). Further alterations in the structural framework of these compounds could be a determining factor to improve their anticholinergic potential which may complement the drug-discovery process against Alzheimer's disease[295] (Table 15).

Gulçin *et al.* (2022) prepared and reported various derivatives of 1,2-aminopropanthiols. These synthesized derivatives were found to be effective inhibitors for the AChE enzyme, with IC_{50} and K_i values in the range of 25.48 to 60.37 μM and 5.76 to 55.39 μM for AChE, respectively.

Particularly, the evaluation of the inhibitory efficacy of compound **322** (IC_{50} = 52.50 μM) against AChE enzyme as compared to the standard tacrine (IC_{50} = 70.87 μM) also indicates the anti-AD potential[296] (Table 15).

Jamalis *et al.* (2022) reported chalcone-based coumarin derivatives and evaluated them as ChE inhibitors for the treatment of AD. The *in vitro* assessment of the synthesized compounds revealed that all of them showed significant activity (IC_{50} ranging from 0.42 to 1.296 μM) towards AChE as compared to the standard drug, galantamine (IC_{50} = 1.142 μM). Amongst the series, compound **323** displayed the most potent inhibitory activity with IC_{50} value of 0.42 μM. Moreover, bromo substitution on C-5 of thiophene ring in chalcone moiety led to decrease in AChE inhibition activity. The obtained results showed that the linker length connecting chalcone moiety and coumarin core played a vital role in AChE inhibition. Hence, the identified compound may be considered as lead for further study in the search of novel AChE inhibitory agent[297] (Table 15).

The SAR studies of the previously mentioned heterocyclic compounds demonstrate that the different derivatives are potent AChE and BChE inhibitors (Fig. 25). All the structural features are performing a significant role in the inhibitory activity, though, a slight variation in the activity of these analogs is due to variability in the nature and positions of substituents on aryl rings. The smaller groups (–CH_3, –OCH_3, –CF_3, –F, –Cl, –NO_2, –OH, *etc.*) attached to the scaffold show higher AChE and BChE inhibitory abilities as compared to the bulky group (benzothiophene, sulfonamide) present on the rings. All the presented analogues so far have shown good to excellent ChE inhibitory abilities with a low risk of toxic side effects. Furthermore, these species are inexpensive and easy to synthesize in the laboratory, making them attractive for viable development and marketing as drugs against cholinesterase.

6 Conclusions and future perspectives

AD is the most common neurodegeneration disease which has a limited number of drug candidates available for its treatment. Currently, anticholinesterase drugs represent the main choice for pharmacotherapy of AD. In this context, the search for new drugs with anticholinesterase activity can be an alternative for treatment and it could be an important form to prolong and improve the life of the patient. This review summarizes the anticholinesterase activity of the most potent *N*-, *O*-, *S*-based heterocyclic compounds. The scope of *N*-, *O*-, *S*-based compounds in medicines is growing daily and their diverse analogs provide a viable and important path for the discovery of drugs with various biological applications. The *N*-, *O*-, *S*-based heterocyclic frameworks offer a high degree of structural diversity that has proven useful for the search of new therapeutic agents with improved pharmacokinetics and other physicochemical features. Research and development of *N*-, *O*-, *S*-based compounds in medicinal chemistry has become a rapidly developing and increasingly active topic. The overwhelming advantages of *N*-, *O*- and *S*-containing drugs in the medicinal field, including easy preparation, low toxicity, less adverse effects, high bioavailability, lower drug resistance, and good biocompatibility, encourage efforts towards further research and development. Although, extensive *in vitro* testing has been reported on compounds summarized in this review, few have selected for *in vivo* tests and subsequent steps for development as drug candidates. Thus, further studies should be performed *in vivo* and more theoretical work should be carried out to predict drug-likeness and drug ability. In addition, we have explored their SAR studies. The SAR studies of the discussed molecules offer a greater understanding of the pattern of substituents on their basic skeleton and appropriate substitutions accountable for their effectiveness and for further exploration of biological efficacy. These significant points confirm the enormous potential of various heterocyclic cores in pharmaceutical applications suggesting a massive scope for these promising moieties because of their diverse molecular targets. We believe that this review article will be valuable for encouraging the structural design and development of sustainable and effective *N*-, *O*-, *S*-based drugs against AD, with minimal side-effects. At last, we hope that this current work could be used as reference to design more potent AChE and BChE inhibitors with excellent inhibitory activity and in the search for new drugs for the treatment of AD.

Abbreviations

AChE	Acetylcholinesterase
ACh	Acetylcholine
AD	Alzheimer disease
BChE	Butyrylcholinesterase
ChE	Cholinesterase
SAR	Structure–activity relationship

Conflicts of interest

There are no conflicts to declare.

Acknowledgements

The authors would like to acknowledge the Deanship of Scientific Research at Umm Al-Qura University, for supporting this work by grant code: 22UQU4320545DSR18. The financial support by the Higher Education Commission of Pakistan (HEC) under Project No. (NRPU-6484 & NRPU-15800) is gratefully acknowledged. Dr Ziad Moussa is grateful to the United Arab Emirates University (UAEU) of Al-Ain and to the Research Office for supporting the research developed in his laboratory (grant no. G00003291).

References

1 N. N. Makhova, L. I. Belen'kii, G. A. Gazieva, I. L. Dalinger, L. S. Konstantinova, V. V. Kuznetsov, A. N. Kravchenko, M. M. Krayushkin, O. A. Rakitin and A. M. Starosotnikov, *Russ. Chem. Rev.*, 2020, **89**, 55.
2 P. M. Amisha, M. Pathania and V. K. Rathaur, *Fam. Med. Prim. Care Rev.*, 2019, **8**, 2328.
3 J. A. Joule, K. Mills and G. F. Smith, *Heterocyclic chemistry*, CRC Press, 2020.
4 A. T. Soldatenkov, A. F. Pozharskii and A. R. Katritzky, *Heterocycles in life and society: An introduction to heterocyclic chemistry, biochemistry and applications*, John Wiley & Sons, 2011.
5 T. Eicher, S. Hauptmann and A. Speicher, *The chemistry of heterocycles: structures, reactions, synthesis, and applications*, John Wiley & Sons, 2013.
6 E. Vitaku, D. T. Smith and J. T. Njardarson, *J. Med. Chem.*, 2014, **57**, 10257–10274.
7 M. D. Delost, D. T. Smith, B. J. Anderson and J. T. Njardarson, *J. Med. Chem.*, 2018, **61**, 10996–11020.
8 H. Zhu, V. Dronamraju, W. Xie and S. S. More, *Med. Chem. Res.*, 2021, **30**, 305–352.
9 A. Gomtsyan, *Chem. Heterocycl. Compd.*, 2012, **48**, 7–10.
10 H. B. Broughton and I. A. Watson, *J. Mol. Graphics Modell.*, 2004, **23**, 51–58.
11 A. Mermer, T. Keles and Y. Sirin, *Bioorg. Chem.*, 2021, **114**, 105076.
12 M. Gupta, *International Journal of Physical, Chemical and Mathematical Sciences*, 2015, **4**, 21–24.
13 E. U. Mugal, A. Sadiq, J. Ashraf, M. N. Zafar, S. H. Sumrra, R. Tariq, A. Mumtaz, A. Javid, B. A. Khan and A. Ali, *Bioorg. Chem.*, 2019, **91**, 103124.
14 E. U. Mughal, M. Ayaz, Z. Hussain, A. Hasan, A. Sadiq, M. Riaz, A. Malik, S. Hussain and M. I. Choudhary, *Bioorg. Med. Chem.*, 2006, **14**, 4704–4711.
15 J. Ashraf, E. U. Mughal, A. Sadiq, N. Naeem, S. A. Muhammad, T. Qousain, M. N. Zafar, B. A. Khan and M. Anees, *J. Mol. Struct.*, 2020, **1218**, 128458.
16 R. J. Obaid, E. U. Mughal, N. Naeem, A. Sadiq, R. I. Alsantali, R. S. Jassas, Z. Moussa and S. A. Ahmed, *RSC Adv.*, 2021, **11**, 22159–22198.
17 J. Ashraf, E. U. Mughal, R. I. Alsantali, R. J. Obaid, A. Sadiq, N. Naeem, A. Ali, A. Massadaq, Q. Javed and A. Javid, *Bioorg. Med. Chem.*, 2021, **35**, 116057.
18 E. U. Mughal, A. Javid, A. Sadiq, S. Murtaza, M. N. Zafar, B. A. Khan, S. H. Sumrra, M. N. Tahir and K. M. Khan, *Bioorg. Med. Chem.*, 2018, **26**, 3696–3706.
19 E. U. Mughal, A. Sadiq, S. Murtaza, H. Rafique, M. N. Zafar, T. Riaz, B. A. Khan, A. Hameed and K. M. Khan, *Bioorg. Med. Chem.*, 2017, **25**, 100–106.
20 J. Ashraf, E. U. Mughal, A. Sadiq, M. Bibi, N. Naeem, A. Ali, A. Massadaq, N. Fatima, A. Javid and M. N. Zafar, *J. Biomol. Struct. Dyn.*, 2021, **39**, 7107–7122.
21 E. U. Mughal, A. Sadiq, M. Ayub, N. Naeem, A. Javid, S. H. Sumrra, M. N. Zafar, B. A. Khan, F. P. Malik and I. Ahmed, *J. Biomol. Struct. Dyn.*, 2021, **39**, 6154–6167.
22 R. I. Alsantali, E. U. Mughal, N. Naeem, M. A. Alsharif, A. Sadiq, A. Ali, R. S. Jassas, Q. Javed, A. Javid and S. H. Sumrra, *J. Mol. Struct.*, 2022, **1251**, 131933.
23 R. J. Obaid, E. U. Mughal, N. Naeem, M. Al Rooqi, A. Sadiq, R. Jassas and S. A. Ahmed, *Process Biochem.*, 2022, **120**, 250–259.
24 M. A. Alsharif, Q. A. Raja, N. A. Majeed, R. S. Jassas, A. A. Alsimaree, A. Sadiq, N. Naeem, E. U. Mughal, R. I. Alsantali and Z. Moussa, *RSC Adv.*, 2021, **11**, 29826–29858.
25 H. Venkatachalam and N. V. A. Kumar, in *Heterocycles-Synthesis and Biological Activities*, IntechOpen, 2019.
26 P. Kaur, R. Arora and N. Gill, *Indo Am. J. Pharm. Res.*, 2013, **3**, 9067–9084.
27 J. Cossy and A. Guerinot, in *Advances in Heterocyclic Chemistry*, Elsevier, 2016, vol. 119, pp. 107–142.
28 C. Rowlands and R. Farley, *Landolt Börnstein*, 2008, vol. 26, p. 308.
29 A. U. Hassan, S. H. Sumrra, M. N. Zafar, M. F. Nazar, E. U. Mughal, M. N. Zafar and M. Iqbal, *Mol. Diversity*, 2022, **26**, 51–72.
30 B. Meyer, *Chem. Rev.*, 1976, **76**, 367–388.
31 R. I. Alsantali, Q. A. Raja, A. Y. Alzahrani, A. Sadiq, N. Naeem, E. U. Mughal, M. M. Al-Rooqi, N. El Guesmi, Z. Moussa and S. A. Ahmed, *Dyes Pigm.*, 2022, **199**, 110050.
32 E. U. Mughal, R. J. Obaid, A. Sadiq, M. A. Alsharif, N. Naeem, S. Kausar, A. A. Altaf, R. S. Jassas, S. Ahmed and R. I. Alsantali, *Dyes Pigm.*, 2022, **201**, 110248.
33 R. J. Huxtable, *Biochemistry of sulfur*, Springer Science & Business Media, 2013.
34 T. H. Maren, *Annu. Rev. Pharmacol. Toxicol.*, 1976, **16**, 309–327.
35 M. S. Wilke, A. L. Lovering and N. C. Strynadka, *Curr. Opin. Microbiol.*, 2005, **8**, 525–533.
36 R. Kaur, S. Chaudhary, K. Kumar, M. K. Gupta and R. K. Rawal, *Eur. J. Med. Chem.*, 2017, **132**, 108–134.
37 M. Baumann, I. R. Baxendale, S. V. Ley and N. Nikbin, *Beilstein J. Org. Chem.*, 2011, **7**, 442–495.

38 N. Arya, A. Y. Jagdale, T. A. Patil, S. S. Yeramwar, S. S. Holikatti, J. Dwivedi, C. J. Shishoo and K. S. Jain, *Eur. J. Med. Chem.*, 2014, **74**, 619–656.
39 Z. Liu, Z. Zhang, W. Zhang and D. Yan, *Bioorg. Med. Chem. Lett.*, 2018, **28**, 2454–2458.
40 S. Jain, V. Chandra, P. K. Jain, K. Pathak, D. Pathak and A. Vaidya, *Arabian J. Chem.*, 2019, **12**, 4920–4946.
41 L. Zhang, X. M. Peng, G. L. Damu, R. X. Geng and C. H. Zhou, *Med. Res. Rev.*, 2014, **34**, 340–437.
42 J. Zhang, S. Wang, Y. Ba and Z. Xu, *Eur. J. Med. Chem.*, 2019, **174**, 1–8.
43 R. Gupta, *Int. J. Comput. Appl.*, 2015, **975**, 8887.
44 N. Kerru, L. Gummidi, S. Maddila, K. K. Gangu and S. B. Jonnalagadda, *Molecules*, 2020, **25**, 1909.
45 V. Polshettiwar and R. S. Varma, *Curr. Opin. Drug Discovery Dev.*, 2007, **10**, 723–737.
46 A. Padwa and S. K. Bur, *Tetrahedron*, 2007, **63**, 5341.
47 D. M. D'Souza and T. J. Mueller, *Chem. Soc. Rev.*, 2007, **36**, 1095–1108.
48 G. Eren, S. Ünlü, M.-T. Nuñez, L. Labeaga, F. Ledo, A. Entrena, E. Banoğlu, G. Costantino and M. F. Şahin, *Bioorg. Med. Chem.*, 2010, **18**, 6367–6376.
49 J. Hepworth and A. Boulton, *Comprehensive Heterocyclic Chemistry*, ed. M. G. McKillop, Pergamon Press, Oxford, 1984, vol. 3.
50 N. A. McGrath, M. Brichacek and J. T. Njardarson, *J. Chem. Educ.*, 2010, **87**, 1348–1349.
51 P. D. Leeson and B. Springthorpe, *Nat. Rev. Drug Discovery*, 2007, **6**, 881–890.
52 R. DeSimone, K. Currie, S. Mitchell, J. Darrow and D. Pippin, *Comb. Chem. High Throughput Screening*, 2004, **7**, 473–493.
53 S. Andreescu and J.-L. Marty, *Biomol. Eng.*, 2006, **23**, 1–15.
54 N. Ben Oujji, I. Bakas, G. Istamboulié, I. Ait-Ichou, E. Ait-Addi, R. Rouillon and T. Noguer, *Sensors*, 2012, **12**, 7893–7904.
55 N. A. Hosea, H. A. Berman and P. Taylor, *Biochemistry*, 1995, **34**, 11528–11536.
56 G. S. Nunes, T. Montesinos, P. B. O. Marques, D. Fournier and J. L. Marty, *Anal. Chim. Acta*, 2001, **434**, 1–8.
57 G. D. Stanciu, A. Luca, R. N. Rusu, V. Bild, S. I. Beschea Chiriac, C. Solcan, W. Bild and D. C. Ababei, *Biomolecules*, 2020, **10**, 40.
58 M. A. DeTure and D. W. Dickson, *Mol. Neurodegener.*, 2019, **14**, 1–18.
59 A. Martinez and A. Castro, *Expert Opin. Invest. Drugs*, 2006, **15**, 1–12.
60 M. Mehta, A. Adem and M. Sabbagh, *J. Alzheimer's Dis.*, 2012, **2012**, 1–8.
61 P. J. Ghumatkar, S. P. Patil, P. D. Jain, R. M. Tambe and S. Sathaye, *Pharmacol., Biochem. Behav.*, 2015, **135**, 182–191.
62 Y. Sun, M. S. Lai, C. J. Lu and R. C. Chen, *Eur. J. Paediatr. Neurol.*, 2008, **15**, 278–283.
63 M. Seto, R. L. Weiner, L. Dumitrescu and T. J. Hohman, *Mol. Neurodegener.*, 2021, **16**, 1–16.
64 A. S. Association, *Alzheimers. Dement.*, 2020, **16**, 391–460.
65 H. Ahmad, S. Ahmad, M. Ali, A. Latif, S. A. A. Shah, H. Naz, N. ur Rahman, F. Shaheen, A. Wadood and H. U. Khan, *Bioorg. Chem.*, 2018, **78**, 427–435.
66 J. D. Ulrich and D. M. Holtzman, *ACS Chem. Neurosci.*, 2016, **7**, 420–427.
67 A. M. Palmer, *Trends Pharmacol. Sci.*, 2011, **32**, 141–147.
68 J.-C. Li, J. Zhang, M. C. Rodrigues, D.-J. Ding, J. P. F. Longo, R. B. Azevedo, L. A. Muehlmann and C.-S. Jiang, *Bioorg. Med. Chem. Lett.*, 2016, **26**, 3881–3885.
69 A. Rahman, M. T. Ali, M. M. A. K. Shawan, M. G. Sarwar, M. A. Khan and M. A. Halim, *SpringerPlus*, 2016, **5**, 1–14.
70 N. Bulut, U. M. Kocyigit, I. H. Gecibesler, T. Dastan, H. Karci, P. Taslimi, S. Durna Dastan, I. Gulcin and A. Cetin, *J. Biochem. Mol. Toxicol.*, 2018, **32**, 22006.
71 M. Xu, Y. Peng, L. Zhu, S. Wang, J. Ji and K. Rakesh, *Eur. J. Med. Chem.*, 2019, **180**, 656–672.
72 D. K. Lahiri, M. R. Farlow, N. H. Greig and K. Sambamurti, *Drug Dev. Res.*, 2002, **56**, 267–281.
73 Z. Najafi, M. Mahdavi, M. Saeedi, E. Karimpour-Razkenari, R. Asatouri, F. Vafadarnejad, F. H. Moghadam, M. Khanavi, M. Sharifzadeh and T. Akbarzadeh, *Eur. J. Med. Chem.*, 2017, **125**, 1200–1212.
74 P. Anand and B. Singh, *Arch. Pharmacal Res.*, 2013, **36**, 375–399.
75 R. M. Lane, S. G. Potkin and A. Enz, *Int. J. Neuropsychopharmacol.*, 2006, **9**, 101–124.
76 N. H. Greig, T. Utsuki, Q.-s. Yu, X. Zhu, H. W. Holloway, T. Perry, B. Lee, D. K. Ingram and D. K. Lahiri, *Curr. Med. Res. Opin.*, 2001, **17**, 159–165.
77 A. Nordberg, C. Ballard, R. Bullock, T. Darreh-Shori and M. Somogyi, *The primary care companion for CNS disorders*, 2013, vol. 15.
78 P. B. Watkins, H. J. Zimmerman, M. J. Knapp, S. I. Gracon and K. W. Lewis, *JAMA*, 1994, **271**, 992–998.
79 H. Khan, S. Amin, M. A. Kamal and S. Patel, *Biomed. Pharmacother.*, 2018, **101**, 860–870.
80 B. Ahmad, S. Mukarram Shah, H. Khan and S. Hassan Shah, *J. Enzyme Inhib. Med. Chem.*, 2007, **22**, 730–732.
81 M. B. Colovic, D. Z. Krstic, T. D. Lazarevic-Pasti, A. M. Bondzic and V. M. Vasic, *Curr. Neuropharmacol.*, 2013, **11**, 315–335.
82 E. C. Ballinger, M. Ananth, D. A. Talmage and L. W. Role, *Neuron*, 2016, **91**, 1199–1218.
83 H. Khan, M. Ali Khan and I. Hussan, *J. Enzyme Inhib. Med. Chem.*, 2007, **22**, 722–725.
84 V. P. Nair and J. M. Hunter, *Critical Care and Pain*, 2004, **4**, 164–168.
85 M. Yuksel, K. Biberoglu, S. Onder, K. G. Akbulut and O. Tacal, *Biochimie*, 2018, **146**, 105–112.
86 H. Khan, M. Saeed, M. A. Khan, N. Muhammad, A. Khan and A. Ullah, *J. Chem. Soc. Pak.*, 2014, **36**, 865–869.
87 S. Zacks and J. Blumberg, *J. Histochem. Cytochem.*, 1961, **9**, 317–324.
88 S. Kuwabara, *Landmark Papers in Neurology* 2015, vol. 12, p. 429.

89 O. Lykhmus, L. Koval, D. y. Pastuhova, M. Zouridakis, S. Tzartos, S. Komisarenko and M. Skok, *Immunobiology*, 2016, **221**, 1355–1361.
90 K. Vrolix, J. Fraussen, M. Losen, J. Stevens, K. Lazaridis, P. C. Molenaar, V. Somers, M. A. Bracho, R. Le Panse and P. Stinissen, *J. Autoimmun.*, 2014, **52**, 101–112.
91 M. Almasieh, Y. Zhou, M. Kelly, C. Casanova and A. Di Polo, *Cell Death Dis.*, 2010, **1**, 27–29.
92 S. H. Song, S. M. Choi, J. E. Kim, J. E. Sung, H. A. Lee, Y. H. Choi, C. J. Bae, Y. W. Choi and D. Y. Hwang, *Neurosci. Lett.*, 2017, **638**, 121–128.
93 N. D. Belyaev, K. A. Kellett, C. Beckett, N. Z. Makova, T. J. Revett, N. N. Nalivaeva, N. M. Hooper and A. J. Turner, *J. Biol. Chem.*, 2010, **285**, 41443–41454.
94 H. Ashton, *Curr. Opin. Psychiatry*, 2005, **18**, 249–255.
95 Y. Dgachi, O. Sokolov, V. Luzet, J. Godyń, D. Panek, A. Bonet, H. Martin, I. Iriepa, I. Moraleda and C. García-Iriepa, *Eur. J. Med. Chem.*, 2017, **126**, 576–589.
96 Q. Li, S. He, Y. Chen, F. Feng, W. Qu and H. Sun, *Eur. J. Med. Chem.*, 2018, **158**, 463–477.
97 H. Zakut, J. Lieman-Hurwitz, R. Zamir, L. Sindell, D. Ginzberg and H. Soreq, *Prenatal Diagn.*, 1991, **11**, 597–607.
98 M. Mesulam, A. Guillozet, P. Shaw and B. Quinn, *Neurobiol. Dis.*, 2002, **9**, 88–93.
99 M.-M. Mesulam, A. Guillozet, P. Shaw, A. Levey, E. Duysen and O. Lockridge, *Neuroscience*, 2002, **110**, 627–639.
100 A. Chatonnet and O. Lockridge, *Biochem. J.*, 1989, **260**, 625–634.
101 A. Mack and A. Robitzki, *Prog. Neurobiol.*, 2000, **60**, 607–628.
102 O. Lockridge, Structure of human serum cholinesterase, *Bioessays*, 1988, **9**, 125–128.
103 C. G. Carolan, G. P. Dillon, D. Khan, S. A. Ryder, J. M. Gaynor, S. Reidy, J. F. Marquez, M. Jones, V. Holland and J. F. Gilmer, *J. Med. Chem.*, 2010, **53**, 1190–1199.
104 B. Li, E. G. Duysen, M. Carlson and O. Lockridge, *J. Pharmacol. Exp. Ther.*, 2008, **324**, 1146–1154.
105 I. Manoharan, R. Boopathy, S. Darvesh and O. Lockridge, *Clin. Chim. Acta*, 2007, **378**, 128–135.
106 N. H. Greig, T. Utsuki, D. K. Ingram, Y. Wang, G. Pepeu, C. Scali, Q.-S. Yu, J. Mamczarz, H. W. Holloway and T. Giordano, *Proc. Natl. Acad. Sci. U. S. A.*, 2005, **102**, 17213–17218.
107 G. Mushtaq, N. H. Greig, J. A. Khan and M. A. Kamal, *CNS and Neurological Disorders-Drug Targets (Formerly Current Drug Targets-CNS and Neurological Disorders)*, 2014, vol. 13, pp. 1432–1439.
108 W. Xie, J. A. Stribley, A. Chatonnet, P. J. Wilder, A. Rizzino, R. D. McComb, P. Taylor, S. H. Hinrichs and O. Lockridge, *J. Pharmacol. Exp. Ther.*, 2000, **293**, 896–902.
109 Q. Li, H. Yang, Y. Chen and H. Sun, *Eur. J. Med. Chem.*, 2017, **132**, 294–309.
110 B. Brus, U. Kosak, S. Turk, A. Pislar, N. Coquelle, J. Kos, J. Stojan, J.-P. Colletier and S. Gobec, *J. Med. Chem.*, 2014, **57**, 8167–8179.
111 D. Knez, B. Brus, N. Coquelle, I. Sosič, R. Šink, X. Brazzolotto, J. Mravljak, J.-P. Colletier and S. Gobec, *Bioorg. Med. Chem.*, 2015, **23**, 4442–4452.
112 S. N. Dighe, G. S. Deora, E. De la Mora, F. Nachon, S. Chan, M.-O. Parat, X. Brazzolotto and B. P. Ross, *J. Med. Chem.*, 2016, **59**, 7683–7689.
113 A. Nordberg, C. Ballard, R. Bullock, T. Darreh-Shori and M. Somogyi, *The Primary Care Companion for CNS Disorders*, 2013, vol. 15, p. 26731.
114 Y. Oda and I. Nakanishi, *The distribution of cholinergic neurons in the human central nervous system*, 2000.
115 M. K. Tripathi, P. Sharma, A. Tripathi, P. N. Tripathi, P. Srivastava, A. Seth and S. K. Shrivastava, *J. Comput.-Aided Mol. Des.*, 2020, **34**, 983–1002.
116 M. Reale, E. Costantini, M. Di Nicola, C. D'Angelo, S. Franchi, M. D'Aurora, M. Di Bari, V. Orlando, S. Galizia and S. Ruggieri, *Sci. Rep.*, 2018, **8**, 1–9.
117 D. J. Selkoe, *Cell*, 1989, **58**, 611–612.
118 S. S. Sisodia and D. L. Price, *FASEB J.*, 1995, **9**, 366–370.
119 A. A. Geronikaki, J. C. Dearden, D. Filimonov, I. Galaeva, T. L. Garibova, T. Gloriozova, V. Krajneva, A. Lagunin, F. Z. Macaev and G. Molodavkin, *J. Med. Chem.*, 2004, **47**, 2870–2876.
120 P. Piplani and C. C. Danta, *Bioorg. Chem.*, 2015, **60**, 64–73.
121 P. N. Tripathi, P. Srivastava, P. Sharma, A. Seth and S. K. Shrivastava, *Bioorg. Med. Chem.*, 2019, **27**, 1327–1340.
122 A. L. Guillozet, S. Weintraub, D. C. Mash and M. M. Mesulam, *Arch. Neurol.*, 2003, **60**, 729–736.
123 C. R. Tyler and A. M. Allan, *Curr. Environ. Health Rep.*, 2014, **1**, 132–147.
124 P. Srivastava, P. N. Tripathi, P. Sharma, S. N. Rai, S. P. Singh, R. K. Srivastava, S. Shankar and S. K. Shrivastava, *Eur. J. Med. Chem.*, 2019, **163**, 116–135.
125 A. Blokland, *Brain Res. Rev.*, 1995, **21**, 285–300.
126 J. Pagonabarraga and J. Kulisevsky, *Neurobiol. Dis.*, 2012, **46**, 590–596.
127 M.-C. Buhot, *Curr. Opin. Neurobiol.*, 1997, **7**, 243–254.
128 A. Easton, V. Douchamps, M. Eacott and C. Lever, *Neuropsychologia*, 2012, **50**, 3156–3168.
129 G. Johnson and S. Moore, *Curr. Pharm. Des.*, 2006, **12**, 217–225.
130 G. V. De Ferrari, M. A. Canales, I. Shin, L. M. Weiner, I. Silman and N. C. Inestrosa, *Biochemistry*, 2001, **40**, 10447–10457.
131 K. Jomova, D. Vondrakova, M. Lawson and M. Valko, *Mol. Cell. Biochem.*, 2010, **345**, 91–104.
132 S. Melov, N. Wolf, D. Strozyk, S. R. Doctrow and A. I. Bush, *Free Radical Biol. Med.*, 2005, **38**, 258–261.
133 W. R. Markesbery, *Free Radical Biol. Med.*, 1997, **23**, 134–147.
134 L. Peauger, R. Azzouz, V. Gembus, M.-L. Tintas, J. Sopková-de Oliveira Santos, P. Bohn, C. Papamicael and V. Levacher, *J. Med. Chem.*, 2017, **60**, 5909–5926.
135 S. Thompson, K. L. Lanctôt and N. Herrmann, *Expert Opin. Drug Saf.*, 2004, **3**, 425–440.
136 T. B. Ali, T. R. Schleret, B. M. Reilly, W. Y. Chen and R. Abagyan, *PLoS One*, 2015, **10**, 0144337.

137 A. Tripathi, P. K. Choubey, P. Sharma, A. Seth, P. N. Tripathi, M. K. Tripathi, S. K. Prajapati, S. Krishnamurthy and S. K. Shrivastava, *Eur. J. Med. Chem.*, 2019, **183**, 111707.
138 E. Mikiciuk-Olasik, P. Szymański and E. Żurek, *Diagnostics and therapy of Alzheimer's disease*, 2007.
139 A. Jain and P. Piplani, *Bioorg. Chem.*, 2020, **103**, 104151.
140 M. S. Malik, B. H. Asghar, R. Syed, R. I. Alsantali, M. Morad, H. M. Altass, Z. Moussa, I. I. Althagafi, R. S. Jassas and S. A. Ahmed, *Front. Chem.*, 2021, **9**, 666573–666584.
141 M. S. Malik, R. A. Alsantali, A. Y. Alzahrani, Q. M. S. Jamal, E. M. Hussein, K. A. Alfaidi, M. M. Al-Rooqi, R. J. Obaid, M. A. Alsharif and S. F. Adil, *J. Saudi Chem. Soc.*, 2022, **26**, 101449.
142 M. S. Malik, S. Farooq Adil, Z. Moussa, H. M. Altass, I. I. Althagafi, M. Morad, M. A. Ansari, Q. M. Sajid Jamal, R. J. Obaid and A. A. Al-Warthan, *Front. Chem.*, 2021, **21**, 630357–630369.
143 R. Mehmood, A. Sadiq, R. I. Alsantali, E. U. Mughal, M. A. Alsharif, N. Naeem, A. Javid, M. M. Al-Rooqi, G.-e.-S. Chaudhry and S. A. Ahmed, *ACS Omega*, 2022, **7**, 17444–17461.
144 M. S. Malik, R. I. Alsantali, Q. M. S. Jamal, Z. S. Seddigi, M. Morad, M. A. Alsharif, E. M. Hussein, R. S. Jassas, M. M. Al-Rooqi and Z. Abduljaleel, *Front. Chem.*, 2021, **9**, 808556–808566.
145 M. S. Malik, R. I. Alsantali, M. A. Alsharif, S. I. Aljayzani, M. Morad, R. S. Jassas, M. M. Al-Rooqi, A. A. Alsimaree, H. M. Altass and B. H. Asghar, *Arabian J. Chem.*, 2022, **15**, 103560.
146 J. Ashraf, E. U. Mughal, R. I. Alsantali, A. Sadiq, R. S. Jassas, N. Naeem, Z. Ashraf, Y. Nazir, M. N. Zafar and A. Mumtaz, *RSC Adv.*, 2021, **11**, 35077–35092.
147 E. M. Hussein, M. S. Malik, R. I. Alsantali, B. H. Asghar, M. Morad, M. A. Ansari, Q. M. S. Jamal, A. A. Alsimaree, A. N. Abdalla and A. S. Algarni, *J. Mol. Struct.*, 2021, **1246**, 131232.
148 E. M. Hussein, M. M. Al-Rooqi, A. A. Elkhawaga and S. A. Ahmed, *Arabian J. Chem.*, 2020, **13**, 5345–5362.
149 E. M. Hussein, M. M. Al-Rooqi, S. M. Abd El-Galil and S. A. Ahmed, *BMC Chem.*, 2019, **13**, 1–18.
150 S. Faazil, M. S. Malik, S. A. Ahmed, R. I. Alsantali, P. Yedla, M. A. Alsharif, I. N. Shaikh and A. Kamal, *Bioorg. Chem.*, 2022, 105869.
151 S. Gauthier, *Can. Med. Assoc. J.*, 2002, **166**, 616–623.
152 J. L. McGaugh and L. F. Petrinovich, *Int. Rev. Neurobiol.*, 1965, **8**, 139–196.
153 A. Weissman, *Int. Rev. Neurobiol.*, 1967, **10**, 167–198.
154 J. J. Sramek, J. Hourani, S. S. Jhee and N. R. Cutler, *Life Sci.*, 1999, **64**, 1215–1221.
155 M. M. Koola, S. K. Praharaj and A. Pillai, *Current Behavioral Neuroscience Reports*, 2019, vol. 6, pp. 37–50.
156 P. Bacalhau, A. A. San Juan, A. Goth, A. T. Caldeira, R. Martins and A. J. Burke, *Bioorg. Chem.*, 2016, **67**, 105–109.
157 A. Fallah, F. Mohanazadeh and M. Safavi, *Med. Chem. Res.*, 2020, **29**, 341–355.
158 M. Danish, M. A. Raza, U. Anwar, U. Rashid and Z. Ahmed, *J. Chin. Chem. Soc.*, 2019, **66**, 1408–1415.
159 P. P. Roy, P. Banjare, S. Verma and J. Singh, *Mol. Inf.*, 2019, **38**, 1800151.
160 R. Shamsimeymandi, Y. Pourshojaei, K. Eskandari, M. Mohammadi-Khanaposhtani, A. Abiri, A. Khodadadi, A. Langarizadeh, F. Sharififar, B. Amirheidari and T. Akbarzadeh, *Arch. Pharm.*, 2019, **352**, 1800352.
161 M. Bajda, K. Łątka, M. Hebda, J. Jończyk and B. Malawska, *Bioorg. Chem.*, 2018, **78**, 29–38.
162 G. Makhaeva, N. Kovaleva, S. Lushchekina, E. Rudakova, N. Boltneva, A. Proshin, B. Lednev, I. Serkov and S. Bachurin, in *Doklady Biochemistry and Biophysics*, Springer, 2018, pp. 369–373.
163 N. Nunes, G. P. Rosa, S. Ferraz, M. C. Barreto and M. de Carvalho, *J. Appl. Phycol.*, 2020, **32**, 759–771.
164 D.-H. Shi, X.-D. Ma, Y.-W. Liu, W. Min, F.-J. Yin, Z.-M. Tang, M.-Q. Song, C. Lu, X.-K. Song and W.-W. Liu, *J. Chem. Res.*, 2018, **42**, 366–370.
165 F. Turkan, A. Cetin, P. Taslimi and İ. Gulçin, *Arch. Pharm.*, 2018, **351**, 1800200.
166 Y. Xu, Z. Zhang, X. Jiang, X. Chen, Z. Wang, H. Alsulami, H.-L. Qin and W. Tang, *Eur. J. Med. Chem.*, 2019, **181**, 111598.
167 Taslimi, F. Türkan, A. Cetin, H. Burhan, M. Karaman, I. Bildirici, I. Gulcin and F. Şen, *Bioorg. Chem.*, 2019, **92**, 103213–103221.
168 G. Gutti, D. Kumar, P. Paliwal, A. Ganeshpurkar, K. Lahre, A. Kumar, S. Krishnamurthy and S. K. Singh, *Bioorg. Chem.*, 2019, **90**, 103080.
169 S. Shaikh, P. Dhavan, G. Pavale, M. Ramana and B. Jadhav, *Bioorg. Chem.*, 2020, **96**, 103589.
170 R. M. Ghalib, R. Hashim, S. F. Alshahateet, S. H. Mehdi, O. Sulaiman, K.-L. Chan, V. Murugaiyah and A. Jawad, *J. Chem. Crystallogr.*, 2012, **42**, 783–789.
171 Y. K. Yoon, M. A. Ali, A. C. Wei, T. S. Choon, K.-Y. Khaw, V. Murugaiyah, H. Osman and V. H. Masand, *Bioorg. Chem.*, 2013, **49**, 33–39.
172 F. Ahmad, M. J. Alam, M. Alam, S. Azaz, M. Parveen, S. Park and S. Ahmad, *J. Mol. Struct.*, 2018, **1151**, 327–342.
173 Y. Xu, H. Wang, X. Li, S. Dong, W. Liu, Q. Gong, Y. Tang, J. Zhu, J. Li and H. Zhang, *Eur. J. Med. Chem.*, 2018, **143**, 33–47.
174 B. Kuzu, M. Tan, P. Taslimi, İ. Gülçin, M. Taşpınar and N. Menges, *Bioorg. Chem.*, 2019, **86**, 187–196.
175 A. I. Almansour, N. Arumugam, R. S. Kumar, D. Kotresha, T. S. Manohar and S. Venketesh, *Bioorg. Med. Chem. Lett.*, 2020, **30**, 126789.
176 I. A. Khodja, H. Boulebd, C. Bensouici and A. Belfaitah, *J. Mol. Struct.*, 2020, **1218**, 128527.
177 B. Barut, S. Sari, S. Sabuncuoğlu and A. Özel, *J. Mol. Struct.*, 2021, **1235**, 130268.
178 M. A. Abbasi, A. Akhtar, K. Nafeesa, S. Z. Siddiqui, K. M. Khan, M. Ashraf and S. A. Ejaz, *J. Chil. Chem. Soc.*, 2013, **58**, 2186–2190.

179 A. Kamal, A. B. Shaik, G. N. Reddy, C. G. Kumar, J. Joseph, G. B. Kumar, U. Purushotham and G. N. Sastry, *Med. Chem. Res.*, 2014, **23**, 2080–2092.
180 M. Mohammadi-Khanaposhtani, M. Mahdavi, M. Saeedi, R. Sabourian, M. Safavi, M. Khanavi, A. Foroumadi, A. Shafiee and T. Akbarzadeh, *Chem. Biol. Drug Des.*, 2015, **86**, 1425–1432.
181 S. Z. Siddiqui, M. A. Abbasi, M. Ashraf, B. Mirza and H. Ismail, *Pak. J. Pharm. Sci.*, 2017, **30**, 1743–1751.
182 A. Ibrar, A. Khan, M. Ali, R. Sarwar, S. Mehsud, U. Farooq, S. Halimi, I. Khan and A. Al-Harrasi, *Front. Chem.*, 2018, **6**, 61.
183 A. Rehman, A. Fatima, N. Abbas, M. A. Abbasi, K. M. Khan, M. Ashraf, I. Ahmad and S. A. Ejaz, *Pak. J. Pharm. Sci.*, 2013, **26**, 345–352.
184 A. Rehman, J. Iqbal, M. A. Abbasi, S. Z. Siddiqui, H. Khalid, S. Jhaumeer Laulloo, N. Akhtar Virk, S. Rasool and S. A. A. Shah, *Cogent Chem.*, 2018, **4**, 1441597.
185 A. Rehman, K. Nafeesa, M. A. Abbasi, S. Z. Siddiqui, S. Rasool, S. A. A. Shah and M. Ashraf, *Cogent Chem.*, 2018, **4**, 1472197.
186 J. Zhang, J.-C. Li, J.-L. Song, Z.-Q. Cheng, J.-Z. Sun and C.-S. Jiang, *J. Asian Nat. Prod. Res.*, 2018, 1090–1103.
187 P. N. Tripathi, P. Srivastava, P. Sharma, A. Seth and S. K. Shrivastava, *Bioorg. Med. Chem.*, 2019, **27**, 1327–1340.
188 P. Mishra, P. Sharma, P. N. Tripathi, S. K. Gupta, P. Srivastava, A. Seth, A. Tripathi, S. Krishnamurthy and S. K. Shrivastava, *Bioorg. Chem.*, 2019, **89**, 103025.
189 A. Tripathi, P. K. Choubey, P. Sharma, A. Seth, P. N. Tripathi, M. K. Tripathi, S. K. Prajapati, S. Krishnamurthy and S. K. Shrivastava, *Eur. J. Med. Chem.*, 2019, **183**, 111707.
190 P. Sharma, A. Tripathi, P. N. Tripathi, S. S. Singh, S. P. Singh and S. K. Shrivastava, *ACS Chem. Neurosci.*, 2019, **10**, 4361–4384.
191 X. Yu, Y.-F. Zhao, G.-J. Huang and Y.-F. Chen, *J. Asian Nat. Prod. Res.*, 2021, **23**, 866–876.
192 A. Fallah, F. Mohanazadeh and M. Safavi, *Med. Chem. Res.*, 2020, **29**, 341–355.
193 P. K. Choubey, A. Tripathi, M. K. Tripathi, A. Seth and S. K. Shrivastava, *Bioorg. Chem.*, 2021, **111**, 104922.
194 A. Tripathi, P. K. Choubey, P. Sharma, A. Seth, P. Saraf and S. K. Shrivastava, *Bioorg. Chem.*, 2020, **95**, 103506.
195 G. Ucar, N. Gokhan, A. Yesilada and A. A. Bilgin, *Neurosci. Lett.*, 2005, **382**, 327–331.
196 V. Jayaprakash, S. Yabanoglu, B. Sinha and G. Ucar, *Turk. J. Biochem.*, 2010, **35**, 91–98.
197 M. D. Altintop, A. Özdemir, Z. A. Kaplancikli, G. Turan-Zitouni, H. E. Temel and G. A. Çiftçi, *Arch. Pharm.*, 2013, **346**, 189–199.
198 S. Chigurupati, M. Selvaraj, V. Mani, K. K. Selvarajan, J. I. Mohammad, B. Kaveti, H. Bera, V. R. Palanimuthu, L. K. Teh and M. Z. Salleh, *Bioorg. Chem.*, 2016, **67**, 9–17.
199 M. S. Shah, S. U. Khan, S. A. Ejaz, S. Afridi, S. U. F. Rizvi, M. Najam-ul-Haq and J. Iqbal, *Biochem. Biophys. Res. Commun.*, 2017, **482**, 615–624.
200 H. E. Temel, M. D. Altintop and A. Özdemir, *Turk. J. Pharm. Sci.*, 2018, **15**, 333.
201 F. Turkan, A. Cetin, P. Taslimi, H. S. Karaman and I. Gulcin, *Arch. Pharm.*, 2019, **352**, 1800359.
202 A. Mumtaz, A. Majeed, S. Zaib, S. U. Rahman, S. Hameed, A. Saeed, H. Rafique, E. Mughal, A. Maalik and I. Hussain, *Bioorg. Chem.*, 2019, **90**, 103036.
203 C. Yamali, H. I. Gul, C. Kazaz, S. Levent and I. Gulcin, *Bioorg. Chem.*, 2020, **96**, 103627.
204 B. Sever, C. Türkeş, M. D. Altıntop, Y. Demir and Ş. Beydemir, *Int. J. Biol. Macromol.*, 2020, **163**, 1970–1988.
205 M. Tuğrak, H. İ. Gül and İ. Gülçin, *J. Res. Pharm.*, 2020, **24**, 464–471.
206 M. Mohammadi-Khanaposhtani, M. Saeedi, N. S. Zafarghandi, M. Mahdavi, R. Sabourian, E. K. Razkenari, H. Alinezhad, M. Khanavi, A. Foroumadi and A. Shafiee, *Eur. J. Med. Chem.*, 2015, **92**, 799–806.
207 M. A. Munawar, F. A. Chattha, S. Kousar, J. Munir, T. Ismail, M. Ashraf and M. A. Khan, *Bioorg. Med. Chem.*, 2015, **23**, 6014–6024.
208 S. P. Mantoani, T. P. Chierrito, A. F. Vilela, C. L. Cardoso, A. Martínez and I. Carvalho, *Molecules*, 2016, **21**, 193.
209 J.-Y. Park, S. Shin, K. C. Park, E. Jeong and J. H. Park, *J. Korean Chem. Soc.*, 2016, **60**, 125–130.
210 G. Wu, Y. Gao, D. Kang, B. Huang, Z. Huo, H. Liu, V. Poongavanam, P. Zhan and X. Liu, *MedChemComm*, 2018, **9**, 149–159.
211 L. Yin, L. Wang, X.-J. Liu, F.-C. Cheng, D.-H. Shi, Z.-L. Cao and W.-W. Liu, *Heterocycl. Commun.*, 2017, **23**, 231–236.
212 Z. Najafi, M. Mahdavi, M. Saeedi, E. Karimpour-Razkenari, R. Asatouri, F. Vafadarnejad, F. H. Moghadam, M. Khanavi, M. Sharifzadeh and T. Akbarzadeh, *Eur. J. Med. Chem.*, 2017, **125**, 1200–1212.
213 Z. Najafi, M. Mahdavi, M. Saeedi, E. Karimpour-Razkenari, N. Edraki, M. Sharifzadeh, M. Khanavi and T. Akbarzadeh, *Bioorg. Chem.*, 2019, **89**, 303–316.
214 M. Son, H. Lee, C. Jeon, Y. Kang, C. Park, K. W. Lee and J. H. Park, *Bull. Korean Chem. Soc.*, 2019, **40**, 544–553.
215 M. Özil, H. T. Balaydın and M. Şentürk, *Bioorg. Chem.*, 2019, **86**, 705–713.
216 A. Rastegari, H. Nadri, M. Mahdavi, A. Moradi, S. S. Mirfazli, N. Edraki, F. H. Moghadam, B. Larijani, T. Akbarzadeh and M. Saeedi, *Bioorg. Chem.*, 2019, **83**, 391–401.
217 A. Singh, S. Sharma, S. Arora, S. Attri, P. Kaur, H. K. Gulati, K. Bhagat, N. Kumar, H. Singh and J. V. Singh, *Bioorg. Med. Chem. Lett.*, 2020, **30**, 127477.
218 M. Yazdani, N. Edraki, R. Badri, M. Khoshneviszadeh, A. Iraji and O. Firuzi, *Mol. Diversity*, 2020, **24**, 641–654.
219 M. Mehrazar, M. Hassankalhori, M. Toolabi, F. Goli, S. Moghimi, H. Nadri, S. N. A. Bukhari, L. Firoozpour and A. Foroumadi, *Mol. Diversity*, 2020, **24**, 997–1013.
220 G. Le-Nhat-Thuy, N. N. Thi, H. Pham-The, T. A. D. Thi, H. N. Thi, T. H. N. Thi, S. N. Hoang and T. Van Nguyen, *Bioorg. Med. Chem. Lett.*, 2020, **30**, 127404.

221 N. Riaz, M. Iftikhar, M. Saleem, S. Hussain, F. Rehmat, Z. Afzal, S. Khawar, M. Ashraf and M. Al-Rashida, *Results Chem.*, 2020, **2**, 100041.
222 M. de Freitas Silva, E. Tardelli Lima, L. Pruccoli, N. G. Castro, M. J. R. Guimarães, F. M. da Silva, N. Fonseca Nadur, L. L. de Azevedo, A. E. Kümmerle and I. A. Guedes, *Molecules*, 2020, **25**, 3165.
223 H. K. Askarani, A. Iraji, A. Rastegari, S. N. A. Bukhari, O. Firuzi, T. Akbarzadeh and M. Saeedi, *BMC Chem.*, 2020, **14**, 1–13.
224 A. Rani, A. Singh, J. Kaur, G. Singh, R. Bhatti, N. Gumede, P. Kisten, P. Singh and V. Kumar, *Bioorg. Chem.*, 2021, 105053.
225 M. Saeedi, A. Maleki, A. Iraji, R. Hariri, T. Akbarzadeh, N. Edraki, O. Firuzi and S. S. Mirfazli, *J. Mol. Struct.*, 2021, **1229**, 129828.
226 I. Khan, M. Hanif, M. T. Hussain, A. A. Khan, M. A. S. Aslam, N. H. Rama and J. Iqbal, *Aust. J. Chem.*, 2012, **65**, 1413–1419.
227 A. Skrzypek, J. Matysiak, M. M. Karpińska and A. Niewiadomy, *J. Enzyme Inhib. Med. Chem.*, 2013, **28**, 816–823.
228 M. Rafiq, M. Saleem, M. Hanif, M. R. Maqsood, N. H. Rama, K.-H. Lee and S.-Y. Seo, *Bull. Korean Chem. Soc.*, 2012, **33**, 3943–3949.
229 A. Skrzypek, J. Matysiak, A. Niewiadomy, M. Bajda and P. Szymański, *Eur. J. Med. Chem.*, 2013, **62**, 311–319.
230 I. Khan, S. Zaib, A. Ibrar, N. H. Rama, J. Simpson and J. Iqbal, *Eur. J. Med. Chem.*, 2014, **78**, 167–177.
231 W.-W. Liu, Q.-X. Li and D.-H. Shi, *Heterocycles*, 2015, **91**, 275–286.
232 X.-J. Liu, L. Wang, L. Yin, F.-C. Cheng, H.-M. Sun, W.-W. Liu, D.-H. Shi and Z.-L. Cao, *J. Chem. Res.*, 2017, **41**, 571–575.
233 D.-H. Shi, H.-L. Zhu, Y.-W. Liu, Z.-M. Tang, C. Lu, X.-D. Ma, X.-K. Song, W.-W. Liu, T. Dong and M.-Q. Song, *J. Chem. Res.*, 2017, **41**, 664–667.
234 R. Ujan, A. Saeed, P. A. Channar, F. A. Larik, Q. Abbas, M. F. Alajmi, H. R. El-Seedi, M. A. Rind, M. Hassan and H. Raza, *Molecules*, 2019, **24**, 860.
235 S. Lotfi, T. Rahmani, M. Hatami, B. Pouramiri, E. T. Kermani, E. Rezvannejad, M. Mortazavi, S. F. Hafshejani, N. Askari and N. Pourjamali, *Bioorg. Chem.*, 2020, **105**, 104457.
236 N. Aggarwal, S. Jain and N. Chopra, Hybrids of thiazolidin-4-ones and 1, 3, 4-thiadiazole: synthesis and biological screening of a potential new class of acetylcholinesterae inhibitors, *Biointerface Res. Appl. Chem.*, 2021, **12**(3), 2800–2812.
237 A. Skrzypek, J. Matysiak, M. Karpińska, K. Czarnecka, P. Kręcisz, D. Stary, J. Kukułowicz, B. Paw, M. Bajda and P. Szymański, *Bioorg. Chem.*, 2021, **107**, 104617.
238 Y.-J. Lee, Y.-R. Han, W. Park, S.-H. Nam, K.-B. Oh, H.-S. Lee, J. Das, R. V. Moquin, A. J. Dyckman and T. Li, *Bioorg. Med. Chem. Lett.*, 2010, **20**, 6865–6881.
239 A. I. Almansour, R. S. Kumar, N. Arumugam, A. Basiri, Y. Kia, M. A. Ali, M. Farooq and V. Murugaiyah, *Molecules*, 2015, **20**, 2296–2309.
240 A. Basiri, B. M. Abd Razik, M. O. Ezzat, Y. Kia, R. S. Kumar, A. I. Almansour, N. Arumugam and V. Murugaiyah, *Bioorg. Chem.*, 2017, **75**, 210–216.
241 L. W. Mohamed, S. M. Abuel-Maaty, W. A. Mohammed and M. A. Galal, *Bioorg. Chem.*, 2018, **76**, 210–217.
242 A. M. Srour, D. H. Dawood, M. N. Khalil and Z. M. Nofal, *Bioorg. Chem.*, 2019, **83**, 226–234.
243 M. A. Youssef, S. S. Panda, R. A. El-Shiekh, E. M. Shalaby, D. R. Aboshouk, W. Fayad, N. G. Fawzy and A. S. Girgis, *RSC Adv.*, 2020, **10**, 21830–21838.
244 H. Girisha, J. N. S. Chandra, S. Boppana, M. Malviya, C. Sadashiva and K. S. Rangappa, *Eur. J. Med. Chem.*, 2009, **44**, 4057–4062.
245 H. Khalid, A. U. Rehman, M. A. Abbasi, R. Hussain, K. M. Khan, M. Ashraf, S. A. Ejaz and M. Q. Fatmi, *Turk. J. Chem.*, 2014, **38**, 189–201.
246 G. Brahmachari, C. Choo, P. Ambure and K. Roy, *Bioorg. Med. Chem.*, 2015, **23**, 4567–4575.
247 P. Meena, V. Nemaysh, M. Khatri, A. Manral, P. M. Luthra and M. Tiwari, *Bioorg. Med. Chem.*, 2015, **23**, 1135–1148.
248 K. S. S. Kumar, C. D. Mohan, K. S. R. Swamy Jagadish, A. Hanumappa and K. S. R. Basappa, *Synthesis*, 2015, **8**, 142–148.
249 N. Karaman, Y. Sıcak, T. Taşkın-Tok, M. Öztürk, A. Karaküçük-İyidoğan, M. Dikmen, B. Koçyiğit-Kaymakçıoğlu and E. E. Oruç-Emre, *Eur. J. Med. Chem.*, 2016, **124**, 270–283.
250 L. Yurttaş, Z. A. Kaplancıklı and Y. Özkay, *J. Enzyme Inhib. Med. Chem.*, 2013, **28**, 1040–1047.
251 S. Hamulakova, J. Imrich, L. Janovec, P. Kristian, I. Danihel, O. Holas, M. Pohanka, S. Böhm, M. Kozurkova and K. Kuca, *Int. J. Biol. Macromol.*, 2014, **70**, 435–439.
252 B. Kaya, Y. Özkay, H. E. Temel and Z. A. Kaplancıklı, *J. Chem.*, 2016, **2016**, 1–7.
253 W. Hussein, B. N. Sağlık, S. Levent, B. Korkut, S. Ilgın, Y. Özkay and Z. A. Kaplancıklı, *Molecules*, 2018, **23**, 2033.
254 M. Saeedi, D. Mohtadi-Haghighi, S. S. Mirfazli, M. Mahdavi, R. Hariri, H. Lotfian, N. Edraki, A. Iraji, O. Firuzi and T. Akbarzadeh, *Chem. Biodiversity*, 2019, **16**, 1800433.
255 P. N. Tripathi, P. Srivastava, P. Sharma, M. K. Tripathi, A. Seth, A. Tripathi, S. N. Rai, S. P. Singh and S. K. Shrivastava, *Bioorg. Chem.*, 2019, **85**, 82–96.
256 Ş. Demirayak, Z. Şahin, M. Ertaş, E. F. Bülbül, C. Bender, S. N. Biltekin, B. Berk, B. N. Sağlık, S. Levent and L. Yurttaş, *J. Heterocycl. Chem.*, 2019, **56**, 3370–3386.
257 M. Abbasi, M. Irshad, S. Siddiqui, H. Junaid, S. Shah and M. Ashraf, *Pharm. Chem. J.*, 2020, **54**, 596–603.
258 P. Szymanski, M. Markowicz, M. Bajda, B. Malawska and E. Mikiciuk-Olasik, *Lett. Drug Des. Discovery*, 2012, **9**, 645–654.
259 Z. Najafi, M. Saeedi, M. Mahdavi, R. Sabourian, M. Khanavi, M. B. Tehrani, F. H. Moghadam, N. Edraki, E. Karimpor-

Razkenari and M. Sharifzadeh, *Bioorg. Chem.*, 2016, **67**, 84–94.
260 Z. Sang, W. Pan, K. Wang, Q. Ma, L. Yu and W. Liu, *Bioorg. Med. Chem.*, 2017, **25**, 3006–3017.
261 M. Eghtedari, Y. Sarrafi, H. Nadri, M. Mahdavi, A. Moradi, F. H. Moghadam, S. Emami, L. Firoozpour, A. Asadipour and O. Sabzevari, *Eur. J. Med. Chem.*, 2017, **128**, 237–246.
262 N. A. Khan, I. Khan, S. Abid, S. Zaib, A. Ibrar, H. Andleeb, S. Hameed and J. Iqbal, *Med. Chem.*, 2018, **14**, 74–85.
263 M. S. Shah, M. Najam-ul-Haq, H. S. Shah, S. U. F. Rizvi and J. Iqbal, *Comput. Biol. Chem.*, 2018, **76**, 310–317.
264 J. Mo, H. Yang, T. Chen, Q. Li, H. Lin, F. Feng, W. Liu, W. Qu, Q. Guo and H. Chi, *Bioorg. Chem.*, 2019, **93**, 103310.
265 J. de Oliveira C Brum, D. C. F. Neto, J. S. F. de Almeida, J. A. Lima, K. Kuca, T. C. C. França and J. D. Figueroa-Villar, *Int. J. Mol. Sci.*, 2019, **20**, 3944.
266 D. N. Rosado-Solano, M. A. Barón-Rodríguez, P. L. Sanabria Florez, L. K. Luna-Parada, C. E. Puerto-Galvis, A. s. F. Zorro-González, V. V. Kouznetsov and L. Y. Vargas-Méndez, *J. Agric. Food Chem.*, 2019, **67**, 9210–9219.
267 I. Bazine, Z. Cheraiet, R. Bensegueni, C. Bensouici and A. Boukhari, *J. Heterocycl. Chem.*, 2020, **57**, 2139–2149.
268 B. Macha, R. Kulkarni, C. Bagul, A. K. Garige, R. Akkinepally and A. Garlapati, *Med. Chem. Res.*, 2021, **30**, 685–701.
269 B. Macha, R. Kulkarni, A. K. Garige, S. Pola, R. Akkinepally and A. Garlapati, *ChemistrySelect*, 2021, **6**, 1947–1957.
270 T. Mohamed, X. Zhao, L. K. Habib, J. Yang and P. P. Rao, *Bioorg. Med. Chem.*, 2011, **19**, 2269–2281.
271 S. Ahmad, F. Iftikhar, F. Ullah, A. Sadiq and U. Rashid, *Bioorg. Chem.*, 2016, **69**, 91–101.
272 T. U. Rehman, I. U. Khan, M. Ashraf, H. Tarazi, S. Riaz and M. Yar, *Arch. Pharm.*, 2017, **350**, 1600304.
273 V. Kumar, B. Kumar, A. Ranjan Dwivedi, D. Mehta, N. Kumar, B. Bajaj, T. Arora, V. Prashar, J. Parkash and V. Kumar, *ChemistrySelect*, 2020, **5**, 8021–8032.
274 S. Manzoor, S. K. Prajapati, S. Majumdar, M. K. Raza, M. T. Gabr, S. Kumar, K. Pal, H. Rashid, S. Kumar and S. Krishnamurthy, *Eur. J. Med. Chem.*, 2021, **215**, 113224.
275 M. Maqbool, A. Manral, E. Jameel, J. Kumar, V. Saini, A. Shandilya, M. Tiwari, N. Hoda and B. Jayaram, *Bioorg. Med. Chem.*, 2016, **24**, 2777–2788.
276 S. Akocak, B. Mehmet, N. Lolak, M. Tuneg and R. K. Sanku, *J. Turk. Chem. Soc., Sect. A*, 2019, **6**, 63–70.
277 N. Lolak, M. Boga, M. Tuneg, G. Karakoc, S. Akocak and C. T. Supuran, *J. Enzyme Inhib. Med. Chem.*, 2020, **35**, 424–431.
278 S. Parlar, G. Bayraktar, A. H. Tarikogullari, V. Alptüzün and E. Erciyas, *Chem. Pharm. Bull.*, 2016, **64**, 1281–1287.
279 F. Pandolfi, D. De Vita, M. Bortolami, A. Coluccia, R. Di Santo, R. Costi, V. Andrisano, F. Alabiso, C. Bergamini and R. Fato, *Eur. J. Med. Chem.*, 2017, **141**, 197–210.
280 R. Ghobadian, M. Mahdavi, H. Nadri, A. Moradi, N. Edraki, T. Akbarzadeh, M. Sharifzadeh, S. N. A. Bukhari and M. Amini, *Eur. J. Med. Chem.*, 2018, **155**, 49–60.
281 S. K. Singh, S. K. Sinha and M. K. Shirsat, *Indian J. Pharm. Educ. Res.*, 2018, **52**, 644–654.
282 N. Sultana, M. Sarfraz, S. T. Tanoli, M. S. Akram, A. Sadiq, U. Rashid and M. I. Tariq, *Bioorg. Chem.*, 2017, **72**, 256–267.
283 T. Mohamed and P. P. Rao, *Eur. J. Med. Chem.*, 2017, **126**, 823–843.
284 M. Sarfraz, N. Sultana, M. Jamil and M. I. Tariq, *Rev. Roum. Chim.*, 2018, **63**, 227–234.
285 U. M. Kocyigit, Y. Budak, M. B. Gürdere, F. Ertürk, B. Yencilek, P. Taslimi, İ. Gülçin and M. Ceylan, *Arch. Physiol. Biochem.*, 2018, **124**, 61–68.
286 T.-S. Tran, M.-T. Le, T.-C.-V. Nguyen, T.-H. Tran, T.-D. Tran and K.-M. Thai, *Molecules*, 2020, **25**, 3916.
287 S. M. Sanad and A. E. Mekky, *J. Iran. Chem. Soc.*, 2021, **18**, 213–224.
288 P. Suwanhom, T. Nualnoi, P. Khongkow, V. Sanghiran Lee and L. Lomlim, *Med. Chem. Res.*, 2020, **29**, 564–574.
289 S. Shaikh, P. Dhavan, M. Ramana and B. Jadhav, *Mol. Diversity*, 2021, **25**, 811–825.
290 Q. Q. Lu, Y. M. Chen, H. R. Liu, J. Y. Yan, P. W. Cui, Q. F. Zhang, X. H. Gao, X. Feng and Y. Z. Liu, *Drug Dev. Res.*, 2020, **81**, 1037–1047.
291 R. Munir, M. Zia-ur-Rehman, S. Murtaza, S. Zaib, N. Javid, S. J. Awan, K. Iftikhar, M. M. Athar and I. Khan, *Molecules*, 2021, **26**, 656.
292 P. Suwanhom, J. Saetang, P. Khongkow, T. Nualnoi, V. Tipmanee and L. Lomlim, *Molecules*, 2021, **26**, 4895.
293 S. Zaib, R. Munir, M. T. Younas, N. Kausar, A. Ibrar, S. Aqsa, N. Shahid, T. T. Asif, H. O. Alsaab and I. Khan, *Molecules*, 2021, **26**, 6573.
294 R. Ujan, P. A. Channar, A. Bahadur, Q. Abbas, M. Shah, S. Rashid, S. Iqbal, A. Saeed, H. S. Abd-Rabboh and H. Raza, *J. Mol. Struct.*, 2021, **1246**, 131136.
295 A. Işık, U. Acar Çevik, A. Karayel, I. Celik, T. Erçetin, A. Koçak, Y. Özkay and Z. Kaplancıklı, *SAR QSAR Environ. Res.*, 2022, **33**, 193–214.
296 A. Huseynova, R. Kaya, P. Taslimi, V. Farzaliyev, X. Mammadyarova, A. Sujayev, B. Tüzün, U. M. Kocyigit, S. Alwasel and İ. Gulçin, *J. Biomol. Struct. Dyn.*, 2022, **40**, 236–248.
297 A. H. Hasan, S. Murugesan, S. I. Amran, S. Chander, M. M. Alanazi, T. B. Hadda, S. Shakya, M. R. F. Pratama, B. Das and S. Biswas, *Bioorg. Chem.*, 2022, **119**, 105572.